博士論文

Study on Ageing Degradation of Nuclear Power Plants Cables using Accelerated Tests
（原子力発電プラントケーブル経年劣化に関する加速試験を用いた研究）

タリク　ジャド　モハマド ジェクティープ

TARIQ ZEYAD MOHAMMAD (ALSHAKETHEEP)

東京大学大学院工学系研究科

原子力国際専攻

The University of Tokyo

Department of Nuclear Engineering and Management

博士論文

Ph.D. Dissertation

Study on Ageing Degradation of Nuclear Power Plants Cables using Accelerated Tests

（原子力発電プラントケーブル経年劣化に関する加速試験を用いた研究）

指導教員　関村 直人 教授

Supervisor: Prof. Naoto SEKIMURA

August 2015

平成 27 年 8 月

学籍番号 37-127311

タリク　ジャド　モハマド　シェクティープ

TARIQ ZEYAD MOHAMMAD (ALSHAKETHEEP)

I dedicate this work to my beloved parents

Acknowledgement

I would like to express my sincere gratitude to my supervisor; Prof. Naoto SEKIMURA for giving me the opportunity to perform my Ph.D. research at his laboratory. His great guidance as well as strong discussion have extensively polished my academic characteristic and developed my understanding for philosophy of research in the field of cables ageing management at nuclear power plants. It is my great honor and pleasure for being his student.

I am very thankful to Prof. Kenta MURAKAMI for his kindness, massive efforts, and advices that helped me improve my performance. I would like to thank him for his help during experimental setup starting from preparing samples of FR-EPR cables, heating oven, tensile testing at Tokai-Mura campus, and volume resistivity measurements. I cannot forget the hundreds of hours of interesting discussion with him even during his rest times and weekends. I totally appreciate his favors.

I would like to thank the secretary of my supervisor; Mrs. Naoko HASE for her kind help and efforts to coordinate laboratory activities as well as arranging meetings with Prof. Naoto SEKIMURA.

I wish to thank all committee members for attending my defense and for their valuable comments.

Special thanks to Prof. Hisaaki KUDO for his discussions and guidance to important references.

I also wish to thank Mr. Masanori KANNO from Japan Nuclear Energy Safety (JNES) Organization for supplying me important references and for his nice discussions.

I wish to thank Prof. Takumi SAITO for his great help regarding FTIR spectroscopy measurements at Asano-campus.

Special thanks to Dr. Lassad BEN YOUNES and Mr. Masaki MURAKAMI for their fruitful discussion and providing aid at Matlab M-file coding. You are nice colleagues and hope you success in your career.

I am grateful to all my warm-hearted family members who stood beside me in the harshest times of this mission. Their contact, encouragement, and support gave me great motivation and relieved my worries.

I direct my thanks to Dr. Ahmed SLIMANI and Mrs. Mari MORISHITA due to their advices during my tense moments. I also would like to express my gratitude to all unmentioned people

who helped me by any mean.

I would like to thank Japanese Ministry of Education, Culture, Sports and Technology (MEXT) for their financial support.

August 2015
Tariq ALSHAKETHEEP

Abstract

Study on Ageing Degradation of Nuclear Power Plants Cables using Accelerated Tests (原子力発電プラントケーブル経年劣化に関する加速試験を用いた研究)

Tariq ALSHAKETHEEP

1. Introduction

Degradation of polymeric-based cable insulator is a key concern for nuclear power plants (NPPs) operation and life management. Survey of good international practices [1-4] resulted in 6 attributes for effectively managing insulator ageing: Cable structure/ materials, environment, category, degradation mechanisms, condition monitoring, and modeling. Management activities through these attributes rely on estimated integrity margins from accelerated ageing tests. Besides, cable integrity is evaluated before installation through the so called environmental qualification (EQ) to assure cable remains functional at design lifetime and design basis accident (DBA). During EQ, integrity is evaluated by accelerated thermal and radiation test simulating normal operation, followed by DBA test that envelop loss of coolant accident (LOCA) conditions, and finally the cable integrity is judged by bending submergence withstand voltage test [3].

On the other hand, the main issues of current EQ as well as relevant research activities on accelerated ageing tests are extracted below:

1-Obtained knowledge from thermal accelerated tests focuses only on insulator material ageing. But during EQ process and real operation, cables are aged including jacket material. Thus, insulator ageing must be well considered within whole cable structure.

2-The equivalency between accelerated test and real conditions is limited to insulator mechanical properties, in particular elongation at break (EAB). Thus, activation energy (E_a) estimations by Arrhenius modeling is mainly dependent on induced mechanisms altered by EAB. But real E_a may differ due to insulator colorant variance, or at extrapolation region due to physical transition mechanisms. Besides, during integrity test, the final judgment relies on electrical properties since they are most vital parameters [1]. Nevertheless, it is difficult to evaluate their time-dependent degradation due to inaccuracies of their conventional measurements by Mega ohmmeter. With above in mind, it is vital to update current knowledge by insulator properties variety and cable structure.

3-Current DBA test only covers LOCA. Some scenarios beyond-DBA (BDBA) conditions may be included in new regulations through the so called design extension conditions (DECs)

Accordingly, this study aims at properly customizing accelerating test to understand cable real degradation during normal operation, and modify cable EQ process to suit with recent progress of NPP safety design. For achieving this goal it is required to:

1-Clarify impact of cable structure on insulator mechanical and electrical properties.

2-Assess utilization of insulator electrical and mechanical properties degradation for trending accelerated ageing from engineering evaluation methods and recent knowledge database.

3-Identify important cables for DECs and propose modification of EQ to suit with some elevated scenarios accompanying DECs.

2. Experimental studies on cable structure impact by accelerated ageing

2.1 Cable materials and test environment

Flame-retardant ethylene propylene rubber (FR-EPR) insulated cables are selected due to their

vast usage in NPPs [4]. Jacket material is polyvinyl chloride (PVC). Cable category is nuclear grade 1E, 3 core, low voltage (LV) (< 600 V) power/control.

Thermal accelerated ageing tests were performed using air-circulated oven at 125 ˚C, 150 ˚C, and 160 ˚C for 5040 hours, 336 hours, and 264 hours, respectively. The assumed degradation mechanisms are chain scission, cross linking, additives immigration while diffusion limited oxidation (DLO) is more efficient at higher test temperatures. Full cable-type (insulator and jacket) ageing is focused, considering that whole cable structure is aged in real NPP environments. But to compare effect of insulator's ageing environment (jacket or air), some specimens were heated after removing their jacket. Maximum scattering of oven temperature is ±4 ˚C.

2.2 Parameters for insulator properties evaluation

Insulator electrical properties were evaluated by volume resistivity (ρ) .Although the induced charged particles from chain scission reactions (i.e. chain scission moieties) by ageing stressors can alter insulator volume resistivity (ρ), conventional insulation resistance (IR) measurements are only pass/fail test and not counted for trending time-dependent ageing, because uncertainty of IR due to the leakage current over cable surface is large. To solve this issue, new electrode for tubular insulator was developed to guard the influence of surface current [5]. By using this electrode and Wheatstone bridge circuit, measurement of ρ in tubular insulator became plausible, provided, however, that $\rho < 1\times10^{15}$ Ωm.

EAB is utilized to evaluate insulator mechanical properties since it is well-known as excellent ageing indicator. Tubular shape tensile samples were made for the three aged insulator colors at each ageing point according to IEC 62582-3:2012.

2.3 Impact of insulator environment on insulator properties

Fig. 1 shows FR-EPR insulator properties behavior with ageing time at 160 ˚C. EAB and ρ slightly varies between insulators colors due to colorant (pigment) variance. But degradation trends are similar implying that degradation mechanisms are identical through insulator environment. However, EAB degradation rate is higher through ageing time when insulator is aged with jacket, revealing that chain-scission and cross linking reactions rate is higher that lead to insulator embrittlement after 210 hours heating. ρ degradation is also more severe after 150 hours heating for insulator aged with jacket, hence chain scission reactions are evident from trending ρ. Mechanisms of large ρ reduction for insulators aged with jacket is attributed to high production of chain-scission moieties, difficulty to cease chain-scissions radicals by anti-oxidants, or induced charged particles from catalyst reactions between insulator and jacket. The increment tendency of ρ after 210 hours heating is due to the change of insulator shape as a result of embrittlement that is trended by EAB reduction. Thus, it is neither correlated to ρ degradation nor recovery.

Similar trend behavior of both EAB and ρ with ageing time was observed for ageing at 125 ˚C even though DLO impacts are less significant. Therefore, jacket-insulator environment enhance

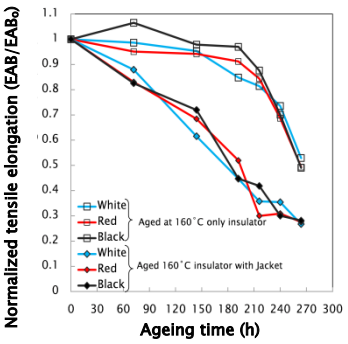

(a) EAB

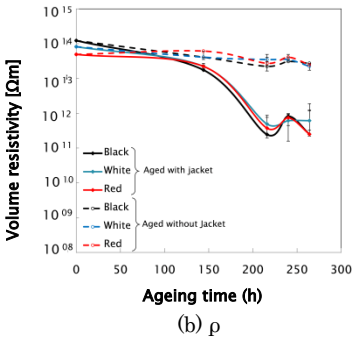

(b) ρ

Fig. 1 Mechanical properties ((a) EAB) and electrical properties ((b) ρ) versus ageing time for FR-EPR insulators aged at 160 ˚C with and without PVC jacket

degradation reactions more severely than air environment. This vital finding is utilized in this study for further evaluations of activation energies (E_a) for equivalent time modeling.

3. Thermal ageing estimations from insulator properties degradation

3.1 Activation energy (E_a) estimation from EAB and ρ degradation

Equivalent time predictions are influenced by E_a determinations from insulator properties degradation. Since both EAB and ρ degradation showed identical trends at 125 ˚C, 150 ˚C, and 160 ˚C ageing, then time-temperature (T-t) superposition approach can be applied to determine E_a as in Fig. 2. However, EAB degradation is continuous with ageing time and exceeds its half-initial value (end-of-lifetime) criterion [1], while ρ degradation is still higher than insulation function acceptance criterion (i.e 1×10^8 Ωm) [1]. Thus, EAB is better indicator for cable integrity at uniform-thermal degradation.

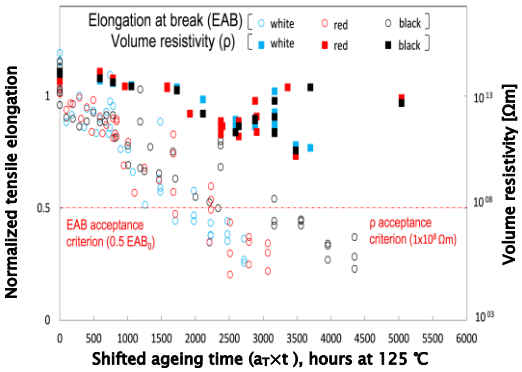

Fig. 2 T-t superposition for FR-EPR insulator thermally aged with PVC jacket from EAB and ρ degradation trends. [Superposed at 125 ˚C]

Time to end-of-lifetime criterion (0.5 EAB_0) at each ageing temperature can be utilized to calculate E_a by Arrhenius model. The values of E_a by T-t approach and Arrhenius model from EAB and ρ degradation are summarized in table 1. Estimated E_a from ρ are different from EAB due to different mechanisms that alter each property. E_a values are very close for each color by T-t approach and Arrhenius model from EAB degradation. This emphasizes that both methods are appropriate for E_a estimation reflecting similar induced mechanisms. E_a for black insulator is largely deviated from other colors when estimations are from EAB due to presence of carbon-black as colorant pigment that acts as anti-oxidant, thus slower degradation rate. But E_a values are very close when estimations by ρ degradation which reveals that impacts of colorant additives are less important.

Table 1 E_a (KJ/mol) estimations for thermally aged FR-EPR insulators

Insulator color	E_a by T-t approach		E_a by Arrhenius model from EAB degradation
	EAB	ρ	
White	90	108	90
Red	93	104	87
Black	113	108	105

3.2 Comparison of thermal ageing estimations with EAB degradation data base

Thermal ageing estimations in current EQ rely on E_a and equivalent time calculations from EAB degradation data base. Accordingly, to evaluate real cable degradation during thermal ageing test, Arrhenius model was utilized to compare E_a and ageing times between EAB degradation for FR-EPR insulators aged with their jacket as in this study with EAB degradation data base for same material but aged with no jacket[3] as shown in Arrhenius plot in Fig. 3. Most E_a values are almost in same range even when ageing method is different. This reveals low possibility for physical transition mechanisms through crystalline melting point[1,6,7] at extrapolation region, and Arrhenius model can be utilized to extrapolate and compare ageing times at 100 ˚C (i.e time to 0.5 EAB_0 at 100 ˚C). For

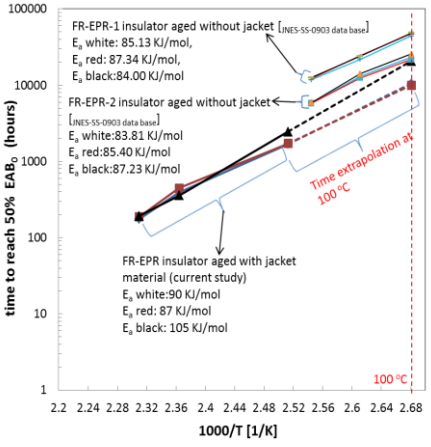

Fig.3 Arrhenius plot of ageing times to 0.5EAB_0 for FR-EPR insulators aged with and without jacket materials

FR-EPR insulators aged with jacket, the ageing times of black insulator was largely deviated above white and red, due to effect of colorant on EAB degradation and E_a estimations. Nevertheless, ageing times of insulators aged with jacket are less than those for insulators aged without jacket. This reveals that the current EQ misestimates degradation of cable insulator due to presence of jacket. But EQ is still suitable considering that cable will pass final integrity withstand voltage test. Thus, excessive ageing time margins at thermal ageing phase can be utilized for DECs.

4. In search of design extension environments for NPPs cables

For BWR-4 case study, 18 targeted electric equipment/cables for DECs were identified from engineering judgment between plant systems understanding with 14 severe accident sequences event trees initiated from LOCA, station black out (SBO) and anticipated transients [8]. These targeted cables were coordinated with other items, as seen in Fig. 4, which can lead to establish knowledgeable-base guideline and predict cable failure behavior based on target accident, cable category, and auto-logic connections with other equipment. Besides, considering cable polymeric based structure, both BDBA temperature and flooding are main stress factors of interest for DECs.

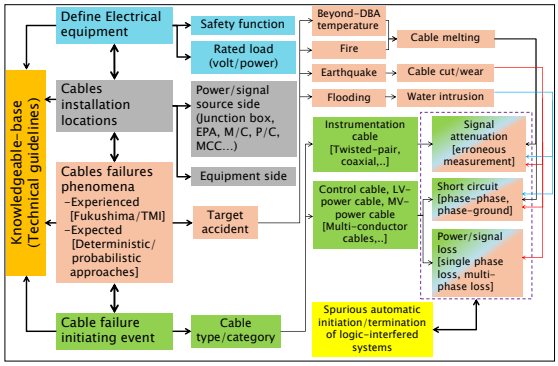

Fig.4 Proactive approach for establishing knowledgeable-base guidelines from targeted cables regarding DECs

Thus, current EQ was reevaluated for both DBA peak temperature and submergence withstand voltage. Cable mechanical integrity criteria limits at 50% absolute and normalized EAB were utilized to extend current DBA peak temperature from 171 ˚C to 230-250 ˚C for thermoset insulator materials. Besides, it was found that targeted cables are LV with withstand voltage (1-2 KV/mm) specified by maker standards, while the current EQ recommendation tests cables by higher values at 3.2 KV/mm. This reveals that current EQ settings for voltage stress include ultimate corresponding environments that can be encountered at any accident scenario of DECs.

5. Conclusions

1-Effect of cable structure on thermal ageing was examined by EAB and ρ. Jacket impact on insulator degradation was very significant, even though colorant pigments effects were evident.

2-Recent EQ process misestimates insulator degradation due to existence of jacket material.

3-Tageted cables for DECs were selected and suitable modification of DBA test was proposed considering BWR plant. DBA peak temperature can be extended from 171 ˚C to 230-250 ˚C for FR-EPR cables inside BWR containment vessel.

References

[1] IAEA, Nuclear Energy Series, No. NP-T-3.6 (2012).

[2] Yamamoto, Minakawa, JNES, System Safety Report, SS-0903 (2009).

[3] Ikeda, Minakawa, JNES, Safety Research Report, RE-2013-2049 (2014).

[4] Sekimura, et al., OECD/NEA, Technical basis for commendable practices on ageing management SCC and Cable Ageing Project (SCAP), Paris (2011).

[5] Alshaketheep, Murakami, Sekimura, E-Journal Adv. Maintenance, Japan Soc. Maintenology,7,pp. 102-107 (2015).

[6] Gillen, et al., Pol. Degrad Stab., 91, pp. 2146 -2156 (2006).

[7] Seguchi, et al., Radiat Phys Chem,80, pp.268-273 (2011).

[8] USNRC, NUREG/CR-2825 (1982)

Table of Contents

Acknowledgement i
Abstract iii
Table of Contents vii
List of Tables ix
List of Figures x
Chapter 1 Introduction 1
1.1 Overview of nuclear power plants (NPPs) cables 1
1.2 Cables ageing management (AM) for long-term operation 3
1.3 Cables AM attributes 5
1.3.1 Cable structure and materials 6
1.3.2 Environment/stressors 8
1.3.3 Classification/category 8
1.3.4 Degradation mechanisms 11
1.3.5 Condition monitoring (CM) 12
1.3.6 Modeling 14
1.4 Cables environmental qualification (EQ) 15
1.5 Current issues on AM activities and EQ process 17
1.5.1 Thermal ageing estimations 20
1.5.2 Design basis accidents conditions 22
1.6 Objectives 24
Chapter 2 Experimental studies on cable structure impact by accelerated ageing 25
2.1 Specimens 25
2.2 Ageing conditions 28
2.3 Experimental setup 31
2.3.1 Tensile testing for elongation at break (EAB) measurement 31
2.3.2 Developed CM technique for electrical volume resistivity (ρ) measurement 34
2.4 Results and discussion 43
2.4.1 EAB 43
2.4.2 ρ 48
2.4.3 Mechanisms investigations by Fourier transform infra-red spectroscopy 52

2.4.4 Discussion on impact of insulation environment on its degradation..... 57
Chapter 3 Thermal ageing estimations from insulator properties degradation 59
3.1 Parameters for thermal ageing characteristics approximations 60
3.2 Activation energy (E_a) estimations 65
3.2.1 Arrhenius model 65
3.2.2 Time-temperature superposition approach 73
3.3 Discussion on thermal ageing estimations from EAB and ρ degradations..... 82
3.4 Comparisons of thermal ageing estimations with EAB degradation data base 84
3.5 Considerations for thermal ageing estimations of current EQ..... 89
Chapter 4 In search of design extension environments for NPPs cables 91
4.1 Cables identifications for design extensions conditions (DECs) 91
4.2 Knowledgeable-base proactive approach for targeted cables regarding DECs 104
4.3 Perception for cable evaluations at DECs..... 107
4.4 Generic approach for modifying current EQ 110
4.5 DBA peak-temperature extension from EAB degradation 116
Chapter 5 Conclusions 125
5.1 Major findings and contributions of this study 125
5.2 Recommendations for future work..... 129
Annex..... 130
Bibliography..... 132

List of Tables

Table 1.1 Cable ageing management guidelines 5
Table 1.2 Polymer materials used in NPPs [14] 7
Table 1.3 Safety classifications for NPPs cables and systems [11] 10
Table 1.4 Cable condition monitoring techniques 13
Table 2.1 Cable specimens' characteristics 26
Table 2.2 Arrangement of ageing temperature, time, and method 30
Table 2.3 bridge arms resistance values for Wheatstone bridge circuit configuration 41
Table 2.4 FTIR spectral peaks of FR-EPR in absorption bandwidth 1700-1800 cm^{-1} and 2500-3000 cm^{-1} 53
Table 3.1 Approximation results of EAB degradation characteristics for FR-EPR insulators aged with SHPVC jacket at 125 °C, 150 °C, and 160 °C 61
Table 3.2 E_a (KJ/mol) estimations from deviated times to 0.5 EAB_0 by technical scattering .. 71
Table 3.3 Acceleration shift factors (a_T) values from ρ degradation curves for thermally aged FR-EPR insulators aged with SHPVC jacket 75
Table 3.4 Acceleration shift factors (a_T) values from EAB degradation curves for thermally aged FR-EPR insulators aged with SHPVC jacket 79
Table 3.5 Activation energy (KJ/mol) values by time-temperature superposed EAB and ρ degradation curves for thermally aged FR-EPR insulators 82
Table 3.6 Acceleration shift factors (a_T) from EAB degradation database for thermally aged FR-EPR insulators 84
Table 3.6 Extrapolated times to 0.5 EAB_0 at 100 °C ageing from FR-EPR insulators aged with and without jacket materials 88

List of Figures

Fig.1.1 Schematic layout for cables in PWR [11,12] 2
Fig.1.2 Key elements of instrementation and control (I&C) cable ageing management program utilizing the systematic ageing management approach [14] 4
Fig.1.3 Cables ageing management attributes 6
Fig.1.4 Schematic diagram for typical safety cables structure [22] 9
Fig.1.5 Type-testing cable environmental qualification method used in Japan 16
Fig.1.6 Illustrative flow-chart for previous research activities on insulator integrity evaluations 18
Fig.2.1 Overview and cross sectional geometry of FR-EPR insulated cable 27
Fig.2.2 Cable-type and tubular-type samples inside oven 29
Fig.2.3 Typical stress-strain (σ-ε) curve for EPR-based elastomers before ageing (a) and after thermal ageing (b) 31
Fig.2.4 Tubular shape tensile test samples and dimensions 33
Fig.2.5 Electrode system for IR and ρ detection 38
Fig.2.6 Electric circuit configuration for IR and ρ measurement 40
Fig.2.7 Volume resistivity versus measurement time for FR-EPR insulators aged at 125 °C for 3480 hours 42
Fig.2.8 Elongation at break versus ageing time for FR-EPR white insulator aged with SHPVC jacket at 160 °C 43
Fig.2.9 Elongation at break versus ageing time for FR-EPR insulator aged with SHPVC jacket at 160 °C 44
Fig.2.10 Elongation at break versus ageing time for FR-EPR insulator aged with SHPVC jacket 45
Fig.2.11 Elongation at break versus ageing time for FR-EPR insulators aged with and without SHPVC jacket at 160 °C 46
Fig.2.12 Elongation at break versus ageing time for FR-EPR insulators aged with and without SHPVC jacket at 125 °C 47
Fig.2.13 Volume resistivity versus ageing time for FR-EPR black insulator aged with SHPVC jacket at 160 °C 48
Fig.2.14 Volume resistivity versus ageing time for FR-EPR insulators aged with SHPVC jacket at 160 °C 49
Fig.2.15 Volume resistivity versus ageing time for FR-EPR insulators aged with SHPVC jacket 50
Fig.2.16 Volume resistivity versus ageing time for FR-EPR insulators aged with and without SHPVC jacket at 160 °C 51
Fig.2.17 Volume resistivity versus ageing time for FR-EPR insulators aged with and without SHPVC jacket at 125 °C 52
Fig.2.18 FTIR spectra for FR-EPR white insulator before and after ageing with SHPVC jacket at 150 °C for 288 hour (bandwidth 1700-1800 cm^{-1}) 54
Fig.2.19 Carbonyl contents versus ageing time for FR-EPR white insulator surface aged with

SHPVC jacket at 150 °C 55
Fig.2.20 Mechanisms schemes by oxidation for FR-EPR white insulator surface aged with SHPVC jacket at 150 °C 56
Fig.2.21 FTIR spectra for FR-EPR white insulator before and after ageing with SHPVC jacket at 150 °C for 288 hour (bandwidth 2500-3000 cm^{-1}) 57
Fig.3.1 Real and approximated ultimate EAB values versus ageing time for FR-EPR insulators aged with SHPVC jacket at 125 °C,150 °C, and 160 °C 62
Fig.3.2 Real and approximated normalized EAB values versus ageing time for FR-EPR insulators aged with SHPVC jacket at 125 °C,150 °C, and 160 °C 64
Fig.3.3 ρ degradation curves for FR-EPR thermally aged with SHPVC jacket 67
Fig.3.4 EAB degradation curves for FR-EPR thermally aged with SHPVC jacket 68
Fig.3.5 Arrhenius plot of FR-EPR insulators ageing times to 0.5 $EAB_{0\,(\mu \pm \sigma)}$ 72
Fig.3.6 ρ degradation curves for FR-EPR thermally aged with SHPVC jacket 74
Fig.3.7 Time-temperature superposed ρ degradation curves to reference temperature of 125 ˚C, for FR-EPR thermally aged with SHPVC jacket 75
Fig.3.8 Arrhenius plot of FR-EPR insulators shift factors by ρ degradation curves superposition 76
Fig.3.9 EAB degradation curves for FR-EPR thermally aged with SHPVC jacket 77
Fig.3.10 Time-temperature superposed EAB degradation curves to reference temperature of 125 ˚C, for FR-EPR thermally aged with SHPVC jacket 80
Fig.3.11 Arrhenius plot of FR-EPR insulators shift factors by EAB degradation curves superposition 81
Fig.3.12 Time-temperature superposed EAB & ρ degradation curves to reference temperature of 125 ˚C, for FR-EPR thermally aged with SHPVC jacket 83
Fig.3.13 Arrhenius plot of ageing times to 0.5 EAB_0 for FR-EPR insulators aged with and without jacket materials 86
Fig.3.14 Perception of design basis methodology for cable EQ 90
Fig.4.1 BWR-4 cut view for RPV, PCV, RHR/LPCS injection valves, and ADS SRVs from system I side 98
Fig.4.2 BWR-4 cut view for primary containment auxiliary systems 102
Fig.4.3 BWR-4 electrical components for design extension conditions 103
Fig. 4.4 Proactive approach for establishing knowledgeable-base guidelines from targeted cables regarding design extension conditions 106
Fig. 4.5 Perception for cable evaluations at design extension conditions 109
Fig. 4.6 General approach for modification of current EQ 111
Fig. 4.7 Temperature schemes of NPPs cables 113
Fig. 4.8 Basis for modifying withstand voltage in order to maintain extended DBA temperature profile 115
Fig. 4.9 Equivalent time for FR-EPR insulators at normal operation temperature of 50 °C extrapolated from accelerated ageing at 125 °C 117
Fig. 4.10 Proposed DBA-temperature profile at peak temperatures of 171°C and 190 °C for FR-EPR cables installed inside BWR containment vessel 119
Fig. 4.11 Rational of DBA-peak temperature extension from EAB retention 121
Fig. 4.12 EAB versus ageing temperature for FR-EPR insulators isochronally aged with SHPVC

jacket for 9 hours, after pre-ageing for 192 hours at 160 °C 123
Fig. 4.13 Proposed DBA-temperature profile at peak temperature of 230-250 °C for FR-EPR cables installed inside BWR containment vessel..... 123

Chapter 1 Introduction

1.1 Overview of nuclear power plants (NPPs) cables

Nuclear power plants (NPPs) play crucial role for supplying low-carbon, reliable and affordable electrical energy. As of May 2015, there are 437 operating and 68 under-construction NPPs located in more than 30 countries [1]. The recorded total world's nuclear share of electricity production was 11% in 2013, while it is expected to be the major contributor with 17% in 2050 [2]

The safe and reliable operation of NPP is directly connected with its structure, systems and components (SSCs). Among SSCs, cables are widely used to deliver electric power and signals for both safety-related and non-safety related systems including relays, motor operated valves, solenoid operated valves, pumps and sensors. Certain cables for safety related systems are required to remain functional during normal operation as well as design basis events (DBE) such as loss of coolant accident (LOCA). Figure 1.1 shows a schematic layout of cables in pressurized water reactor (PWR). Cables are usually placed in raceways; metallic conduits or cable trays that are not sealed from surrounding environment [3]. Depending on their installation locations and usage; cables are continuously vulnerable to variety of environmental stressors like high temperature, gamma radiation, humidity, chemicals and mechanical stresses. The level of temperature and gamma radiation is more significant inside reactor containment vessel (RCV) with average of 50 ^{o}C and 10^{-3} Gy/h, respectively [4,5].

Long-term exposure for environmental stressors may cause cable materials degradation; in particular insulator component which can lead to cable failure by different modes including short circuits between cable conductors, short circuit between any conductor with shield/ground, open circuit, and breakdown of cable insulator [6,7]. Under some accidental stressors, cable can fail in relatively short period. Depending to cable function, the failure may lead to transients and plant shutdown.

During Brown Ferry NPP accident, over 1600 instrument, power, and control circuits' cables were damaged by fire leading to hot short (i.e short circuit between energized conductors) [8,9,10]. Accidental consequences like hot short can cause specific systems to operate in unanticipated behavior and lead to spuriously initiate accidents like LOCA and station black out (SBO) thus challenging NPP response

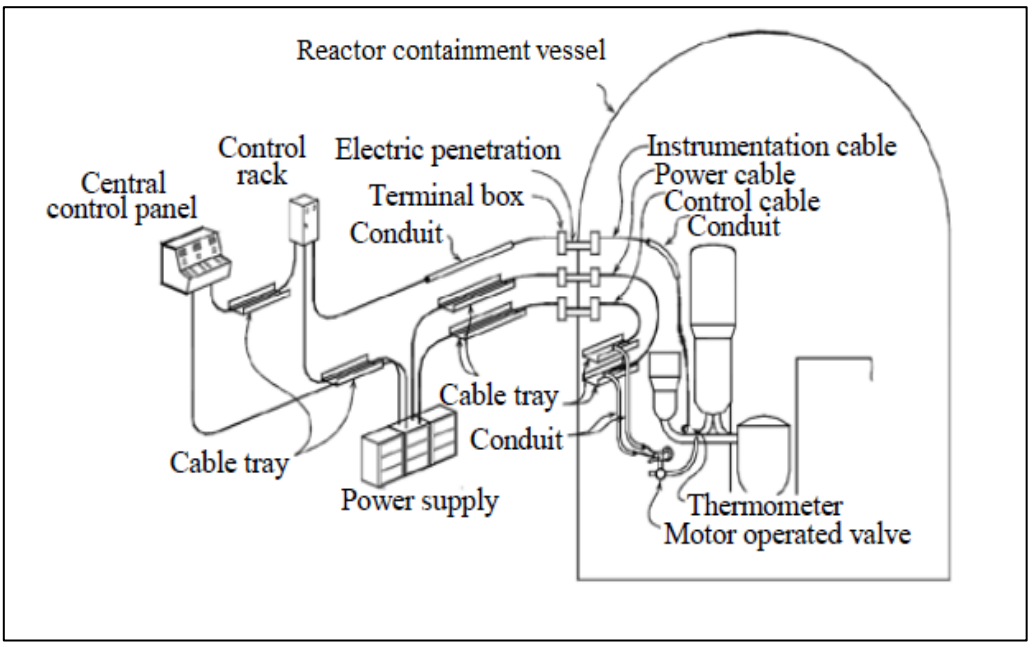

Fig.1.1 Schematic layout for cables in PWR [11,12]

A typical boiling water reactor (BWR) includes around 700 Km of cables with various categories, while the total number of cables inside PWR containment building can reach 1600 Km [3]. With such enormous length, wholesale replacement of cables to counter their possible ageing effects is neither prudent nor feasible. Accordingly, there is massive need for developing ageing management strategies to assure cables integrity during their design lifetimes and possible extended life within whole plant lifetime extensions.

1.2 Cables ageing management (AM) for long-term operation

Nuclear power plants experience two kinds of time dependent changes: (i) Physical ageing of SSCs, which results in degradation, i.e. gradual deterioration in their physical characteristics; (ii) Obsolescence of SSCs, i.e. their becoming out of date in comparison with current knowledge, standards and technology.[13].Cables are one of the components of utmost concern of ageing management that counter measure ageing degradation and obsolescence, especially in recent plants that will approach initial design life of 40 years and seeking license renewal for life extensions to 60-80 years operation.

Effective ageing management throughout the service life of NPPs cables requires the use of a systematic approach to managing ageing that provides a framework for coordinating all programs and activities relating to the understanding, control, monitoring, and mitigation of ageing effects of the plant cables. The elements of such approach can be coordinated within closed loop program as in figure 1.2[14], which is an adaptation of Deming's 'PLAN–DO–CHECK–ACT' cycle to the ageing management of an SSC [11,13,14]. The established ageing management program shall take into account the main nine generic attributes defined by IAEA safety guide NS-G-2.12 [13]. Among these elements, understanding cable ageing is the key element since it can mutually affect the items of adjacent elements. For example, understanding properties of cable polymeric materials and their degradation mechanisms is essential for updating environmental qualification sequences and regulation requirements. Besides, identification of hot spot locations will result in corrective actions in the form of mitigating these environments or relocating cable to milder environments, thus help avoid cable failures by expected design scenarios at original places. Ongoing development of cable inspections and monitoring methods is in need, especially when considering that cable evaluations by conventional visual/tactile methods during walkdowns activities become very difficult at some restricted elevated dose rates areas or at inaccessible cable portions inside conduits or trenches. Such testing shall be implemented periodically, even though cable

qualification can prejudge cable integrity before installation, and that is because cable qualification cannot itself guarantee reliable service for cable life especially during unexpected accident scenarios. On the other hand, the use of normally sacrificial aged samples at cable deposits near real operating cables is useful for research activities on cable degradation since it has similar ageing environmental stressors and does not require systems disconnections of real cables. Cables management against obsolescence requires specifically replacing specific cables materials based on the latest knowledge such as halogenated cables.

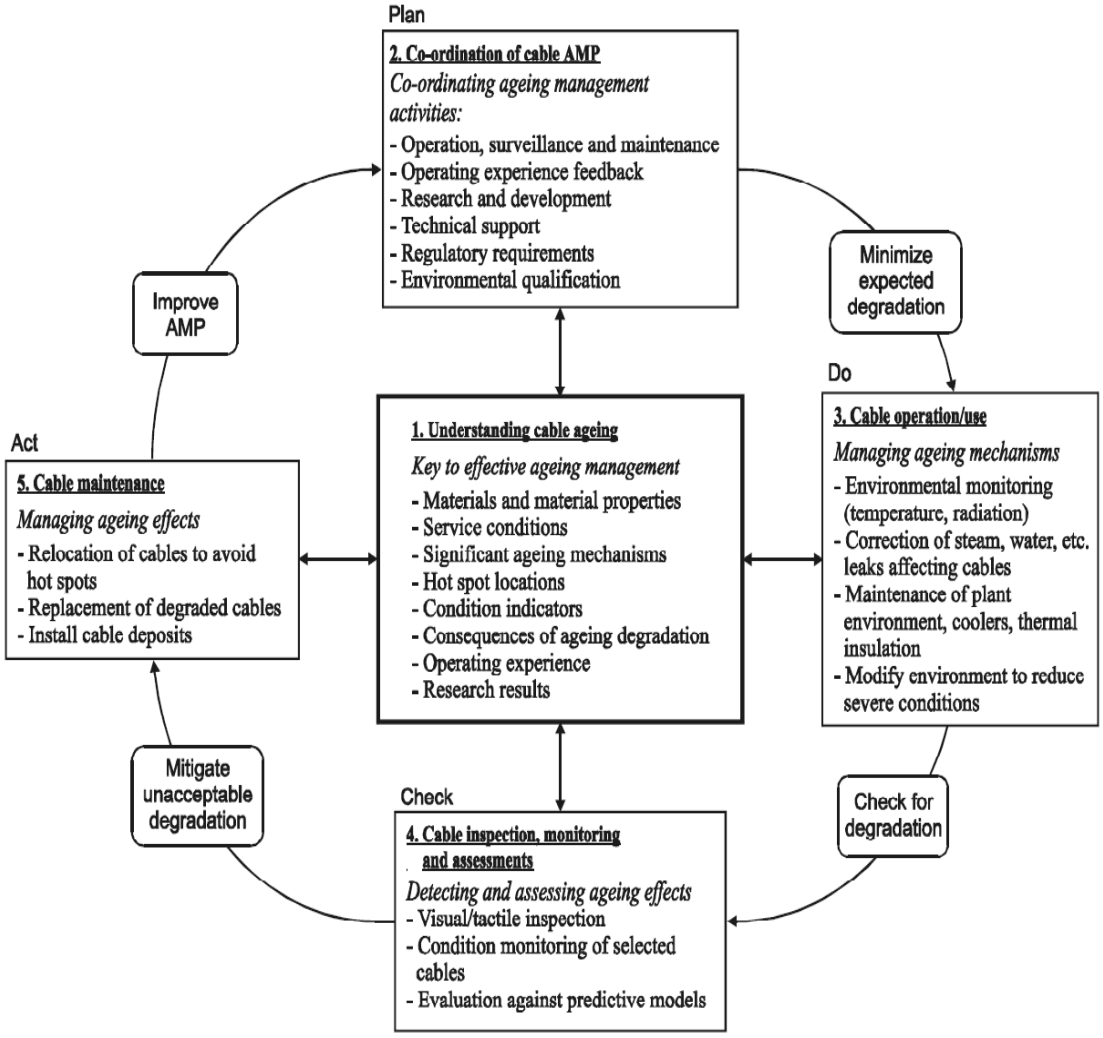

Fig.1.2 Key elements of instrumentation and control (I&C) cable ageing management program utilizing the systematic ageing management approach [14*]

1.3 Cables AM attributes

With increasing awareness of cables ageing importance for plant safety and long term operation, the intense of research activities regarding cable ageing management has recently increased. The recent knowledge of cable ageing degradation research has been well coordinated into useful guidelines that can help NPP personnel as well as non-nuclear plants with cables operation at elevated environments, in particular temperatures. This study surveyed various cables guidelines and addressed updated knowledge for cables ageing management in table 1.1[7,11,12,14,15,16,17,18,19]. Surveying these guidelines resulted in main sex attributes for efficient ageing management during normal operation and accident conditions as shown in figure 1.3.

Table 1.1 Cable ageing management guidelines

Guideline title	Organization	No.
- Assessment and management of ageing of major NPP components important to safety : In containment I&C cables	IAEA	TECDOC-1188
- Assessing and managing cable ageing in NPPs	IAEA	NP-T-3.6
- Approaches to ageing management for NPPs, international generic ageing lessons learned (IGALL) final report	IAEA	TECDOC-1736
- Review manual for technical assessment for ageing management : Insulation degradation of electric/instrumentation equipment	JNES	SS-0511-02
- Assessment of cable ageing for NPPs	JNES	SS-0903
- Technical basis for commendable practices on ageing management, SCC and cable ageing project (SCAP)	NEA	CSNI/R(2010)15
- IEEE standards for qualifying class 1E electric cables and filed splices for nuclear power generating stations	IEEE	383
- Essential elements of an electric cable condition monitoring program	U.S.NRC	NUREG/CR-7000
- Condition monitoring of cables, task 3 report: Condition monitoring techniques for electric cables	U.S.DOE	BNL-90735-2009-IR

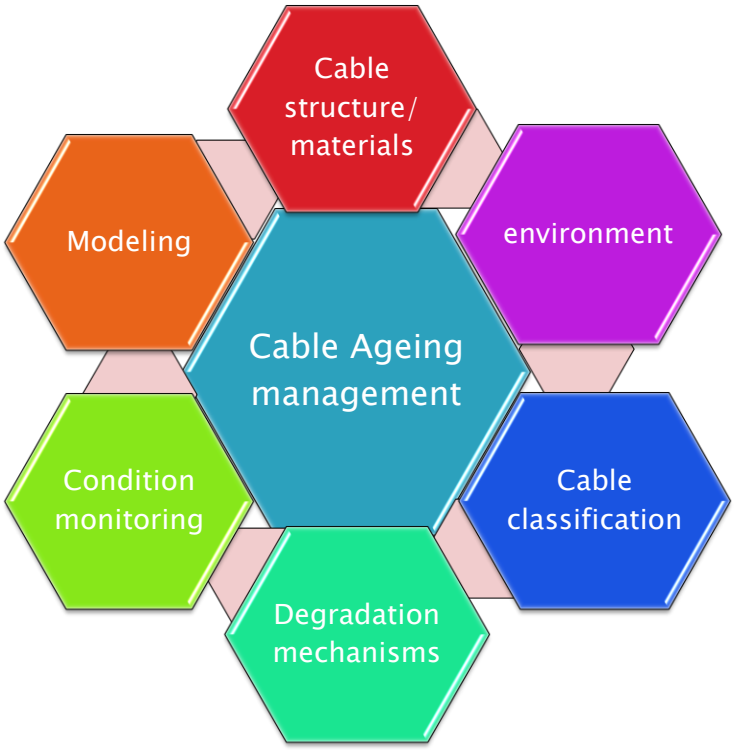

Fig.1.3 Cables ageing management attributes

The basic information about each attribute is summarized as below:

1.3.1 Cable structure and materials

Typical construction of cable includes conductor, insulator, filler, tape (or shield), and jacket as in figure 1.4. Conductor is generally made from solid or stranded annealed copper. Conductor copper is often coated with tin, lead, tin-lead alloy, nickel, or silver to minimize oxidation, enhance solder ability, and allow operation at higher conductor temperatures [3]. Insulator is the major sub-component that assures electric independence between the multiple conductors together or between conductors with ground. Jacket acts as first defense barrier to protect cable from the variety of surrounding stressors like mechanical pressing, moisture, chemical contaminants, and fire. Cable insulation and jacket are made from various polymeric-based compounds as summarized in table 1.2. EPR/EPDM and XLPE are the dominant insulator materials while CSPE is mostly used as jacket material [11,14,20]. Cables regulations require cease the usage of halogenated insulated cables inside containment, such as

PVC, due to concern over halogen emissions in the event of fire [3,11,14] .Many additives like antioxidants (for quenching free radicals during ageing), flame retardants (endow flame retardance property), pigments (provide insulator colors), fillers (to enhance roundness of multi conductor cables), plasticizers (to decrease glass transition temperature and endow flexibility), and cross-linkers (for polymers chains linking during curing) are also used within cable base polymers to enhance the polymer stability and workability during manufacturing process and as well as operation at elevated temperature and radiation levels. The amount and type of these additives varies as proprietary manufacturers and usually remain undisclosed. From whole cable structure, jacket and insulator materials will experience ongoing degradation since they are directly vulnerable to various levels of stressors (such as temperature) during normal operation and accident conditions.

Table 1.2 Polymer materials used in NPPs [14]

Material	**Insulation**	**Jacket**
Cross-linked polyethylene/polyolefin (XLPE/XLPO)	✓	
low and high molecular weight polyethylene (LMWPE, HMWPE)	✓	
ethylene propylene based elastomers (EPR, EPDM)	✓	
chlorosulphonated polyethylene (CSPE), also known as Hypalon		✓
ethylene vinyl acetate (EVA)	✓	✓
polyvinyl chloride (PVC)	✓	✓
silicone rubber (SiR)	✓	✓
polyether ether ketone (PEEK)	✓	
ethylene tetrafluoroethylene (ETFE), also known as Tefzel	✓	
polyphenylene oxide (PPO), also known as Noryl	✓	
butyl rubber (BR)	✓	✓
polyimide, also known as Kapton	✓	✓
polychloroprene, also known as Neoprene		✓

1.3.2 Environment/stressors

NPPs cables are continuously susceptible to various environmental and operational stressors depending on their location and function. The main stressors that cause insulator/jacket degradation include elevated temperatures, gamma-ray dose rate, humidity (moisture or submergence), mechanical stress (or manipulation), chemical contaminants, voltage stress, and self-ohmic heating (for medium voltage cables) [3,7].

In most areas within NPPs, the levels of environmental stressors are less severe than plant design environments which result in very slow degradation. However, some portions of cables are located in limited number of adverse localized environments (i.e. hot spots), thus degradation rate becomes faster. Cables ageing become important for the scope of management when the level of some stressors exceeds specific values, such as cables located in locations with temperatures higher than 40 °C[20,21]. Adverse localized environments can be identified through wide range of activities like reviewing environmental qualification (EQ) zone maps, feedbacks from plant technical staff and industry operating experience, and periodic inspections by infrared thermography[11,16]. Typical hot spot locations can be found in vicinity of main stream isolation valves and pipe tunnels, pressurizer compartments, electrical cabinets, and drywell neck region [3,14,16].In Japanese NPPs, temperature can elevate in hot spot areas to 85 °C and 80 °C for BWR and PWR, respectively while radiation dose rate values are usually much lower than 0.3 Gy/h [11].

1.3.3 Classification/category

Considering the huge number of cable systems that can cover around 17,000 circuits [20],only certain cables are required to remain operational during in-service period as well as during and following design basis accidents conditions. Cables are generally classified according to their function and safety. In light of their functions, cables are categorized into power cables, instrumentation and control (I&C) cables with structures as typically illustrated in figure 1.4. In side reactor building, power cables are either medium voltage (4.6KV/6.9 KVac) providing electric power to

electric equipment with high current capacity such as emergency core cooling pumps and feed water pump, or low voltage (<1KVac/dc) providing electric equipment with lower current capacity such as motor operated valves, solenoid operating valves, motor control centers, batteries, transformers, heaters, and oil pumps.

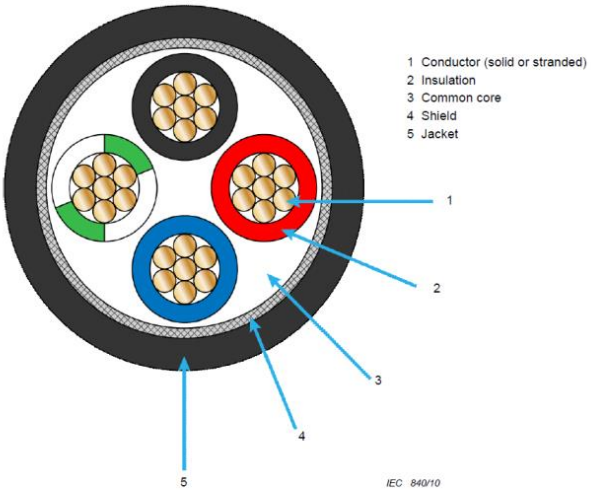

a) Power cable

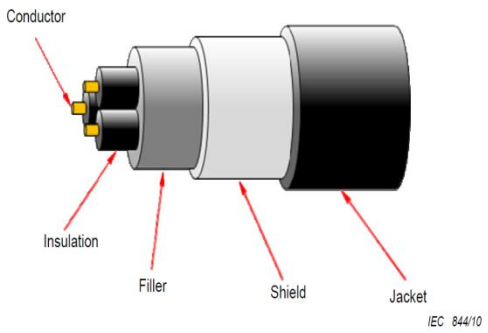

b) Multi-conductor shielded control cable

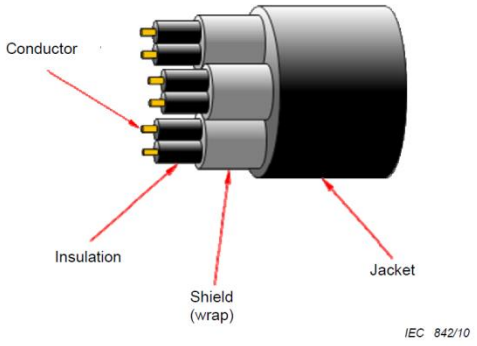

c) Twisted pair shielded instrumentation cable

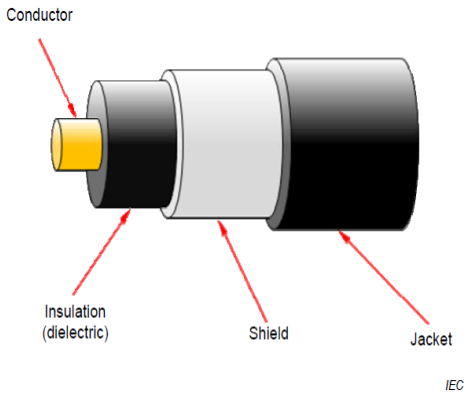

d) Co-axial instrumentation cable

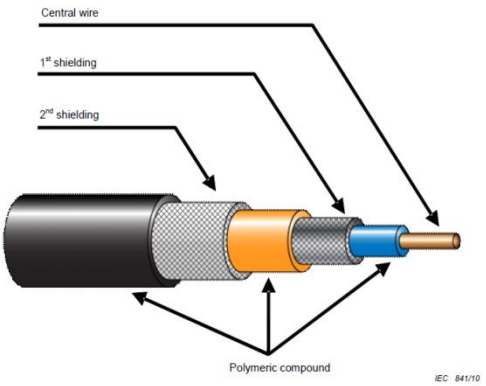

e) Tri-axial instrumentation cable

Fig.1.4 Schematic diagram for typical safety cables structure [22*]

Control cables are low voltage cables used to interconnect control circuits such as limit switches, control switches, relays and valve controllers. They can transmit feedback signals about the current state of component such as “valve closed” and “motor running” [3].Instrumentation cables are low voltage cable in the class of 24/48 V and transmit mili ampere or micro ampere current from various kinds of transducers [4]. Their configuration depends on the interconnecting devices. For example, twisted pair cables can be used with resistance temperature detectors, pressure transducers, and thermocouples extension wires. Coaxial, twin-axial and tri-axial cables are generally used for radiation detection. Some I&C cables are shielded to protect transmitted signals against electro-magnetic interference. The bulk majority of NPPs cables are low voltage power cables and I&C cables [14].

In light of safety importance, cables are primarily categorized into cables with operational significance (whose failure will cause plant trip or affect plant power production), and cables with nuclear safety significance that are required to prevent and mitigate design basis events and support emergency core coolant to prevent likelihood of core melting and containment breach. Most of safety cables are in standby mode and not exposed to accident environment, but since they are required to be functional during and following accident conditions, they are qualified at simulated accident environments prior to their installation through the so called environmental qualification process (EQ). The detailed classification for safety cables is variable between countries and guidelines as can be noticed in table 1.3.

Table 1.3 Safety classifications for NPPs cables and systems [11]

<table>
<tr><th>National or international standard</th><th colspan="4">Classification of the importance to safety</th></tr>
<tr><td rowspan="2">IAEA</td><td colspan="3">Systems important to safety</td><td rowspan="2">Systems not important to safety</td></tr>
<tr><td colspan="2">Safety</td><td>Safety related</td></tr>
<tr><td rowspan="2">IEC 61226</td><td colspan="3">Systems important to safety</td><td rowspan="2">Unclassified</td></tr>
<tr><td>Category A</td><td>Category B</td><td>Category C</td></tr>
<tr><td>France N4</td><td colspan="2">1E</td><td>2E</td><td>IFC/NC</td></tr>
<tr><td>European utility requirements</td><td>F1A (automatic)</td><td>F1B (automatic and manual)</td><td>F2</td><td>Unclassified</td></tr>
<tr><td>Japan</td><td>PS1/MS1**</td><td>PS2/MS2**</td><td>PS3/MS3**</td><td>Non-nuclear safety</td></tr>
<tr><td rowspan="2">USA</td><td rowspan="2">1E, safety related, or safety</td><td colspan="3">Non-safety related</td></tr>
<tr><td>Important to safety</td><td colspan="2">Balance of plant (BOP)</td></tr>
<tr><td rowspan="3">CANADA (CSA Std N209.14)</td><td colspan="3">Important to safety</td><td>Not important to safety</td></tr>
<tr><td colspan="3">Safety, safety related</td><td>Not safety, not safety related</td></tr>
<tr><td>Category 1</td><td>Category 2</td><td>Category 3</td><td>Category 4</td></tr>
</table>

1.3.4 Degradation mechanisms

Degradation mechanisms of cable insulator or jacket materials in NPPs are generally categorized into chemical mechanisms or physical mechanisms [14]. The chemical mechanisms include oxidation, chain scission of molecular chains, and cross-linking of adjacent molecular polymer chains. Chemical reactions affect the molecular structure of material that leads to degraded mechanical and electrical properties as will be explained in section 1.5. Physical degradation mechanisms will affect polymer macroscopic composition such as macroscopic density change, glass transition temperature value, discoloration change, and plasticizers evaporation/ immigration [14,23,24]

Under air environment, degradation of polymer is roughly attributed to oxidation which can be further accelerated at increased temperatures and ionizing radiation [11,14,15,24,25,26,27]. Several schemes have been introduced to understand evolved mechanisms by oxidative chain-scission and cross linking reactions under various accelerated temperature and radiation levels [4,5,14,24,25,28,29,30,31]. A conventional mechanism scheme is represented by the following chemical reactions [25]:

$$\text{Polymer (RH)} \longrightarrow \text{R}^{\cdot}\ \text{(polymer alkyl radical)} + \text{H}^{\cdot}\text{(proton)} \qquad 1.1$$

$$\text{R}^{\cdot} + \text{O}_2 \longrightarrow \text{R-O-O}^{\cdot}\ \text{(peroxy radical)} \qquad 1.2$$

$$\text{R-O-O}^{\cdot} + \text{RH} \longrightarrow \text{R-O-OH (hydroperoxide)} + \text{R}^{\cdot} \qquad 1.3$$

$$\text{R-O-OH} \longrightarrow \text{R-O}^{\cdot}\ \text{(poly-oxy radical)} + {}^{\cdot}\text{OH (hydro-oxy radical)} \qquad 1.4$$

$$\text{R-O}^{\cdot} \longrightarrow \text{chain scissions (carbonyl compounds, alcohol)} \qquad 1.5$$

$$\text{R-O-O}^{\cdot}\ (\text{R-O}^{\cdot}) + \text{AX (antioxidant)} \longrightarrow \text{R-O-OX (R-OX)} + \text{AY} \qquad 1.6$$

In first equation (1.1), polymer alkyl radical is initiated from the chain scission of polymer by temperature and radiation energy. The free radical will react with surrounding oxygen (1.2) and converts to peroxy radical which abstracts hydrogen from the neighbor polymer through chain scission reaction (1.3) to regenerate same alkyl radical of (1.1) and hydro peroxide. The hydro peroxide decomposes (1.4) into poly-oxy radical and hydro-oxy radical. Chain scission of poly-oxy radicals (1.5) produces carbonyl compounds (C=O) and some impurities like alcohol. Carbonyl

compounds are mutually converted by chain scission and cross linking reactions to several products that have different functional group but all indicate polymer degradation by oxidation [28,29,32]. The role of antioxidant is essential since it can quench the propagated free radicals (1.6) and thus terminate the oxidative degradation reactions. Literature review reports that minimum amount of antioxidant is sufficient to inhibit oxidation during accelerated ageing [24,25,33]. However, antioxidant content in polymer matrix decreases by evaporation during thermal ageing, with higher rates at higher temperatures, and with dose by irradiation decomposition [24,25].

In accelerating ageing tests, excessive temperatures and dose rates raise free radicals initiations rate leading to enhance oxygen consumption with much higher rates than its diffusion within polymer material. This phenomenon is known as "diffusion limited oxidation (DLO)", and lead to concentrated oxidative profiles in limited portion of polymer thickness (heterogeneous degradation) [14,27,34]. Effect of DLO has been modeled through estimating the sample thickness by which oxidation is homogeneous (i.e. DLO is insignificant) [35,36]. In addition, since real service conditions involve synergetic effects from various stressors, in particular temperature and radiation, predominant diagrams are developed to predict dominant ageing zones by single stressors and can help set up accelerated ageing conditions[14].

High humidity or submergence cause moisture intrusion, electrochemical reactions, micro void paths forming water treeing that evolve to carbonized paths by high voltage stress which in turn alters electrical properties as will be explained in section 1.5.

1.3.5 Condition monitoring (CM)

Condition monitoring (CM) inspections and tests can provide the means for evaluating the level of aging degradation of electric cables. Some of CM techniques can trend time-dependent degradation such as elongation at break (EAB), indenter modulus (IM), oxidation induction time (OIT), while other techniques can identify cable fault locations within cable length (or locating hot spot areas) such as time (frequency) domain reflectometry (TDR/FDR), and line impedance resonance

analysis (LIRA). Despite the variety of CM techniques, until now there is no universal single CM technique can assess the condition of in-service cable design varieties [3,37], thus in-service cables are evaluated by a combination of measurements that cover polymer chemical structure change and degraded mechanical and electrical properties. Ongoing research activities are still presenting new CMs for more reliable estimations from cable ageing degradation [38,39,40]. The most recent cable CM techniques are categorized in table 1.4 according to inspected property of insulator polymer. IAEA established a range of requirements for ideal CM considerations of in-service cables such as applicability to all polymer materials, ability for in-situ testing, not destructive nor intrusive, well correlated with real cable degradation, good indicator of structural integrity with electrical functionality, and cost effective [15]. Both NUREG/CR-7000 and BNL-90735-2009-IR guidelines provide detailed description of cable CM test and their features based on test type, property measured, applicable cable materials, intrusiveness, applicable stressors, detected ageing mechanisms, advantages, and limitations [7,19].

Table 1.4 Cable condition monitoring techniques

Mechanical measures	**Chemical measures**	**Electrical measures**
- Elongation at break (EAB)	- Fourier transform infrared (FTIR)	- Insulation resistance (IR)
- Indenter modulus (IM)	- Oxidation induction time/ temperature (OIT/OITP)	- Polarization index (PI)
- Microhardness profiling	- Differential scanning calorimetry (DSC)	- AC voltage withstand
- Indenter recovery time	- Thermogravimetric analysis (TGA)	- Partial discharge (PD)
- Dynamic mechanical analysis (DMA)	- Gel fraction	- Dielectric loss (tan δ)
	- Oxygen consumption rates	- Time/ frequency domain reflectometry (TDR/FDR)
	- Electron microprobe analysis (EMPA)	- Inductance capacitance resistance (LCR)
		- Line impedance resonance analysis (LIRA)
		- Age alert micro sensor

1.3.6 Modeling

Among the multiple purposes of cables accelerated ageing at higher temperature and dose rates is to predict their degradation behavior and extrapolate their design lifetimes at real NPP operating conditions. Accordingly, predictive models are utilized from trending time-dependent induced degradation of insulator properties. The basic model under thermal accelerated ageing is Arrhenius model that correlates degradation rate exponentially with temperature inverse and activation energy (E_a) [6,12,15,17,41,42]. Extrapolations by Arrhenius require similar E_a values between extrapolation temperature and ageing temperature. For semi-crystalline polymer materials (such as XLPE), If accelerated thermal ageing is performed at higher temperatures than crystalline melting points (such as 90-120°C for XLPE), physical transition reactions will occur leading to different degradation mechanisms and E_a values, thus Arrhenius is inapplicable. Nevertheless, extrapolations are still plausible by "same acceleration factor" model developed by JNES-SS-0903[12]. Once radiation dose is involved at accelerated ageing, other models are used to extrapolate accelerated ageing such as superposition of time dependent data, superposition of dose to equivalent damage, and power law extrapolation model [12,15]

1.4 Cables environmental qualification (EQ)

NPPs safety cables are tested before their installation through the so called environmental qualification (EQ) process. The objective of EQ is to provide reasonable assurance that the cable will operate or demand, under specified service conditions, to meet system performance requirements. The specified service conditions include both normal operating conditions and design basis events (DBE) conditions at the end of its expected service life. Cables can be qualified in several ways, like type testing, operating experience and analysis [15]. The preferred method of qualification is type testing, which is described in various standards, national requirements or recommendations [3,18]. In a type test, cable samples are exposed to test conditions in order to simulate degradation during the qualified life period and design-basis events. Based on acceptance criteria, it is verified whether the cable is capable of performing expected safety function at the time of a DBE, even after their in-service period.

Current EQ for Japanese NPPs cables are described as in figure 1.5 that is based on JNES-SS-0511-02 [17]. Testing activities through this EQ process are based on recommended practices of institute of electrical engineering in Japan (IEEJ) technical report division II, No.139 [43] that is an adaption of IEEE-323-1974 and IEEE-383-1974 [44,45]. Testing activities include sequential accelerating ageing by temperature followed by radiation that corresponding to 40-60 years normal operation at real plant conditions. Arrhenius model is used to set accelerated thermal ageing conditions. For example, test conditions of 121 °C × 168 hours simulate real operation conditions of 66°C×40 years. There are no specific values for acceleration factors during temperature and radiation accelerated ageing. Radiation dose rates can rise to 10 KGy/h and total dose can reach 2 MGy (including accident dose) [3,12]. But IAEA recommends using accelerated ageing temperatures below 120 °C and dose rates less than 100 Gy/h due to concerns over diffusion limited oxidation (DLO) effects [15]. Following accelerated ageing test, the cable is tested at design basis accident (DBA) conditions that envelop loss of coolant accident (LOCA). DBA steam profile includes

both elevated temperature and pressure conditions with values assigned by plant specific considerations. For Japanese boiling water reactor (BWR) cables installed inside containment vessel, the DBA temperature profile consists of a primary peak temperature of 171 °C for a 9 hours period followed by a secondary temperature of 121 °C for 13 days period [12]. Cable integrity is finally judged by submergence bending withstand voltage test. Cable is bended and attached to a mandrel with diameter larger than cable outer diameter by 40 times. The mandrel is merged in water for minimum period of one hour "soak period", followed by applying alternating current (AC) volt value of 3.2 KV/mm insulation thickness to tested cable for 5 minutes [17].

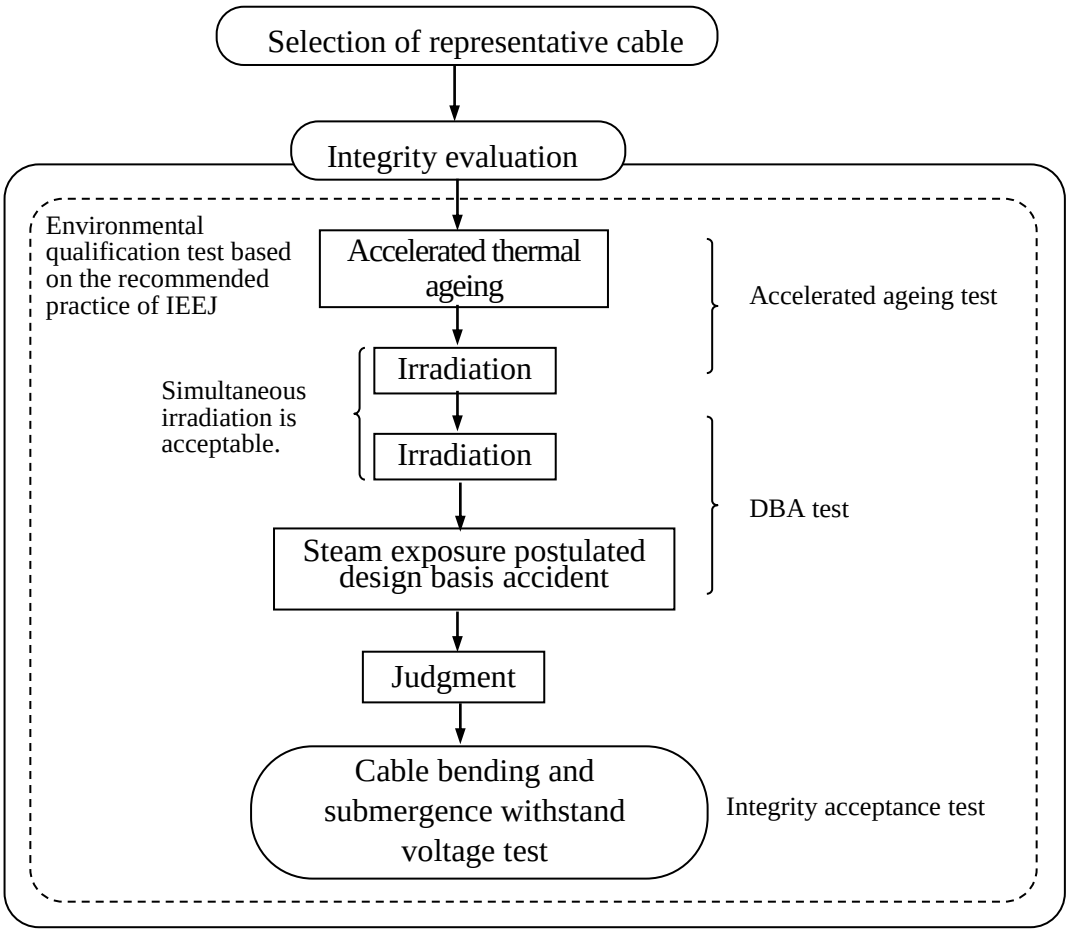

Fig.1.5 Type-testing cable environmental qualification method used in Japan

1.5 Current issues on AM activities and EQ process

The integrity of cable insulator materials is mainly determined from mechanical and electrical parameters [15]. Mechanical and electrical changes are the outcome of insulator structure damage of polymer by the variety of ageing stressors. A wide range of research activities for cable ageing management have been reviewed to understand current situation on insulator integrity evaluations from dominant ageing stressors [3,7,14,27,46,47,48,49,50] as summarized in figure 1.6. The short-term excessive mechanical stressors (such as cable bending, pressing and vibration) can lead to rapid cable cracking, wear and damage [7]. For remaining stressors (high temperature, radiation, moisture and volt stress), the long-term exposure can lead to change of chemical structure that is in turn may affect insulator by evolved cracking and increased leakage current [7,51]. The increased leakage current is better attributed by decreased insulation resistance measurements, in particular volume resistivity through insulation thickness [6,16]. Under the singular or combined exposure to high temperature and gamma-radiation, the dominant mechanisms are chain scission of polymer backbone and formation of free radicals with presence of oxygen [27].The free radicals will also lead to cross linking between polymer chains [23]. Chain-scission and cross linking reactions will alter molecular weight and cause loss of ductility of macromolecular chains and embrittlement which can lead to thermo-oxidative initiated cracking. Moisture/humid environment concurrent with voltage stress in medium voltage cables will lead to electrochemical reactions and form micro-cavities (water treeing), and by considering the effect of self-ohmic heating temperature and long-term voltage stress, carbonized micro-channels can form and water tree will grow larger to become electrical tree producing partial discharging, loss of dielectric strength, and increased leakage current (reduced resistivity) [7,17,52,53,54] .

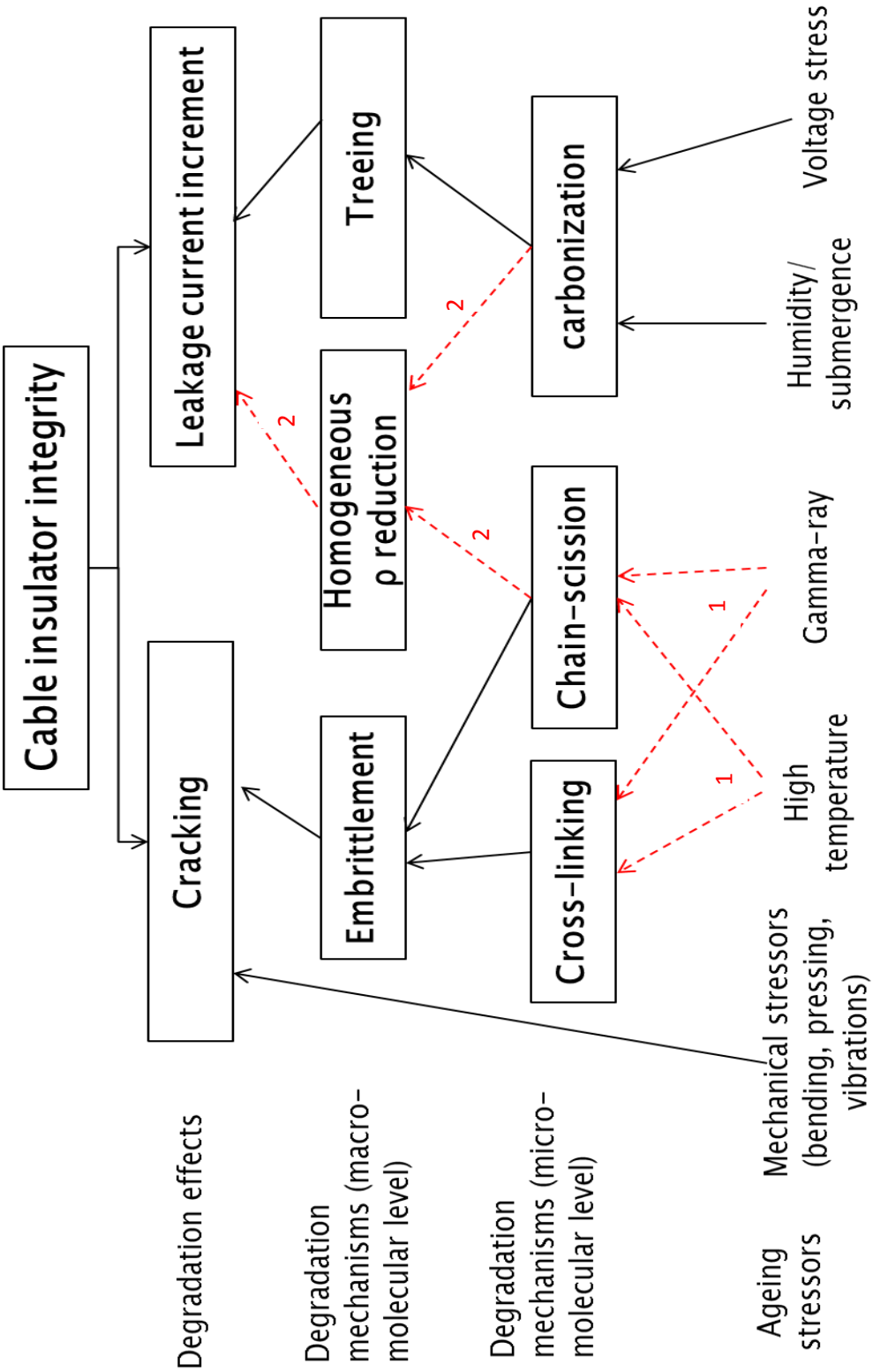

Fig.1.6 Illustrative flow-chart for previous research activities on insulator integrity evaluations

The main lack of aforementioned research activities are represented by the red-dashed arrows in figure 1.6 and categorized into two main findings:

1- Impact of environmental ageing stressors by temperature and radiations on chain-scission and cross linking reactions is still not systemically studied. There is massive need for reliable modeling from kinetic mechanism behavior of polymer microstructure that consider the complex set of these reactions rates and their dependence on variety of insulator backbone structure, additives, and insulation thickness profiling. The current investigated models are semi-empirical, while some degradation effects from non-Arrhenius behavior, oxygen concentration, anti-oxidants additives, and inverse temperature are still not addressed for modeling or under investigations [4,5,14]. Determinations of type-testing conditions during EQ process must be dependent on such developed degradation models for more precise predictions.

2- Trending time-dependent reduction of volume resistivity (ρ) is very difficult from the homogenous ageing by induced chain-scissions moieties and carbonized paths. Current evaluations of insulator integrity for IR or ρ is based on pass/fail testing. That is because of inaccuracies of conventional measurement methods by Mega ohmmeter that also include large uncertainties from surface restively over cable surface[6].

Since the outcome of cable AM research activity is reflected on EQ, the above mentioned consideration will affect EQ testing and conditioning, in particular for thermal ageing estimations considering that the temperature is the main ageing stressor for field-aged cables [26]. Besides, DBA phase of current EQ was reviewed and essential findings were addressed for the scope of this study. The main issues on EQ process from thermal ageing estimations and DBA phase are illustrated more thoroughly as below:

1.5.1 Thermal ageing estimations

Applicability of Arrhenius model is complicated by polymer morphological structure, dose rate effect, and synergetic effects. Thus thermal ageing test may misestimate real lifetime predictions. This can lead to unnecessary replacement of early aged cables or risky operation of over degraded cables. Issues for thermal ageing estimations are categorized as below:

1- **Cable structure**: Recent research activities for cable ageing focus on degrading cable insulator material [12,24,25,55,56,57],since cable integrity and functionality are mainly determined from trending insulator properties. In addition, it is assumed that the existence of jacket, binder-tape and other filler materials can lead to diffusion limited oxidation (DLO) causing less oxidative-degradation within insulator depth, thus cable components are disassembled in advance to assure higher level of thermo-oxidative degradation. On the other hand, during EQ process, cable insulator is degraded including the variety of cable insulator colors as well jacket material. In the comparative tests of JNES-SS-0903 project between cable-type ageing (ageing whole cable) and tubular-type ageing (ageing only insulator), degradation progress was considered similar between the two ageing methods from surface hardness profiling, X-ray microanalyses (XMA) profiling, and discoloration observations. Accordingly, it was decided to perform ageing after removing jacket and conductors to avoid firm adherence with insulator materials. Nevertheless, reviewed surface hardness measurements of SiR Insulators along their thickness showed more increment tendency with ageing time progression for cable type [12]. Besides, thickness profiling analysis by XMA is diagnostic qualitative condition monitoring, thus it is difficult to judge which ageing method was considerably significant. In addition, at same study, significant discoloration for SHPVC insulator aged with jacket was considered to be promoted by catalyst effect of copper conductor. Literature review reported that catalyst reactions by copper diffusion into insulator material increased macroscopic density at regions approaching insulator internal

side (near conductor) during thermal ageing [56,58]. Based on all above considerations, cable insulator are necessarily to be degraded within whole cable structure in order to clarify its real degradation with ageing method and for better extrapolations during accelerated thermal ageing phase of EQ process.

2- **Arrhenius model extrapolations from insulator properties parameters:** Current EQ utilizes Arrhenius model for establishing thermal ageing test conditions that is equivalent to real conditions operation. Estimations by Arrhenius model require previous determination of activation energy (E_a) from research activities. The values of E_a are assumed similar between accelerated thermal ageing temperature and extrapolated temperature near real plant operation conditions. However, literature review reports that Arrhenius model estimations from same E_a at accelerated ageing region and extrapolation region is complicated by physical transition reactions at crystalline melting temperature point for semi-crystalline polymeric insulators, and for inverse temperature effects [15,24,25,56]. Beside these morphological effects, insulator degradation by aforementioned cable structure effects can cause E_a differences from current knowledge that depend ageing of insulator material only. In addition, E_a estimations for EQ process is generally based on induced mechanisms from insulator mechanical properties degradations, in particular elongation at break (EAB) [12,56]. But chemical changes in insulator material cause also degradation of its electrical properties. Electrical parameters such as voltage withstand and IR (or ρ) are most vital parameters for insulator functionality [15] .In addition the final integrity judgment test is based on evaluations from insulator voltage breakdown. Nevertheless, E_a estimations from induced electrical properties degradation are still not addressed due to inaccuracies of trending thermal ageing degradation as mentioned before. This means that current thermal ageing estimations are limited to induced mechanisms from mechanical degradation of insulator material. Accordingly, current knowledge for thermal ageing estimations by Arrhenius model shall also consider the evaluation of the insulator degradation by mechanical as well as electrical properties.

1.5.2 Design basis accidents conditions

In all current type-testing EQ process, the worst environment to verify cable integrity include postulated accident scenarios at loss of coolant accident (LOCA) or high energy line break (HELB) [12,17]. These settings were established to suit with previous consideration of NPP safety design principle. In the previous design, LOCA was considered among the most vital DBA. This required utilizing engineered safety features and accident procedures of NPPs to settle down the postulated single initiating events at DBA without core melting thereby achieving level 3 of defense-in-depth (DiD) principle [59]. Based on these assumptions, Safety or safety-related components and their connecting cables were evaluated to withstand harmful conditions that have been previously induced as design basis.

However, the new principle of NPP design has been enhanced to countermeasure some elevated scenarios with multiple failures and sever accidents. This means that accident scenarios that was considered as beyond-DBA (BDBA) of existing NPPs are now originally induced in the design basis or considered as DBA for newly installed NPPs [59]. In other words, DiD-level 3 should include some accident scenarios that were previously considered with DiD-level 4. Such rational of DiD evolutions can be expressed by the so called design extension [59, 60]. Accordingly, NPPs shall initially be designed to include some scenarios of multiple failure and core melting accidents, or the so called design extension conditions (DECs).

To realize these facts, new accident environments for cable EQ may be higher than those previously established at LOCA. In the new condition-based qualification process, both fire testing and seismic vibration testing were addressed for cable evaluations according to country specific requirements[15]. But no evaluation approach was introduced considering accidents sequences initiated by these events. Besides, the endurance limit by which cable integrity rapidly fails have been previously estimated by “Cable Response to Live Fire (CAROLFIRE)” project[8,9,10]. In CAROLFIRE project, the average fire induced electrical failure (threshold temperature) was

estimated to 200-250 °C and 400-450 °C for thermoplastic and thermoset cables, respectively [8,9,10].

With all above in mind, there is massive necessity to modify cable EQ test at current DBA conditions through systemically utilizing cable integrity between severe accidents scenarios beyond LOCA environments and below threshold failure limits that can suit with some scenarios of DECs.

1.6 Objectives

This study aims at properly customizing accelerating test in order to understand the real degradation of cable during normal operation, in addition to modify environmental qualification (EQ) process to suit with recent progress of NPP safety design.

In order to achieve this objective, research activities for this study are arranged to:

1- Distinguish the impact of cable structure in light of additives variance and insulator environment change on cable insulator degradation considering both mechanical properties, in particular elongation at break (EAB) as well as electrical properties, in particular volume resistivity (ρ).

2- Utilize obtained knowledge from insulator electrical and mechanical properties degradation in order to assess accelerated ageing from view point of engineering evaluation methods and recent knowledge data base.

3- Finally, identify NPP cables that are important for design extension conditions (DECs) and propose modification of EQ process at DBA phase to suit with some elevated accident scenarios accompanying DECs.

Chapter 2 Experimental studies on cable structure impact by accelerated ageing

This chapter aims at investigating the effect of cable structure on insulator mechanical and electrical properties during accelerated thermal ageing. Flame-retardant ethylene propylene rubber (FR-EPR) insulated cables were thermally aged at different temperatures as described in sections 2.1 and 2.2. Both mechanical properties (elongation at break) and electrical properties (volume resistivity) evaluation procedures are explained in section 2.3. The results of accelerated thermal ageing are shown in section 2.4. Some aged samples were analyzed by Fourier transform infrared spectroscopy to understand embedded degradation mechanisms. The degradation effects were more significant when ageing was performed with jacket material while colorant pigments are still unclear.

2.1 Specimens

For the purpose of this study, the nuclear grade-cable specimens were selected based on their function, and the portion of their insulator material usage inside current operating NPPs. The cable was bought from Japanese manufacturer and designated as PSHV. Figure 2.1 shows an illustrative view of tested cable. The specimens are characterized by following aspects:

1- **Category:** Nuclear grade 12 American wire gauge (AWG) cables were used as specimens of this study. Cable kind is FR-PSHV based on Japanese standards. Cable characteristic are shown in Table 2.1. Safety-related, 1E, three-phase (3-ϕ), low voltage (LV) control/power (<600 V), 12 American wire gauge (AWG) cable was used in this study. Maximum current ratings for power transmission is 9.3 A.[61] The voltage category is similar to electrical equipment with nominal rated voltage of 3-ϕ, 480 V such as low

pressure coolant injection (LPCI) and low pressure core spray (LPCS) motor operated valves (MOVs).

Table 2.1 Cable specimens' characteristics

Item	Details
Name [Japanese standards]	FR-PSHV
Safety classification	Safety-related , 1E
Power/voltage rate	Low voltage power /control (600V)
Core no.	3-phase (3-ϕ) (white, red and black)
Core size	12 American wire gauge (AWG)
	(3.5 mm^2, Φ :2.1 mm)
Max. current capacity	9.3 A
conductor type	Copper
No. of wires per core	7 stranded wires
Insulator type	Flame retardant ethylene propylene rubber (FR-EPR)
Insulator thickness	1 mm
Jacket type	Special heat resistant poly vinyl chloride (SHPVC)
Jacket thickness	2 mm
Cable overall diameter	12 mm

2- **Insulator material:** Flame-retardant ethylene propylene rubber (FR-EPR) are selected as insulator, since EPR based polymers are the dominant insulating material used in current operating NPPs covering about 45 % of control/power cables and 75% of instrumentation cables [11,20,42]. Usually, EPR term can be characterized by either copolymer structure named ethylene propylene monomer (EPM) or by terpolymer structure named ethylene propylene diene monomer (EPDM). EPM includes saturated ethylene and propylene monomers as base polymer material, hence it is only vulcanized (cross-linked) from peroxide systems, while EPDM and due to existence of the third diene monomer thereby causing unsaturation of molecules, thus can be vulcanized by both sulfur and peroxide curing systems [62].

Ethylene-propylene ratio is ranging from 45%-75% with crystallinity evolution by higher ethylene ratios [56]. The cable specimens have three colored insulators; white, red and black. The thickness of each insulator is 1mm.

3- **Jacket material:** Jacket material is special heat-resistance polyvinyl chloride (SHPVC). SHPVC is an improved type of PVC with heat resistant plasticizers (that endure up to 80 ^{o}C) and polyvinyl chloride resins with high degree of polymerization that make it preferred for use in specifically high temperatures hot-spot locations [56]. The jacket thickness is 2 mm.

4- **Conductor:** Stranded copper (7 wires) with a total diameter of 2.1 mm was embedded inside each of the three insulators.

Further information about material formulation such as plasterer type, anti-oxidant additives and fillers are unknown for this study since they are manufacturer proprietary.

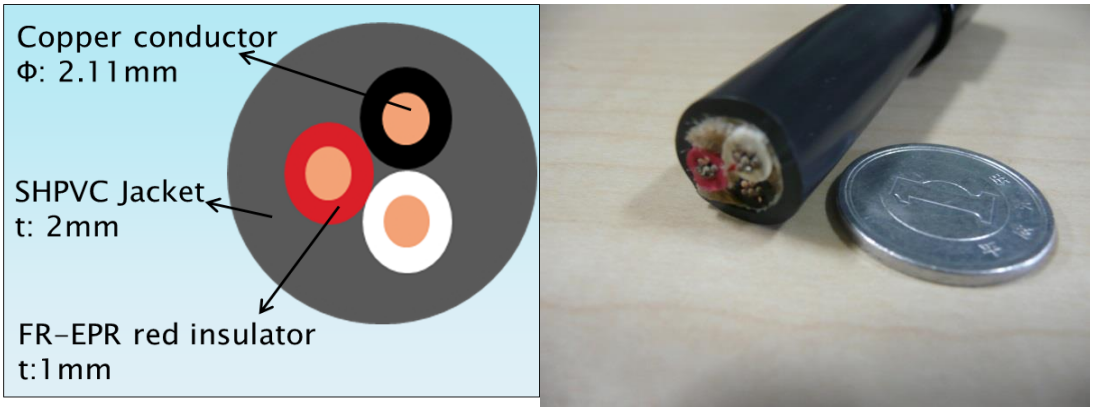

Fig.2.1 Overview and cross sectional geometry of FR-EPR insulated cable

2.2 Ageing conditions

The characteristics of ageing conditions were mainly determined by both test environment and ageing method (insulator environment):

1- **Temperature:** Accelerated thermal ageing was considered for the scope of this study since temperature is the utmost important stressor that jeopardizes cable integrity. During normal operation conditions temperature can typically increase to 50 ^{o}C while radiation dose rate is generally less than 0.05 Gy/h at hot-spot areas [56]. For homogeneous (uniform) degradation and at higher temperatures, the induced thermal degradation mechanisms are predominant compared to radiation mechanisms even at higher dose rates [14].During design basis accident conditions, temperature-peak values can increase to 171 ^{o}C and 190 ^{o}C in the case of Japanese's BWRs and PWRs respectively [12]. Temperature levels can further increase and exceed threshold failure values of 200-250 ^{o}C (for thermoplastic cables) and 400-450 ^{o}C (thermoset cables), in case of fire or elevated accident scenarios [8,9,63,64]. In this study, three ageing temperature set points and periods were considered as the following:

- 125 ^{o}C heating up to 210 days (5020 hours).
- 150 ^{o}C heating up to 14 days (336 hours).
- 160 ^{o}C heating up to 11 days (264 hours).

Expected degradation mechanisms include chain-scission, cross-linking, additives (such as anti-oxidant) evaporation [25,27] while diffusion limited oxidation (DLO) will increase with increasing ageing temperature [34]. For SHPVC jacket material quick elimination of chlorine (Cl) is certain. [14,49]

Heating was performed inside air-circulated fan ovens. Temperature was measured with 4 K-type thermocouples connected to KEYENCE NR-1000 data acquisition system. Measured temperature was deviated between ± (1-4) ^{o}C.

2- **Cable treatment inside oven:** The focus of degradation during this study was mainly on insulation material within whole cable structure since insulation is degraded while surrounded by other cable components (jacket,

filler, binder, and shield) at normal operation conditions and during environmental qualification process. Accordingly, FR-EPR insulator samples were aged including SHPVC jacket material, or the so called cable-type samples. On the other hand, in order to assess the effect of insulator environment on insulator properties degradation, some FR-EPR insulators were aged after stripping out SHPVC jacket material, hence insulator will be surrounded by air and the effect of DLO is less significant compared to cable-type ageing. FR-EPR insulators samples which aged without jacket are also called tubular-type samples. Figure 2.2 shows both cable-type and tubular-type samples which were vertically mounted by metallic hangers inside test oven. During thermal ageing, the samples were spun up-side-down periodically to ensure uniform thermal distribution through whole sample surface.

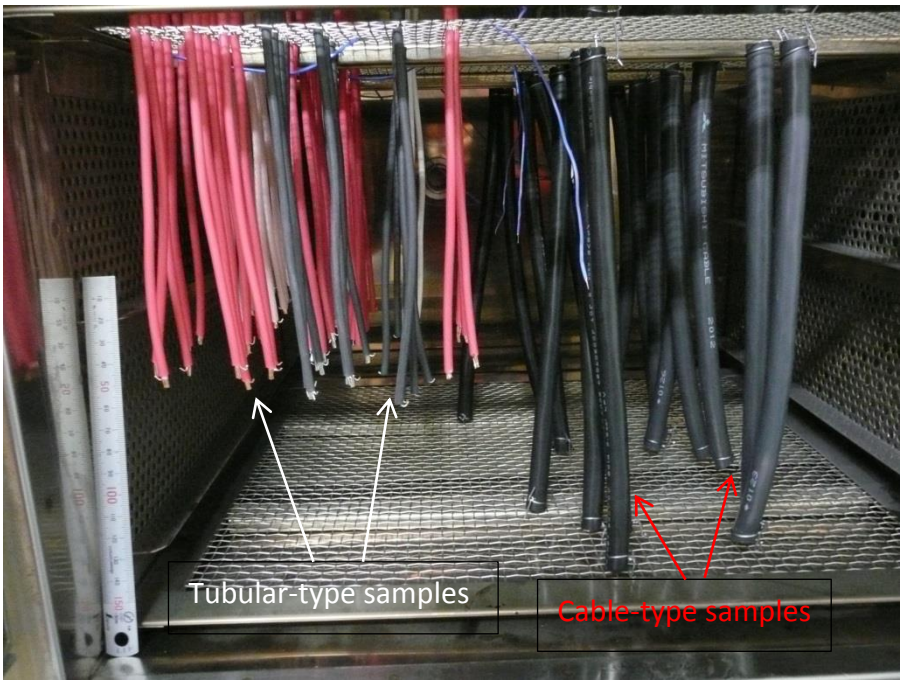

Fig.2.2 Cable-type and tubular-type samples inside oven

Arrangement of ageing method with ageing temperature and ageing time are shown in table 2.2. Aged samples were picked out periodically from thermal oven. For cable-type aged samples, the SHPVC jacket, binder tape and filler were removed. Samples were prepared only from the FR-EPR insulator for further evaluations of

both mechanical and electrical properties. Samples were conditioned at laboratory temperature (20±2) ^{o}C before measurement.

Table 2.2 Arrangement of ageing temperature, time, and method

Ageing method	**Ageing temperature (^{o}C)**	**Ageing time (hours)**
Cable-type (Insulator with jacket)	125	5020
	150	336
	160	264
Tubular-type (Only insulator)		
	125	5020
	160	264

2.3 Experimental setup

2.3.1 Tensile testing for elongation at break (EAB) measurement

Mechanical properties are key measure for the chemical change by chain scission and cross linking reactions during thermal ageing which results in change of molecular structure. Tensile testing is generally used to evaluate the level of mechanical integrity in aged samples by stretching samples until their break; thus obtaining stress-strain curve as can be seen in figure 2.3. In stress-strain curve, stress is measure for insulator strength at break (tensile strength) while strain is measure for insulator ductility (or elongation at break point (EAB)). The ultimate EAB is mathematically described by equation 2.1, while Ts is described by equation 2.2:

$$EAB(\%) = \frac{L_1 - L_0}{L_1} \times 100 = \varepsilon \times 100 \qquad 2.1$$

$$Ts\ (MPa) = \sigma = \frac{F}{A} \qquad 2.2$$

Where L_0 is initial sample length before testing (gauge length) [mm], L_1 is sample length at break point [mm], ε is strain, F is applied load at break [N] and A is the cross-sectional area of tested sample [mm^2].

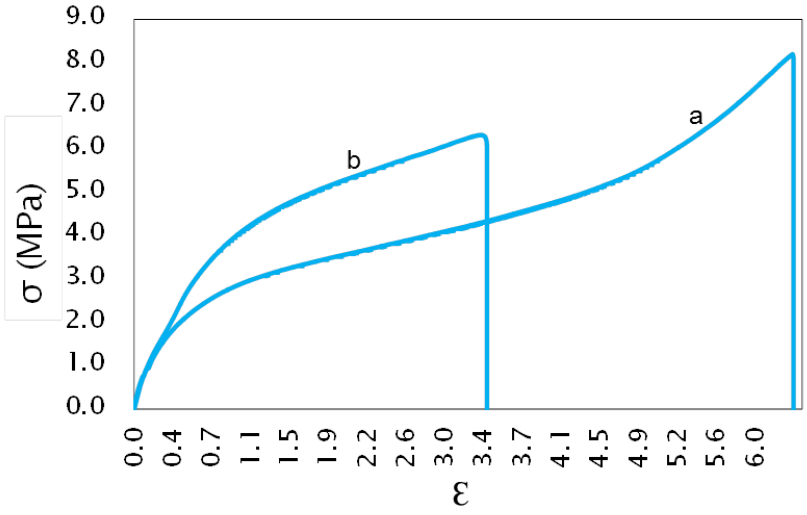

Fig.2.3 Typical stress-strain (σ-ε) curve for EPR-based elastomers before ageing (a) and after thermal ageing (b)

Literature review reports that EAB is better indicator than tensile strength (Ts) because the strength value can increase and then decrease with ageing while EAB directly decrease with ageing time [6,23]. The reason that Ts increases and then decreases is due to Ts reliance on cross linking density and effective network chains. Ts will primarily increase with increased cross linking density and then decrease with further increase of cross linking density. When the cross linking density reaches very high levels, the molar mass of chain between two successive crosslink points decrease and hence the chain mobility is restricted and the network chain orientation is limited which in turn will reduce the number of effective network chains and hence the decrement of Ts.[32]. For EAB, it has been considered as main parameter for cable structural integrity during ageing management. A value of 50 % normalized EAB is considered as indicator end-of life time for ageing [15,40] while 50% absolute EAB limit insures adequacy against mechanical stress during DBEs such as LOCA [6,14,15]. However, EAB evaluation through tensile testing has some disadvantages, in particular for being destructive, intrusive and requiring plant outage during cable removal and replacement. Thus, it is recommended to use sacrificial cables inside samples deposits at real plant conditions [11,14,15] and also to correlate with other non-destructive CM techniques such as oxidation induction time/ temperature[14] and indenter modulus [12,65].

Based on above, EAB is considered in this study to evaluate the mechanical integrity. Samples for tensile testing were prepared according to IEC 62582-3:2012 International Standard [66*]. Due to relatively small diameter of cable insulator, tubular type tensile specimens (Fig.2.4) were made from aged FR-EPR insulator only after stripping out SHPVC jacket and extracting stranded wires of conductor copper. During sample preparation, special care was considered for removing conductor wires due to their stacking with insulator inner surface as results of thermal ageing, which can add more degradation to insulation if not well removed. More details of this procedure can be referred from IEC 62582-3:2012 Annex B [66].

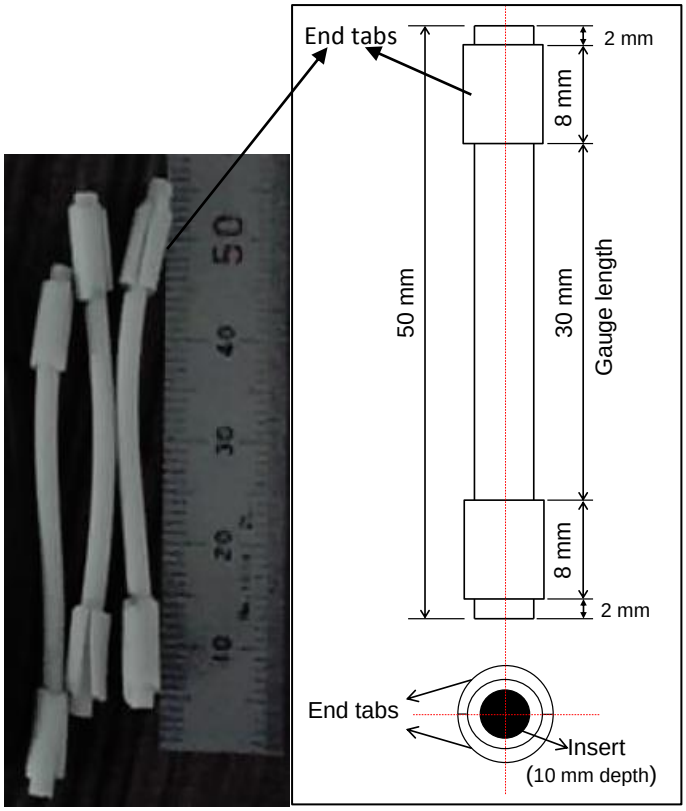

Fig.2.4 Tubular shape tensile test samples and dimensions

The main parameters of tensile testing experiment are shown below:

- Sample type: Tubular- type
- Tube cross-section area: 9.6 mm^2
- Sample length: 50 mm
- Gauge length (L_0): 30 mm
- End tabs: 8 mm
- Inserts: 10 mm
- Testing machine/Clamping: SHIMADZU AUTOGRAPH AG-X /mechanical grips
- Strain rate (testing speed): 50 mm/min.

Samples were stored for at least 24 hours at laboratory conditions (20±2) ^oC before tensile testing as recommended by IEC 62582-3:2012 [66]. Both inserts and end tabs were made from same aged samples with same Young modulus (σ/ε) in order to avoid excessive stress in specimens at clamping positions and to emulate the use of

dumbbell type samples where stress is concentrated in the longitudinal axis during testing [66].

2.3.2 Developed CM technique for electrical volume resistivity (ρ) measurement

Electrical properties are most vital parameters for cable insulation functionality such as insulation resistance (IR), dielectric strength and voltage breakdown [15] Nevertheless, IR is only used as a pass fail/test during normal operation, as well as during accelerated thermal/radiation ageing and DBE conditions of EQ test [15,46,50]. Voltage breakdown and dielectric strength are also evaluated as a pass/ fail judgment during withstand voltage integrity test of EQ process [15,17]. Very recent studies showed that dielectric strength parameters, in particular real and imaginary parts permittivity (ε) can trend induced degradation from both temperature and simultaneous temperature/gamma-ray ageing in wide range of frequency bandwidth [3,17,27].

For IR measurements, the main parameter of interest is volume resistivity (ρ) that is corresponding to leakage current content through insulation thickness. The higher leakage current reduces volume resistivity, thus more degraded insulation. IR is responsive to long-term moisture-related degradation with high temperatures which leads to moisture-diffusion, softening, swelling and increase of water content inside insulator [46,47]. Besides, during moisture/submergence-related ageing, the influence of temperature on IR degradation is more substantial compared to humidity influence, and that is due to the induced insulation embrittlement and cracking which increase water intrusion [46,67]. In contrast, trending and monitoring the time-dependent behavior of thermal degradation for IR is difficult [46], even though oxidation chain-scission moieties (charged particles) can alter volume resistivity [46,68]. That is due to uncertainties of current IR measurement by Mega ohmmeter (Megger) system that contains (beside volume resistivity (ρ)) leakage current over cable surface (i.e surface resistivity) [6] in addition to other impacts like cable length, humidity, and surface contaminations [7]. Accordingly, a main driving force for this study is to

precisely detect ρ behavior along thermal ageing through improved electrical condition monitoring (CM) technique.

ρ measurement by the developed CM is characterized by three aspects: (Tubular electrode, electric configuration, and measurement time setup for aged samples).

1- **Tubular electrode:** Specific electrodes having same tubular shape of three aged insulators (white, red and black) at each ageing temperature were designed as in figure 2.5. Sample surface was wiped by ethanol after removing jacket material. Insulator conductive wires were maintained inside aged samples since it was found that ρ detection was only plausible by keeping same copper wires rather than replacing these wires with copper tube-inserts. That can be explained by the non-uniform cross sectional area of insulator inner surface that has small arcaded voids, thus when replacing the original wires with uniform cylindrical-shape conductive tube, there will be some air clearance between inserted tube and insulator inner surface and that complicates leakage current passage and IR (or ρ) detection. In contrast, thermal ageing lead to stacking of insulator conductive wires with its inner surface and this enhance contact to facilitate leakage current passage. Both guarded and guarded electrodes were made from copper foil with conductive adhesive tape on one side. Electrode thickness is 39 μm and resistance is 0.02 Ω/cm^2. The electrodes were made by gently pasting the copper foil on insulator outer surface from adhesive side. The guarded electrode (L) counts for facilitating the leakage current from insulator conductor to insulator surface through its thickness to detect IR and ρ. Guard electrode is used to remove surface leakage current and reduce the errors from stray current and current lines fringing [69]. The width of gap between guarded and guard electrodes affect length of fringing from current lines at both guarded electrode length. The dimensions of tubular system are shown in figure 2.5. The value of resistive leakage current through cable thickness is corresponding to the insulation resistance (R_x) of the whole cylindrical volume surrended by electrodes and insulator conductor. The basic correlation between R_x and ρ for homogeneous cylindrical cable insulation is expressed by equation 2.3:

$$\boldsymbol{Rx} = \int_{r1}^{r2} \frac{\rho}{2\pi Leff.} \frac{dr}{r} \qquad 2.3$$

Where R_x is insulation resistance [Ω], ρ is insulation volume resistivity [Ωm], r is radius of equipotential surface within insulator thickness. r_1 [m] and r_2 [m]are the radii of inner and outer insulator surfaces respectively (i.e radii of copper conductor and insulator outer surface). $L_{eff.}$ [m] is the actual effective length of guarded electrode (L) and the extended length by current lines fringing at both electrode edges (2(g/2-δ)) [70], i.e:

$$\boldsymbol{L_{eff.}} = L + (g\text{-}\delta/2) \qquad 2.4$$

Where δ is dimensionless constant determined by equation 2.5[70]:

$$\boldsymbol{\delta} = t(2/\pi) ln cosh[(\pi/4)(g/t)] \qquad 2.5$$

Where *t* is insulation thickness [m], and g is the gap width [m] between guarded electrode and guard electrode [m]. After performing integration of equation 2.3 and substituting the variables of equations 2.4 and 2.5, the volume resistivity (ρ) can be expressed as in equation 2.6:

$$\boldsymbol{\rho} = \frac{2\pi\big(L + (\mathrm{g} - \delta/2)\big)Rx}{\ln(\frac{d_2}{d_1})} \qquad 2.6$$

Where d_1 is diameter of copper conductor d_2 is diameter of insulator outer surface. From equation 2.6 it can be noticed that ρ relies on tubular electrode-dimensions, in particular guarded electrode length (L), insulator diameters (d_1, d_2) and also gap width to thickness ratio (g/t) from equation 2.5. In our study, g/t ratio is designed in between 1.5-2 (Fig. 2.5), thus effective length ($L_{eff.}$) becomes:

$$\boldsymbol{L_{eff.}} = L + 0.5\mathrm{g} \qquad 2.7$$

Accordingly, ρ can be expressed as in equation 2.8:

$$\boldsymbol{\rho} = \frac{2\pi(L + 0.5\mathrm{g})Rx}{\ln(\frac{d_2}{d_1})} \qquad 2.8$$

By substituting the numerical values of L, g, d_2 and d_1 (Fig 2.5), the value of ρ [Ωm] can be directly correlated from measured R_x [Ω] as in equation 2.9:

$$\boldsymbol{\rho} = 0.49R_x \qquad 2.9$$

The value of Rx was electrically detected by connecting the tubular electrode by two configurations, direct measurement and Wheatstone bridge.

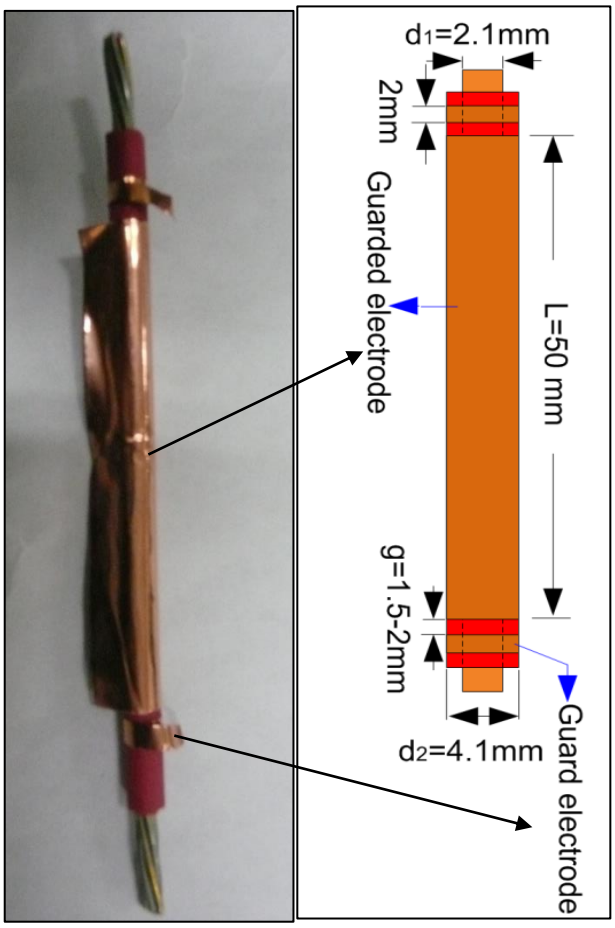

a) Top view

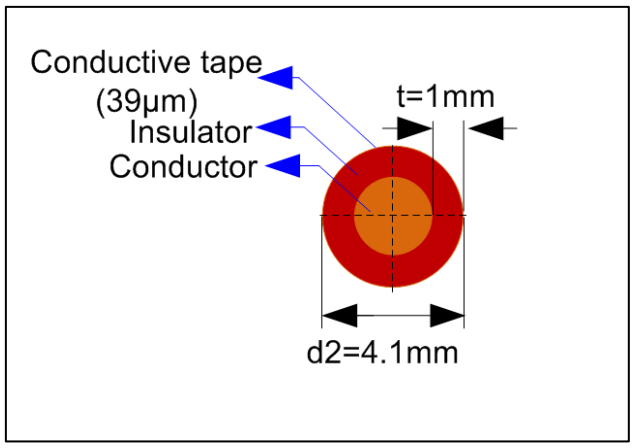

b) Cross sectional view

Fig.2.5 Electrode system for IR and ρ detection

2- **Electric circuit configurations:** In order to obtain Rx value, the tubular electrode in figure 2.5 was electrically connected by either Wheatstone bridge configuration or direct measurement configuration as can be seen in figure 2.6. In the direct configuration, the value of (R_x) can be directly calculated based on Ohm's law:

$$\boldsymbol{R_x} = V_{dc}/I_x \qquad 2.10$$

Where V_{dc} is the applied direct-current voltage [V], while I_x is the resistive leakage current passing through tubular electrode [A]. 500 Vdc was used as a voltage source [70]. TOA PM-18 U analog Pico-ammeter was used to detect leakage current with range of (3 pA - 100 μA) and resolution of 0.1 μA. For the Wheatstone bridge configuration, the tubular electrode was connected with three bridge arms; two have fixed resistance values (R_B, R_N) while the other arm is potentiometer (R_A) with variable resistance (0-999 K Ω) for balancing the bridge (zeroing the Pico ammeter). At balance conditions, the value of Rx is calculated by equation 2.11:

$$\boldsymbol{R_x} = R_B\, R_N / R_A \qquad 2.11$$

The values of bridge arms are shown in table 2.3. When the detected Rx values were lower than 0.5 TΩ, the bridge arm resistor R_B was replaced by

another resistor with smaller resistance value due to the limitation of potentiometer (R_A) readings above (1MΩ).

The value of R_x for both configurations was recorded after 60 seconds from circuit electrification [70]. The reason for this procedure is to ensure vanishing of capacitive charging current and dielectric absorption current [3,42], while the remaining current is the resistive leakage current corresponding to induced chain-scission ions from insulator thermal degradation.

In order to interpose and shunt away stray currents from R_x measuring circuits, a guard-system has been made from guard electrodes rings and one of Pico-ammeter terminals constituting a three-terminal network [70,71]. For Wheatstone bridge configuration, the guard system was connected with the two lower-valued resistance arms (R_B and R_A), while for direct measurement circuit, the guard-system was connected with ground junction of voltage source.

R_x measurement by Wheatstone bridge is considered more accurate than direct measurement. That is because balancing Wheatstone bridge arms resistors will minimize the error from internal resistance of both voltage power source and Pico-ammeter in addition to connecting wiring resistance and bridge arms resistance tolerance at balancing conditions. The variation of measured R_x between Wheatstone bridge and direct measurement was less than 5% for most cases. Based on above, the results of resistivity shown in the following parts of this study are taken from Wheatstone bridge configuration. Detailed values of Wheatstone bridge arms resistances and values of R_x from direct measurement are shown in Annex 1 for some aged FR-EPR samples at randomly selected conditions.

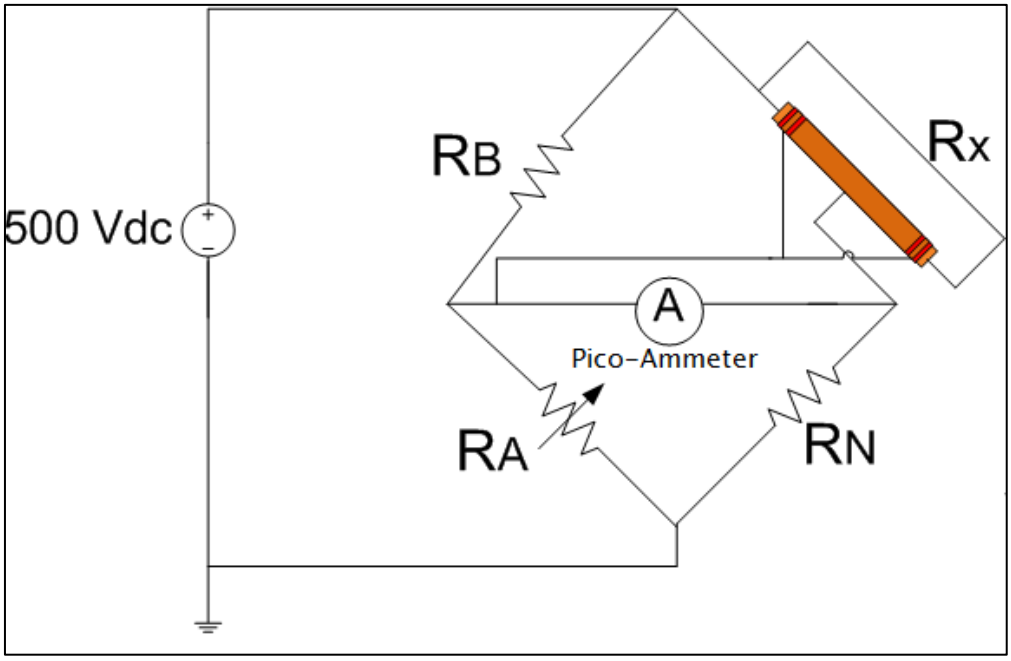

a) Wheatstone bridge circuit diagram [40]

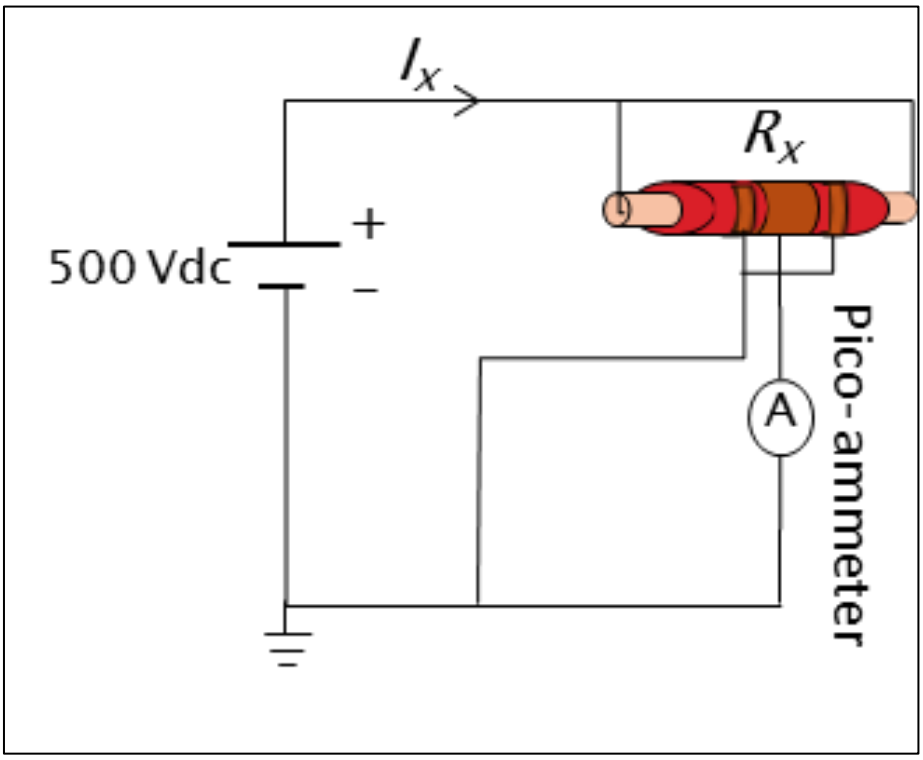

b) Direct measurement circuit diagram

Fig.2.6 Electric circuit configuration for IR and ρ measurement

Table 2.3 bridge arms resistance values for Wheatstone bridge circuit configuration

Bridge Arm	**Resistance (Ω)**	
	$Rx> 5\times10^{11}$	$Rx< 5\times10^{11}$
R_B (fixed resistor)	500×10^{6}	1×10^{6}
R_N (fixed resistor)	1×10^{9}	1×10^{9}
R_A (potentiometer)	$0\text{-}999 \times 10^{3}$	$0\text{-}999 \times 10^{3}$

3- **ρ measurement time setup for aged samples:** the measurement times for mechanical properties has been well established considering recovery/decay behavior after accelerated ageing. For EAB evaluations, tubular-shapes specimens are recommend to be tensile tested after 24 hours from oven sampling as previously mentioned in section.2.3.1. For indenter modulus (IM) evaluations, decay behavior is considered for hygroscopic polymers after dry thermal ageing due to restoration of normal moisture content when subjected to laboratory climate conditions [72]. Accordingly, it is necessary to assess post-ageing curve of ρ for FR-EPR insulator in order to fit measurement time after oven sampling and thus better trending of ρ degradation. To achieve this, tubular electrodes were made from FR-EPR aged insulators at 125 ^{o}C for 3480 hours and the values of ρ were continuously measured for 28 days. At the first 13 days, the samples were stored inside desiccator with temperature of 20 ±2 ^{o}C and RH of 25 %. After that samples were stored at laboratory climate conditions with same temperature and increased RH level up to 60%. Figure 2.7 shows ρ results with measurement time in days. In the first seven days, the value of resistivity for the three colored insulators is oscillating between recovery/decay and that is due to some transients from chains-scissors reactions that are still producing charged particles. After that, recovery behavior is dominant due to the terminations of chains scission reactions by cross-linking, thus the amount of charged moieties are stabilized. The value of ρ recovered to highest order level 10^{13} Ωm after 10 days of

measurement. The recovery trend is still continuous even after changing the environment of sample storage to higher RH values. Based, on these findings recovery behavior is considered to be dominant after thermal ageing, and measurement time of all aged samples through this study were made after 10 days at laboratory conditions (20±2) ^{o}C.

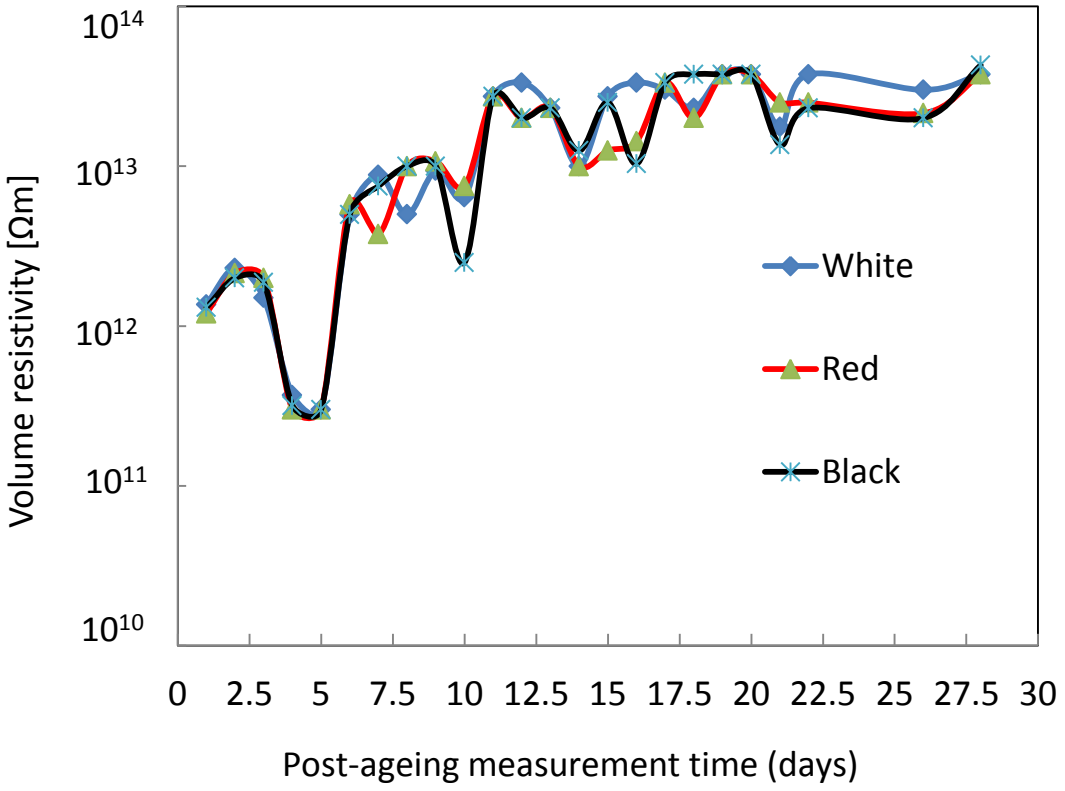

Fig.2.7 Volume resistivity versus measurement time for FR-EPR insulators aged at 125 °C for 3480 hours

2.4 Results and discussion

2.4.1 EAB

Figure 2.8 shows the results of ultimate EAB along ageing time for white FR-EPR insulator aged with SHPVC jacket material at 160 °C. The error bars represent maximum and minimum EAB values for three repeated samples at each sampling time. The variation of EAB value for three samples at each sampling time is a result of technical scattering by ageing temperature variation of ± (1-4°C), preparation of tubular-type tensile samples, and tensile testing machine. In spite of this scattering, EAB decrement with ageing time is obvious. EAB varies from initial value 500 % which indicates high ductility and tough viscoelastic behavior of mechanical property for EPR elastomer [70]. With increased time, EAB gradually decreases reaching around 100% at end of thermal ageing time indicating mechanical property degradation by induced chain-scission and cross linking reactions, thus cracking and embrittlement were initiated. EAB decrement exceeded half its initial value (EAB_0) that is considered indicator of thermal ageing and for Arrhenius model extrapolations.

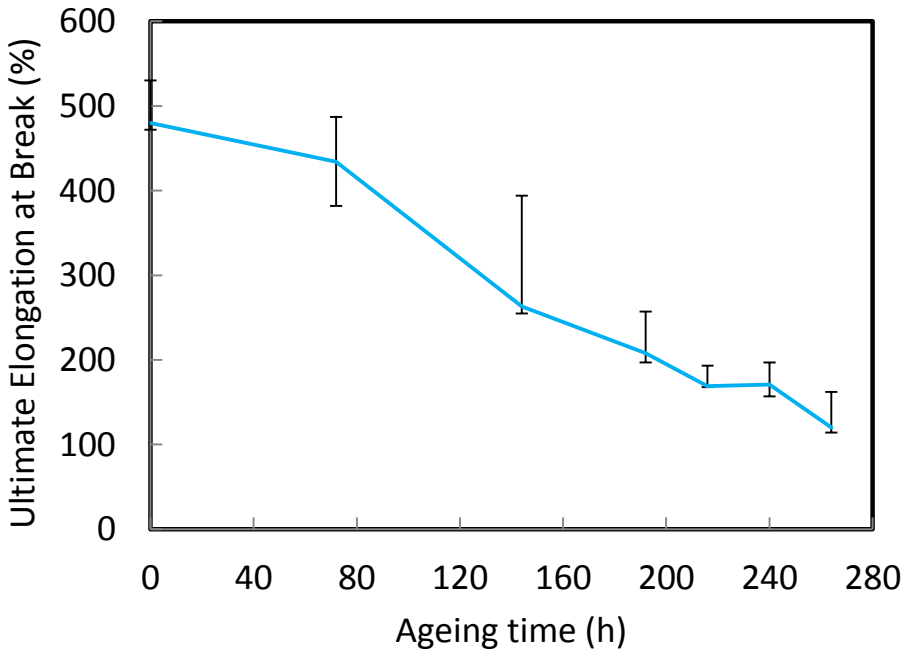

Fig.2.8 Elongation at break versus ageing time for FR-EPR white insulator aged with SHPVC jacket at 160 °C

Figure 2.9 shows ultimate EAB results versus ageing time for three FR-EPR insulators colors (white, red, and black) aged at 160 °C. Error bars represent minimum and maximum EAB values of three repeated samples for each insulator color at each sampling time. EAB values of the three insulators colors decrease with ageing time in similar tendency exceeding their corresponding half-initial values (0.5 EAB_0) criterion and approaching around 100 % by end of ageing time due to embrittlement and cracking. This reveals that degradation mechanisms by chain-scission and cross linking reactions are also similar between colors. EAB variance between colors can be due to technical scattering, but it also can be due to the different structure by colorant pigments additives [49]. However, since error bars of the three colors are mutually interposing, it becomes difficult to distinguish the effect of color difference with technical scattering separately. Thus, the impact of cable structure difference by colorant pigments is still unclear from EAB trending results with ageing time.

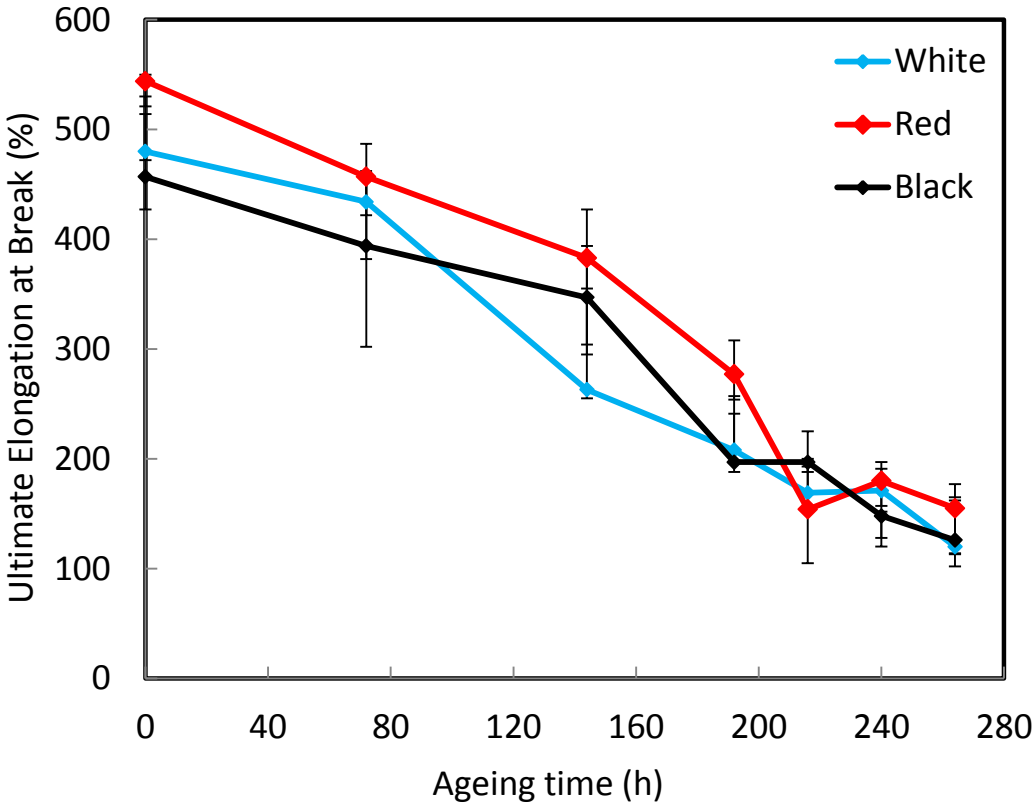

Fig.2.9 Elongation at break versus ageing time for FR-EPR insulator aged with SHPVC jacket at 160 °C

Figure 2.10 shows EAB versus ageing time for the three FR-EPR insulator colors aged at 125 °C, 150°C and 160 °C including SHPVC jacket. In order to compare effect of ageing temperature on insulation degradation, EAB are normalized to their un-aged initial values (EAB_0). Degradation trends between the three insulators are almost similar at each ageing temperature. Accordingly similar degradation mechanisms between the three insulators are evolved through ageing temperatures span (125 °C-160°C). Besides, the EAB decrement rate increase with increasing ageing temperature due to increment of corresponding chain-scissions and cross linking reactions rates at higher temperatures.

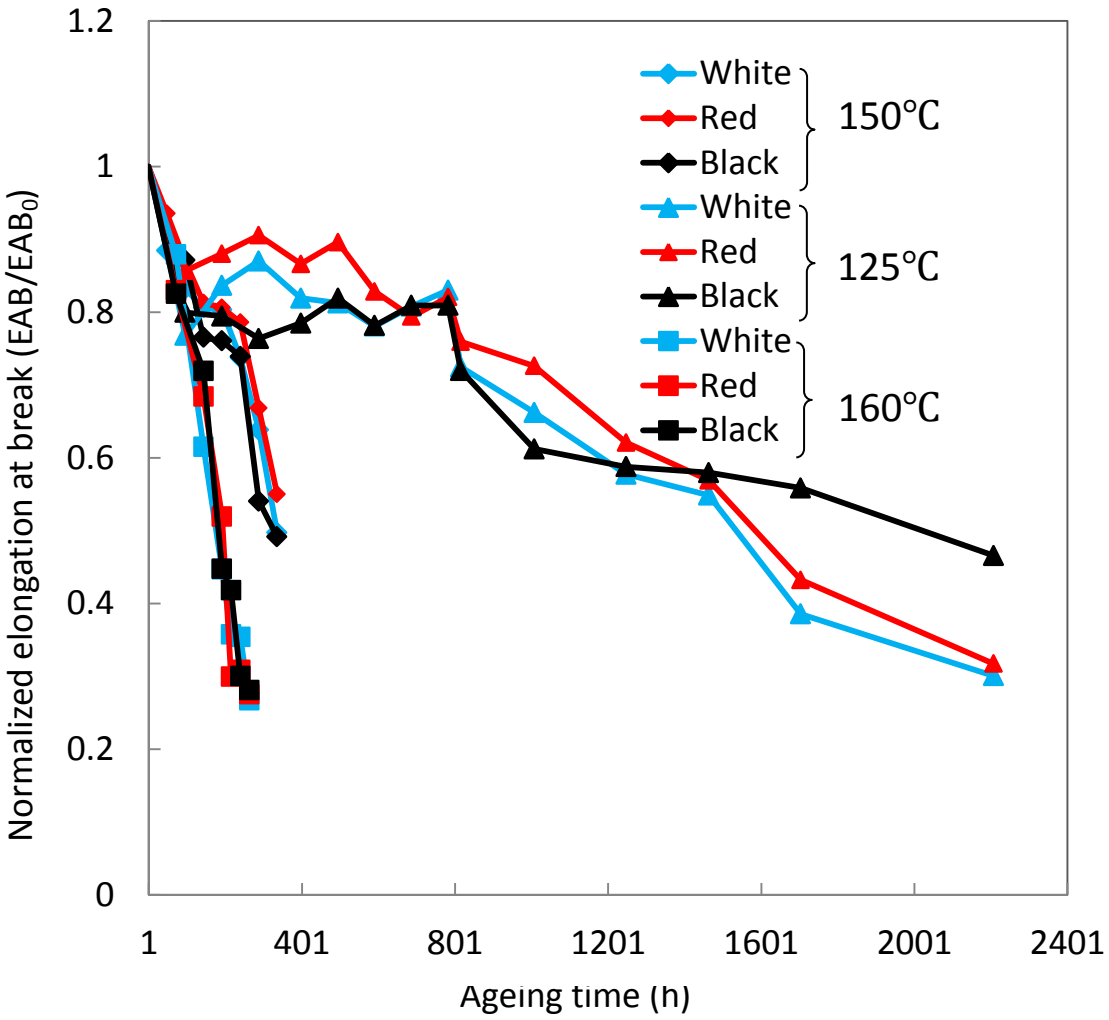

Fig.2.10 Elongation at break versus ageing time for FR-EPR insulator aged with SHPVC jacket

In order to investigate the impact of ageing with/without jacket on mechanical property degradation of insulator, normalized EAB are trended with ageing time for FR-EPR insulators aged with and without jacket at 160 °C and 125 °C as can be seen in figures 2.11 and 2.12, respectively. At 160 °C ageing (Fig. 2.11), degradation behavior for insulators aged with jacket has linear tendency with ageing time In contrast, when insulators are only aged, EAB varies in small rate until ageing time of 200 hours then decrement rate becomes higher. EAB values for ageing with jacket are lower than corresponding values when ageing as only insulator material. Mechanical property of insulators that aged solely reaches same degradation level criteria for insulators aged with jacket (i.e. 0.5 normalized EAB) after about 90 hours heating

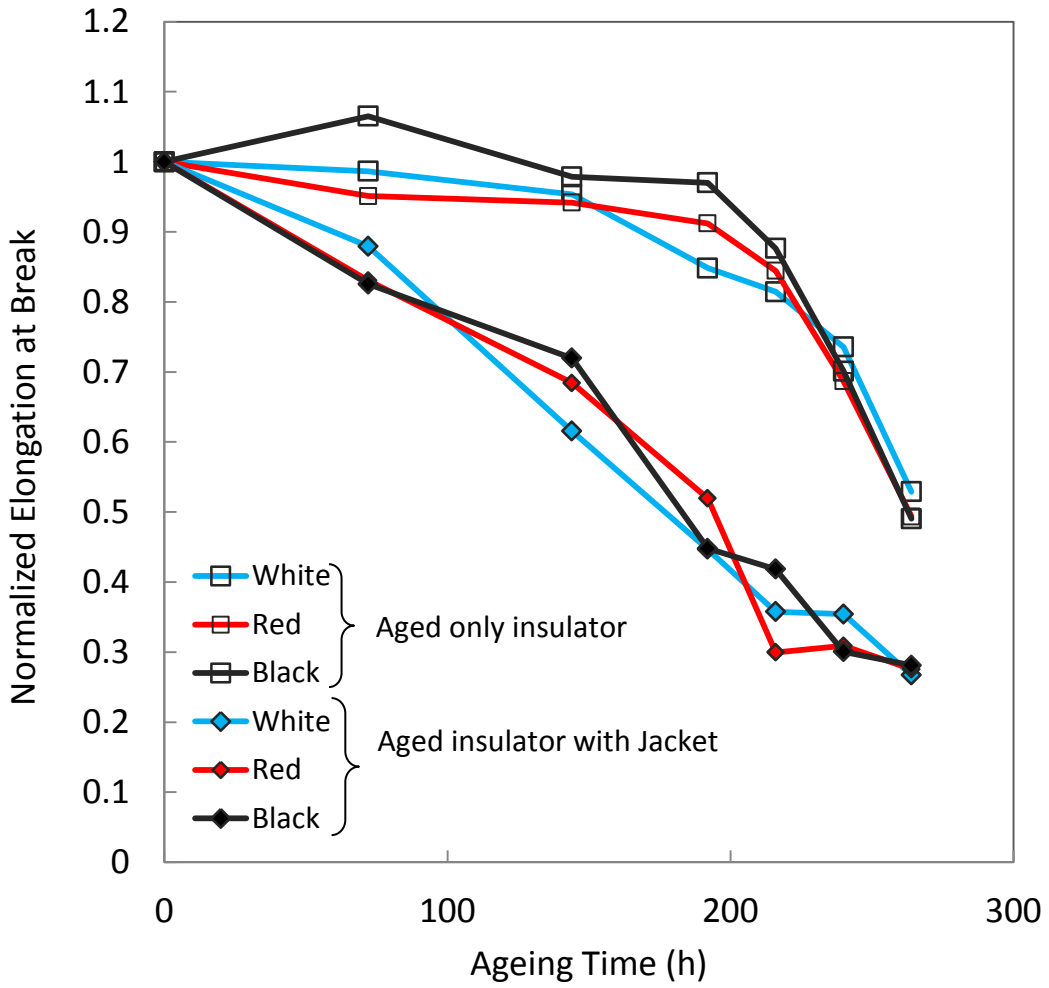

Fig.2.11 Elongation at break versus ageing time for FR-EPR insulators aged with and without SHPVC jacket at 160 °C

At early period for ageing at 125 °C (Fig. 2.12), the values of EAB are close for insulator aged with and without jacket. But at ageing time of 800 hours, EAB degradation rate increases for insulators aged with jacket and it becomes more obvious that EAB for insulators solely aged are larger than EAB for insulators aged with jacket. For insulators aged without jacket, EAB reaches same degradations level of 0.5 EAB_0 after 900-1700 hours compared to ageing with jacket. Further discussions on impact of insulator environment on its degradation will be explained in section 2.4.4 after better understanding from electrical properties results in section 2.4.2 as well as degradation mechanisms by Fourier transform Infrared (FTIR) spectra analysis in section 2.4.3.

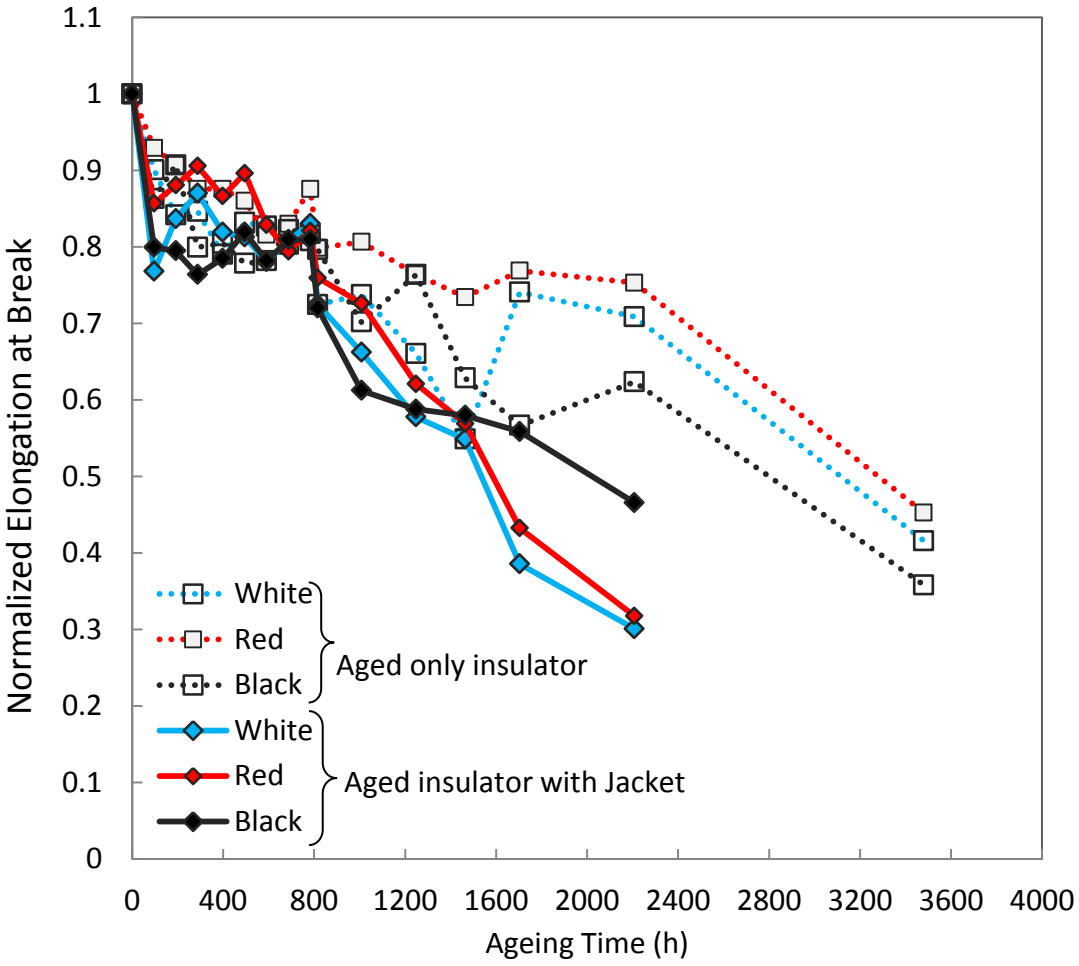

Fig.2.12 Elongation at break versus ageing time for FR-EPR insulators aged with and without SHPVC jacket at 125 °C

2.4.2 ρ

Figure 2.13 shows the results of volume resistivity (ρ) along ageing time for black FR-EPR insulator aged with SHPVC jacket material at 160 °C. The error bars represent maximum and minimum ρ values for three repeated samples at each sampling time. It can be seen that effect of technical scattering on ρ is very small. For Un-aged sample, the highest detected ρ from developed electrode (section 2.3.2) is in the order level of 10^{14} Ωm. ρ varies slightly with ageing time until 140 hours where ρ reduction becomes faster and reach order level of 10^{11} Ωm at ageing time 200 hours due to induced charged moieties from chain-scission reactions[23,68]. Nevertheless, ρ reduction is still higher by 3 orders of magnitude above IAEA established insulator functionality criterion of 1×10^{8} Ωm.[15]. After 200 hours heating, ρ have increment tendency. This increment is not real ρ recovery nor degradation, but caused by the change of insulator shape that resulted from thermally induced embrittlement and cracking that were previously evidenced by gradual EAB decrement at such high ageing time (Fig. 2.8 and Fig. 2.9). The induced embrittlement and cracking will overlap ρ real behavior and it becomes difficult to be trended with ageing time.

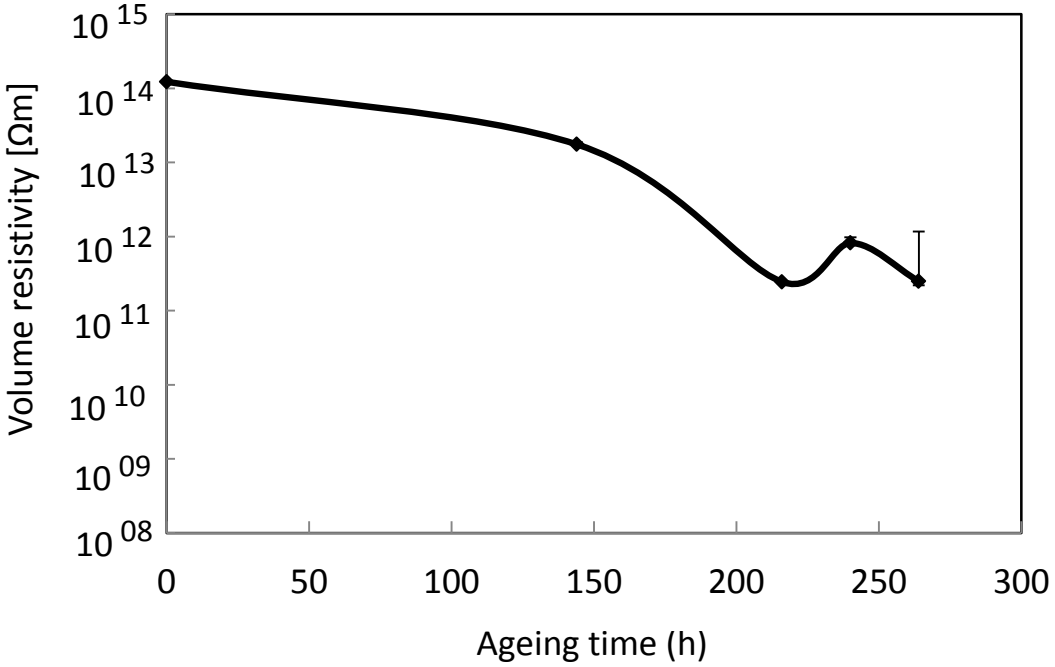

Fig.2.13 Volume resistivity versus ageing time for FR-EPR black insulator aged with SHPVC jacket at 160 °C

Figure 2.9 shows ρ results versus ageing time for three FR-EPR insulators colors (white, red and black) aged at 160 °C. Error bars represent minimum and maximum ρ values of three repeated samples for each insulator color at each sampling time. ρ degradation trends are similar for the three insulators, thus their relevant degradation mechanisms are similar. The slight variance of ρ between the three colors is by mutual effect of technical scattering and colorant pigments variance. Although it is difficult to distinguish ρ variance by colorants pigments, however pigments effect to induced ions from chain scission reactions is limited. Increment tendency after 200 hours ageing is by thermally induced embrittlement as discussed in figure 2.13.

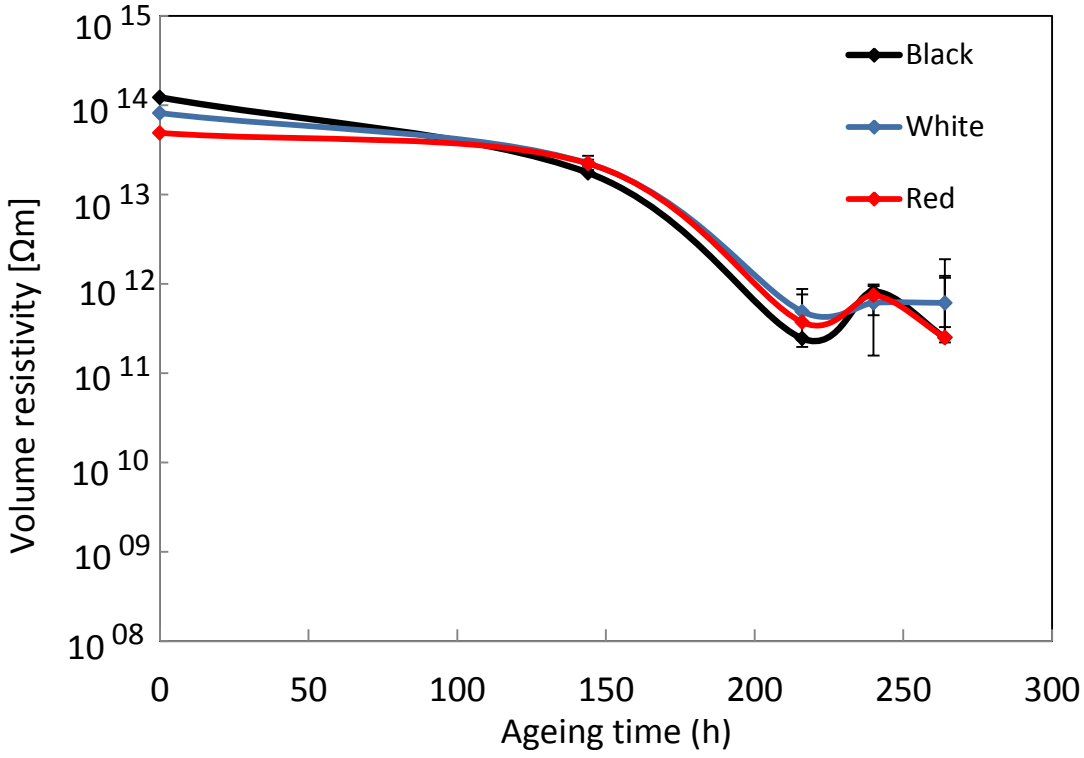

Fig.2.14 Volume resistivity versus ageing time for FR-EPR insulators aged with SHPVC jacket at 160 °C

Figure 2.15 shows ρ versus ageing time for the three FR-EPR insulator colors aged at 125 °C, 150°C and 160 °C including SHPVC jacket. Degradation trends between the three insulators are almost similar at each ageing temperature except for red color aged at 150 °C where there is still no large ρ reduction up to end of ageing time at 336 hours. Thus, the pigments in red color caused mechanism kinetics that

delayed resistivity sharp reduction at this temperature. This affected degradation rate and it might require a slight more ageing time to achieve large reduction of ρ as in other insulator colors. Nevertheless, similar degradation mechanisms are expected through ageing temperatures span (125°C-160°C). Besides, ρ decrement rate increases with increasing ageing temperature that accelerates chain-scission ions production. For ageing at 125°C, increment tendency after 3480 hours ageing is due to thermally induced embrittlement which overlaps ρ detection as discussed previously.

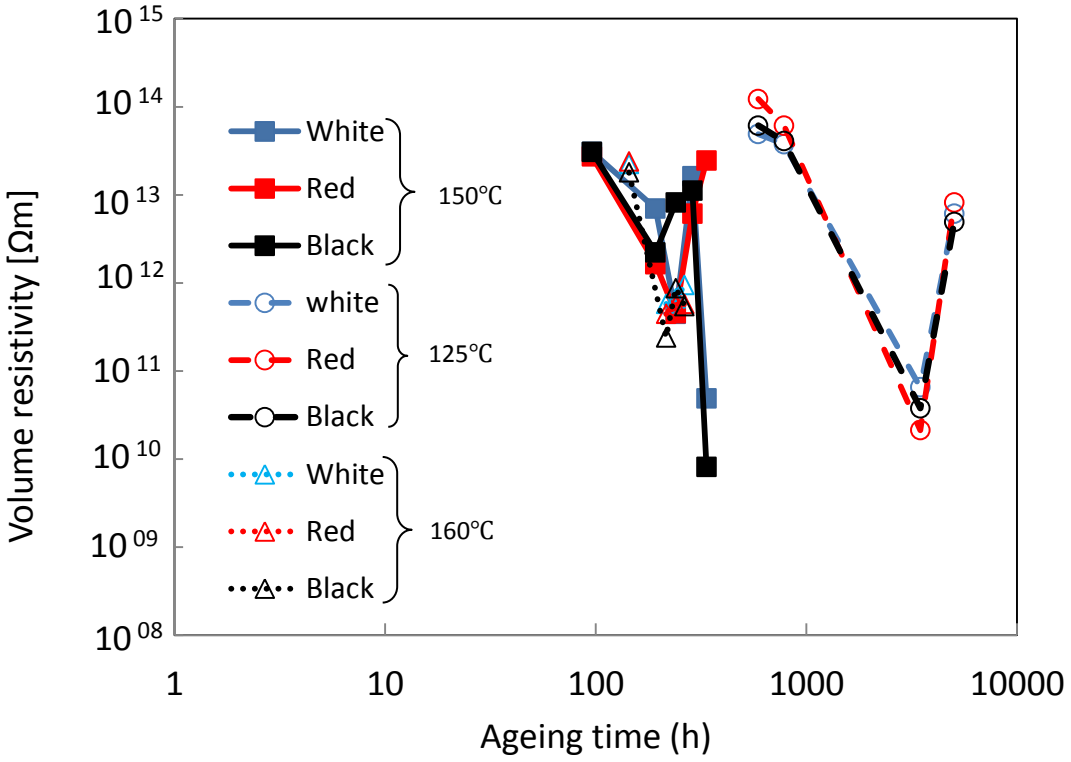

Fig.2.15 Volume resistivity versus ageing time for FR-EPR insulators aged with SHPVC jacket

In order to investigate the impact of ageing with/without jacket on electrical property degradation of insulator, ρ are trended with ageing time for FR-EPR insulators aged with and without jacket at 160 °C and 125 °C as can be seen in figures 2.16 and 2.17, respectively. At 160 °C ageing (Fig. 2.16), ρ degradation tendency is very slow for both ageing with and without jacket until ageing time of 140 hours. After 140 hours, ρ for insulators aged with jacket sharply decreases by (2-3) orders of magnitude below corresponding ρ values for insulators that are only aged. ρ for

insulator only aged keeps slow decrement rate and remains at order level of 10 $^{13}\Omega$m by end of ageing time.

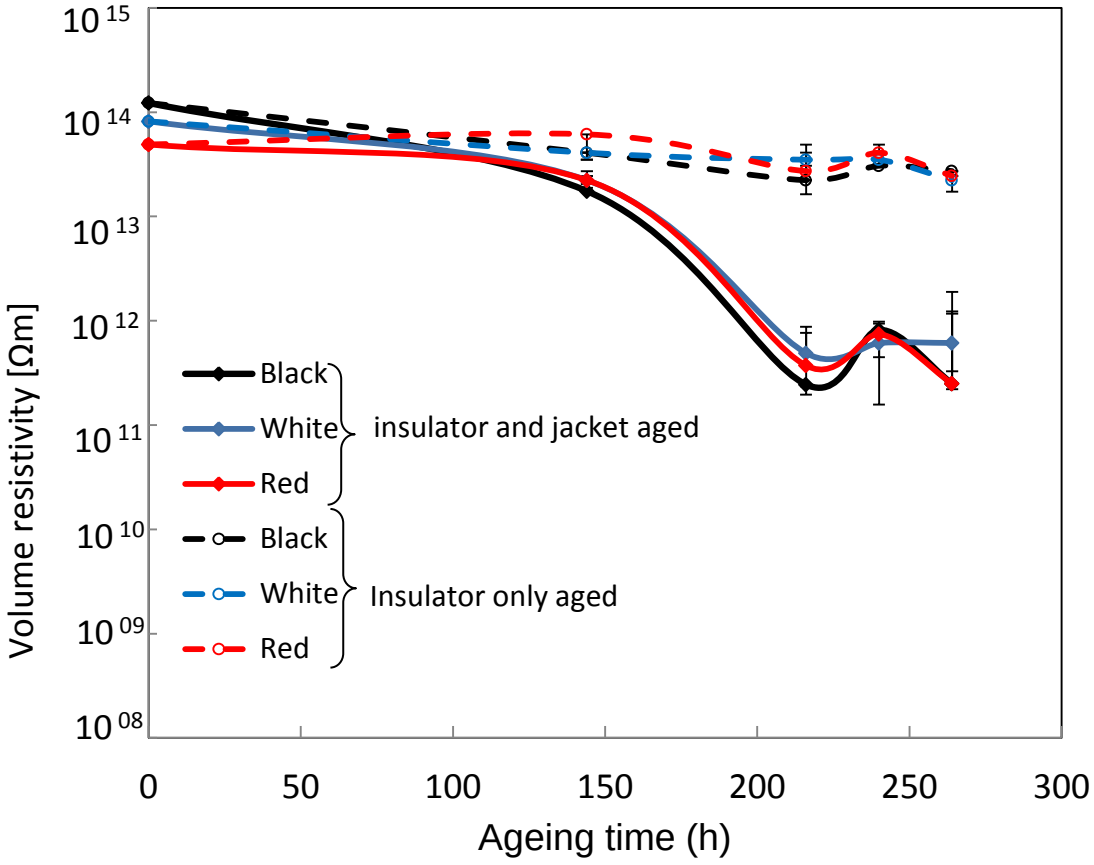

Fig.2.16 Volume resistivity versus ageing time for FR-EPR insulators aged with and without SHPVC jacket at 160 °C

At 125 °C ageing (Fig. 2.17), ρ degradation tendency is almost similar between the three colors for each ageing method as in higher temperature of 160 °C (Fig. 2.16). The values of ρ are close for insulator aged with and without jacket until 800 hours. After 800 hours, ρ for insulators aged with jacket decreases and reaches order level 10^{10} Ωm at 3480 hours. At same ageing time, corresponding ρ values for only aged insulators are higher by 3 orders of magnitude. ρ for only aged insulators keeps slow degradation behavior reaching 10^{13} Ωm by end of aging time.

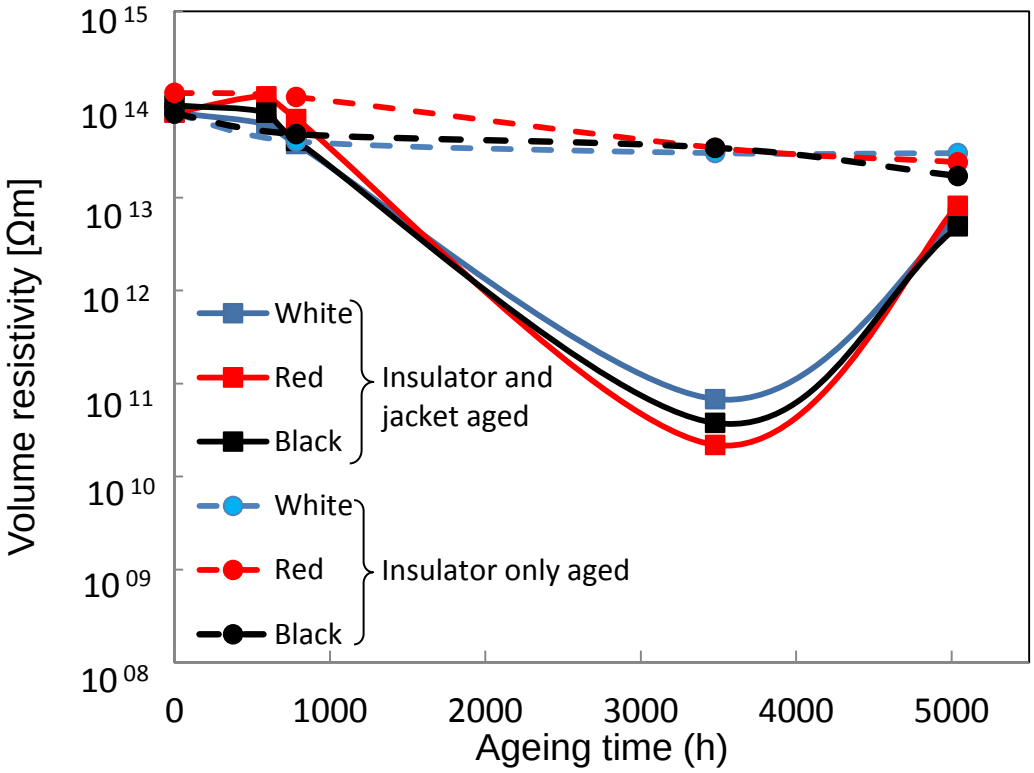

Fig.2.17 Volume resistivity versus ageing time for FR-EPR insulators aged with and without SHPVC jacket at 125 °C

It is necessary to understand evolved mechanics by thermal ageing before further discussion of impact of insulator environment on ρ degradation. Thus FTIR was utilized to understand mechanisms in following section (2.4.3) and then discussion will be continued in section 2.4.4.

2.4.3 Mechanisms investigations by Fourier transform infra-red spectroscopy

Fourier transform infrared spectroscopy (FTIR) was utilized to analyze the molecular structure of FR-EPR insulator as indication of ageing. The basic principle behind FTIR is that during applying infrared light to material surface, a particular chemical bond of material will absorb light and starts vibration at specific wave number. The amount of reflected light to spectrometer will determine the peak of that chemical bond. FTIR spectroscopy was performed by PIKE TECHNOLOGIES horizontal attenuated total reflectance (HATR) spectrometer using Zinc Selenide (ZnSe) crystal. The samples were prepared as rectangular shape with dimensions 6

mm × 72 mm and attached with ZnSe crystal from outer surface side after wiping by ethanol. Insulator outer surface was only investigated without thickness profiling. That is due to tubular-shape of insulator which complicates thickness slicing by microtome. Thus, FITR absorbance is limited to depth of less than 10 μm from sample surface.

In section 2.4.1 and 2.4.2, the results of EAB and ρ degradation were more severe when FR-EPR was aged including jacket material. Thus, FTIR was only performed on insulators that aged with jacket material. Besides, since EAB and ρ degradation trends are almost similar between three colors as well as mechanism are same by different ageing temperatures, then FTIR analysis was performed for only one insulator color aged at single ageing temperature for specific ageing times, i.e FR-EPR white insulator aged at 150 °C aged up to 288 hours. For FR-EPR elastomer, the characteristic chemical bonds of interest, and their corresponding wavenumbers are summarized in table 2.4.

Table 2.4 FTIR spectral peaks of FR-EPR in absorption bandwidth 1700-1800 cm^{-1} and 2500-3000 cm^{-1}

Wavenumber (cm^{-1})	**Vibration assignment**	**Functional group**
1715	>C=O stretch	Carboxylic acid (C=O)
1735	>C=O stretch	Carboxylic aldehyde (C=O)
1749	>C=O stretch	Carboxylic ester (C=O)
1772	>C=O stretch	Carboxylic anhydride (C=O)
2853	-C-H asymmetric stretch	Methylene ($-CH_2-$)
2920	-C-H symmetric stretch	Methylene ($-CH_2-$)
2952	-C-H stretch	Methyle ($-CH_3$)

Carbonyl peaks with absorption bandwidth between (1700-1800) cm^{-1} are main indicator for oxidation. Thus, to investigate surface degradation by oxidation, FR-EPR samples were scanned at un-aged conditions and after 288 hours ageing as

shown in figure 2.18 in the bandwidth (1700-1800) cm^{-1}. The observed four peaks are attributed to carboxylic compounds originated from oxidative chain-scission and cross linking reactions. Peaks assignment are as followings; 1715 cm^{-1} is assigned to carboxylic acid $\left[\underset{R-C-OH}{\overset{O}{\overset{\|}{}}} \right]$, 1735 cm^{-1} is assigned to carboxylic aldehyde $\left[\underset{R-C-H}{\overset{O}{\overset{\|}{}}} \right]$, 1749 cm^{-1} is assigned to carboxylic ester $\left[\underset{R-C-OR}{\overset{O}{\overset{\|}{}}} \right]$, and 1772 cm^{-1} is assigned to carboxylic anhydride $\left[\underset{R-C-O}{\overset{O}{\overset{\|}{}}} \underset{-C-R}{\overset{O}{\overset{\|}{}}} \right]$[28,30,73]. The results show that the peaks intensity increases for the four carbonyl compounds after 288 hours ageing and EAB decrement to 399 %. Thus, surface degradation by oxidation is evident for FR-EPR insulators aged with jacket material.

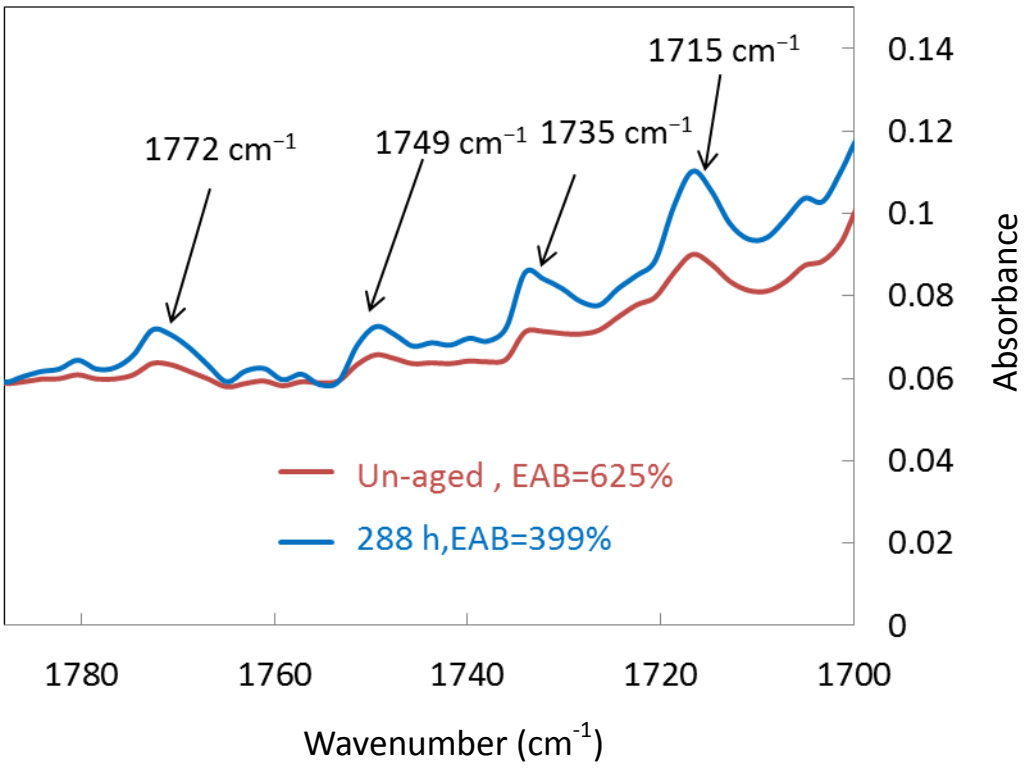

Fig.2.18 FTIR spectra for FR-EPR white insulator before and after ageing with SHPVC jacket at 150 °C for 288 hour (bandwidth 1700-1800 cm^{-1})

To understand mechanisms schemes of oxidation, the four carboxylic compounds at (1700-1800) cm^{-1} were trended with ageing time as shown in figure 2.19. The degradation level from carbonyl absorbance is determined relative to absorption band 1464 cm^{-1} (assigned to $-CH_2-$ bending vibration) [29]. The four compounds have very

close trends with time. It can be seen that the major oxidation product is carboxylic acid while aldehyde, ester, and anhydride are secondary products. The reason for high carboxylic acid portion is due to its production by chain scission of polymer alkyl radical ($R^{\cdot}$) in presence of oxygen (O_2) after EPR back bone chain scission [24,25,28] ,or indirectly from carboxylic aldehyde chain-scission reactions [30]. The aldehyde is generated from chain scission of Poly-oxy radical [30] that was initiated after hydro peroxide (ROOH) thermal decomposition [25,30]. Carboxylic ester can be formed by chain scission reaction of carboxylic acid with alcohol compounds (ROH), while carboxylic anhydride is cross linking reaction product of carboxylic acid at high ageing temperature [28]. The aforementioned mechanisms schemes are illustrated in figure 2.20.

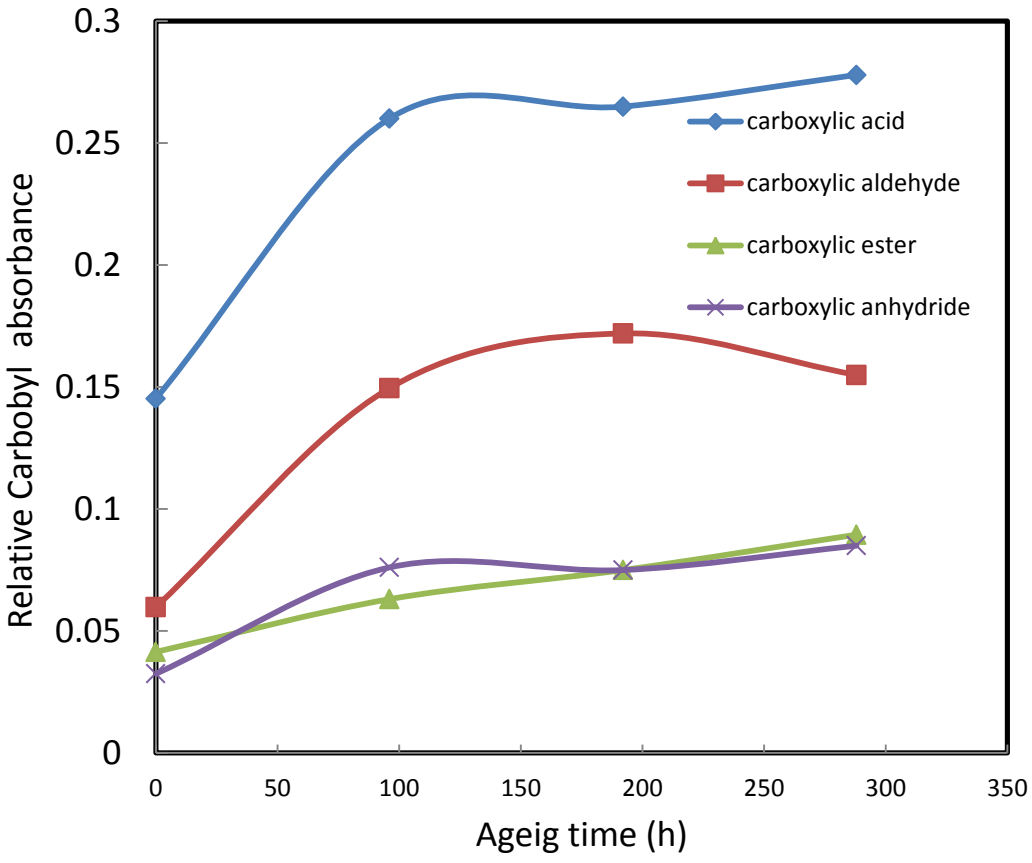

Fig.2.19 Carbonyl contents versus ageing time for FR-EPR white insulator surface aged with SHPVC jacket at 150 °C

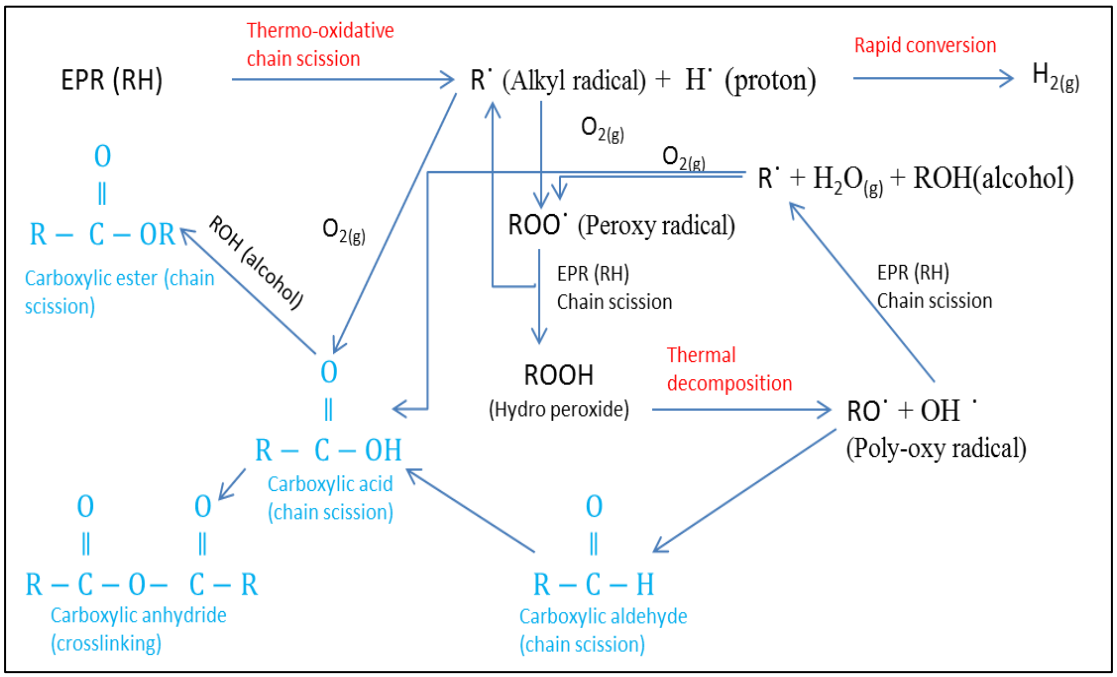

Fig.2.20 Mechanisms schemes by oxidation for FR-EPR white insulator surface aged with SHPVC jacket at 150 °C

For PVC jacket material, thermal degradation leads to PVC molecular chains breaking and inducing chlorine (Cl) ions that form with protons ($H^{\cdot}$) hydrochloric acid (HCl) which eliminates from PVC jacket material to surrounding vicinity. This process is called HCl elimination and involves dehydrochlorination of PVC macromolecular chains resulting in formation of double bonds (polyenes) that present liable sites for oxidation and cause material discoloration with advanced ageing.[14,49]. This process becomes more important at temperatures above (70~80)°C [15,49]. HCl is highly corrosive and may attack cable, conductor, and also connecting devices[49]. Literature review shows that HCl by dehydrochlorination has characteristic absorbance bandwidth at (2926-2932 cm^{-1}) [74]. Accordingly, FTIR spectroscopy was utilized to investigate the bandwidth (2926-2932 cm^{-1}) on FR-EPR insulator surface and judge whether PVC jacket affected FR-EPR insulator by HCl elimination as can be seen in figure 2.21. The spectrum peak at 2920 cm^{-1} is assigned to asymmetric stretching vibration of methylene ($-CH_2-$) in the saturated hydrocarbon backbone, while the peak at 2853 cm^{-1} is assigned to symmetric stretching vibration of methylene ($-CH_2-$) [29]. The shoulder peak at 2952 cm^{-1} is assigned to methyl ($-CH_3$) stretching vibration [75]. As can be seen from figure 2.21, there is no evolved peaks at bandwidth (2926-2932 cm^{-1}) up to ageing time of 288 hours even though EAB

decreased to 399%. Accordingly, effect of PVC jacket dehydrochlorination on FR-EPR insulator degradation is not evident from FTIR inspections on surface within depth below 10 μm. Effect of dehydrochlorination is also not evident through whole thickness of aged FR-EPR insulator.

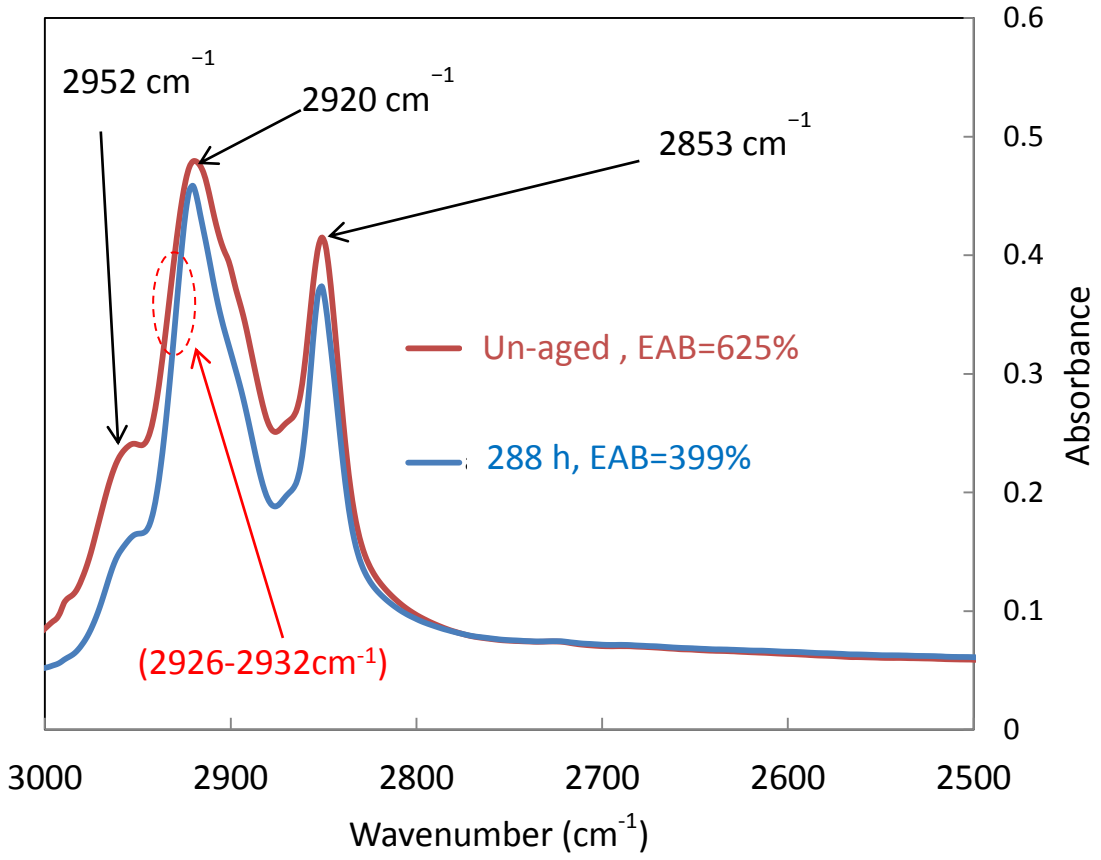

Fig.2.21 FTIR spectra for FR-EPR white insulator before and after ageing with SHPVC jacket at 150 °C for 288 hour (bandwidth 2500-3000 cm^{-1})

2.4.4 Discussion on impact of insulation environment on its degradation

EAB and ρ results show that the degradation of FR-EPR insulator mechanical and electrical properties is more significant when ageing with SHPVC jacket materials. For ageing at 160 °C (Fig. 2.11), EAB for insulator aged with jacket have degradation rate higher than without jacket which reveals that chain-scission and cross linking reactions rate are higher. The results from ρ degradation as well as carbonyl components (acid, ester and aldehyde) emphasize that chain-scission reactions are more dominant than cross linking for insulators aged with jacket.

Besides, sharp EAB reduction behavior at ageing time of 200 hours (Fig. 2.11) for only aged insulators is well-known and called “induction-time” behavior due to the large reduction of anti-oxidant amount as result of thermo-oxidative degradation at that time (200 hours)[47,56]. Thus oxidation is more dominant for insulators aged without jacket. For insulators aged with jacket even though evolved carbonyl compounds (Fig. 2.18 and 2.19) are indications from oxidation reactions, but from ρ degradation trends at ageing temperature of 160 °C (Fig. 2.16), it can be observed that the ρ degradation is more severe when ageing with jacket , while for ρ is still high when insulator is only aged. This reveals that chain-scissions reactions are not governed by oxidations and the jacket material will accelerate chain-scission ions generation or will complicate ions absorption and quenching by ant-oxidant. Even at lower ageing temperature of 125 °C ,where the effects of diffusion limited oxidations (DLO) are less significant than ageing at 160 °C, EAB and ρ degradation curves (Fig. 2.12 and 2.17) show that insulator aged including jacket materials experienced higher degradation level and this emphasizes that effect of jacket environment on insulator degradation is more significant than oxidation.

Immigrated additives and reaction products from PVC jacket into FR-EPR insulation during thermal ageing is also possible. But effect of HCL dehydrochlorination from PVC jacket material into insulator degradation is not evident as investigated from FTIR spectra analysis at bandwidth (2926-2932 cm^{-1}) (Fig. 2.21)

Chapter 3 Thermal ageing estimations from insulator properties degradation

This chapter aims at reflecting the obtained knowledge of cable structure in previous chapter into engineering estimation of thermal degradation during normal operation conditions through:

1-Examine appropriateness of volume resistivity (ρ) degradation for trending thermal ageing

2-Evaluate activation energy (E_a) and equivalent time considering accelerated test uncertainties.

In section 3.1, JNES-SS-0903 logistic function was utilized to approximate elongation at break (EAB) for better understanding of EAB thermal ageing and post-ageing evaluations. In section 3.2, E_a was evaluated considering the variance of cable structure by insulator colorants pigments impact which was clear and distinguished from technical scattering. Besides, time-temperature (T-t) superposition was applied to obtain E_a from volume resistivity (ρ) and EAB degradation curves. In section 3.3, thermal ageing estimations by both insulator properties (EAB & ρ) were evaluated by T-t superposed degradation curves. The superiority of EAB compared to ρ was obvious for post ageing evaluations in the light of equivalent time predictions. In section 3.4, comparison was made for thermal ageing estimations from EAB degradation of this study with JNES-SS-0903 degradation database. It was found that degradation progress is faster for aged FR-EPR insulators with jacket used in this study, thus considerations for thermal ageing estimations by current environmental qualifications (EQ) process were discussed in section 3.5.

3.1 Parameters for thermal ageing characteristics approximations

In chapter 2, it was found that EAB degradation of FR-EPR insulator was more significant when insulator is aged within whole cable structure. Thus, in chapter 3, post thermal ageing analysis of cable integrity shall rely on EAB degradation curves for FR-EPR insulators that were aged with SHPVC jacket material. This requires in advance understanding the characteristic of EAB thermal degradation curves. Accordingly, JNES-SS-0903 logistic function was utilized [12]: JNES-SS-0903 proposed non-linear regression logistic function to approximate the experimental EAB data points with ageing time, through correlating with four parameters (A_1, A_2, x_0, and p) as in equation 3.1 :

$$EAB = \frac{A_1 - A_2}{1 + \left(\frac{t}{x_0}\right)^p} + A_2 \qquad 3.1$$

Where:

EAB: Approximated (fitted) ultimate elongation at break [%]

t: Ageing time [hour]

A_1: Initial EAB, i.e. EAB of un-aged sample [%]

A_2: Minimum EAB [%]

p: Degradation rate constant (gradient)

x_0: Time to $(A_1+A_2)/2$ [hour]

The best fitted values of A_1, A_2, x_0, and p were found based on least-square error coding by using MATLAB software, M-file codes. The values of these parameters are tabulated in table 3.1 for the three FR-EPR insulators colors (white, red, and black) at all ageing temperatures (125 °C, 150 °C and 160 °C). As a result, approximation of real experimental EAB degradation curves becomes plausible as can be seen in figure 3.1. The approximated thermal degradation curves properly fit their corresponding

experimental data points, thus further thermal ageing estimations will rely on analysis of approximated curves.

Table 3.1 Approximation results of EAB degradation characteristics for FR-EPR insulators aged with SHPVC jacket at 125 °C, 150 °C, and 160 °C

Ageing temperature	**Approximation parameters**				**Least square error**
	A_1	A_2	x_o	p	
FR-EPR white					
125 °C	541.39	9.94E-05	1681.61	2.56	15697.71
150 °C	578.67	2.34E-14	392.32	2.26	6254.23
160 °C	493.12	1.44E-12	174.90	2.30	25451.15
FR-EPR red					
125 °C	580.06	2.47E-06	1709.90	2.41	6722.43
150 °C	615.12	3.92E-09	445.43	1.73	4411.07
160 °C	515.04	2.36E-07	187.23	2.86	39316.80
FR-EPR black					
125 °C	543.04	4.05E-12	2457.25	1.30	17439.46
150 °C	603.75	2.51E-06	356.32	1.73	5064.55
160 °C	444.65	4.53E-09	192.16	2.86	30519.96

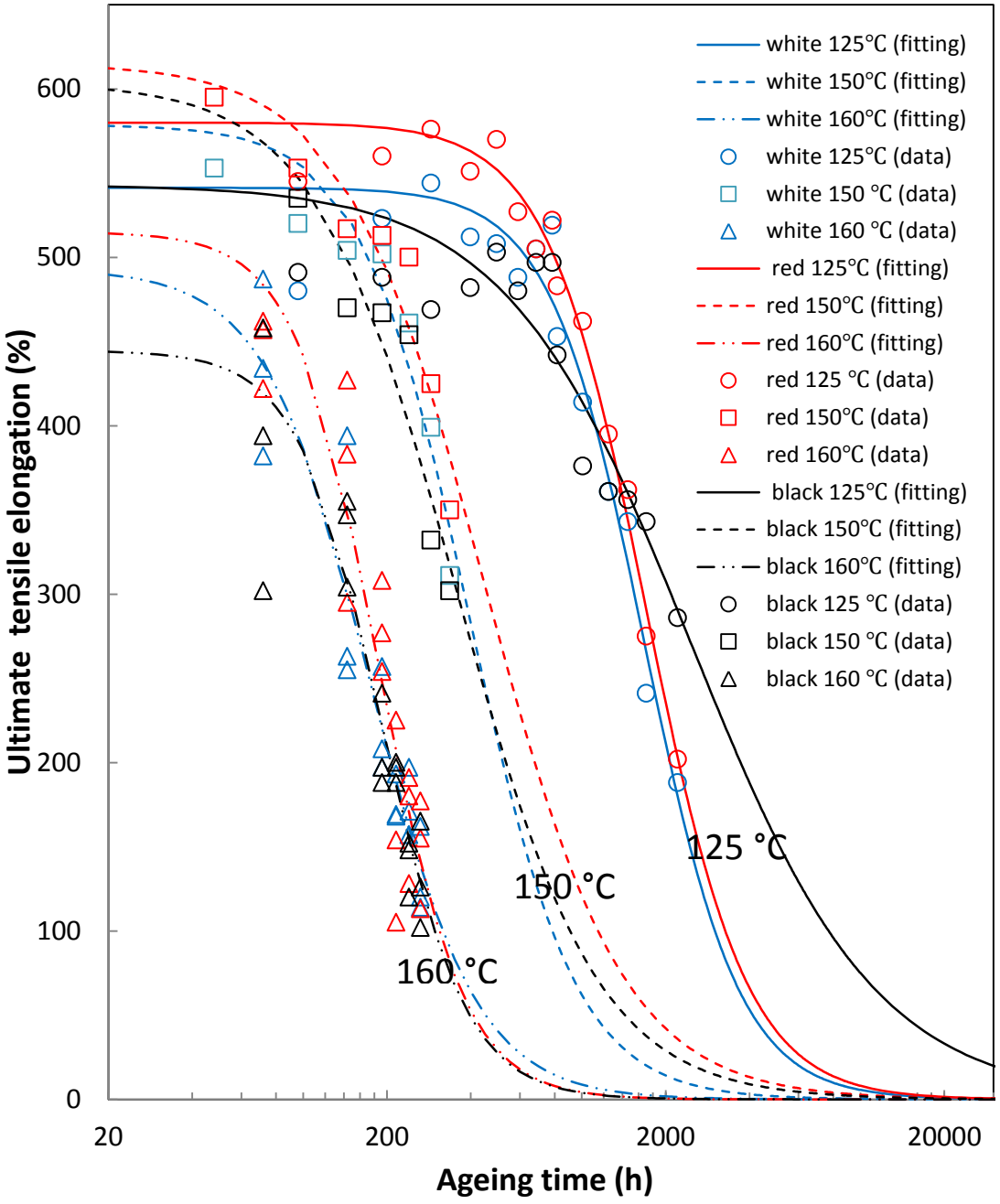

Fig.3.1 Real and approximated ultimate EAB values versus ageing time for FR-EPR insulators aged with SHPVC jacket at 125 °C,150 °C, and 160 °C

In figure 3.1, the trend of thermal ageing characteristics is classified as in the first trend of JNES-SS-0903:"*Almost no progress of degradation is recognized in the early period, but the progress of degradation becomes rapid from certain point*" [12]. A_2 have almost zero values, revealing that the minimum EAB values will decrease to zero due to severely induced cracking at late degradation periods. The time parameter

(x_0) is dependent on ageing temperature and material type, and it is inversely proportional to increased temperature. And since A_2 is zero, x_0 becomes the time for EAB to reach its half initial values (0.5 EAB_0). Besides, initial EAB values (i.e. A_1) differ with insulator color. A_1 values even vary for same insulator color at each ageing temperature. This variance is due to initial differences of cross linking degree at manufacturing that leads to variance of cross-linking densities during vulcanization [12,76] in addition to photo-oxidation impacts during storage. [30]. Nevertheless, the initial variance of EAB is not significant on degradation progress between colors, because at each ageing temperature, the rapid degradation starts at very close time. Accordingly, the ultimate EAB values can be normalized to their corresponding A_1 values in order to better understand degradation rates behavior. The normalized EAB degradation curves for all FR-EPR colors aged at three temperatures set points are shown in figure 3.2.

In figure 3.2, EAB reduction rates are similar for both white and red color insulators. But for black insulator, EAB reduction rate becomes slower at ageing temperature of 125 °C. This is reflected in the parameter for degradation rate constant or slope (p) in table 3.1, where the value of "p" for all insulator colors at all temperatures are between 1.7-2.8, except for black color aged at 125 °C, the value is 1.3 which indicates lower degradation rate. The reason of this behavior is due to the possible effect of insulator additive, in particular colorant pigment. Even though the detailed components of cable insulators were difficult to know in this study, but according to investigations of JNES-SS-0903 data base, all FR-EPR black insulators samples contained carbon-black as colorant agent pigments. Besides, literature review reports that carbon-black can slow down ageing process and act as mild thermal anti-oxidant, where carbon-black can act as a trap for propagating radicals as a result of the free radical quenching action of the surface groups on carbon black [77]. With all above in mind, it is considered that effect of carbon-black colorant additives was responsible for delayed degradation rate of FR-EPR black insulator and thus delayed corresponding x_0 value to 2457.25 hours compared to 1681.61 hours and 1709.90 hours for white and red insulators, respectively when ageing at 125 °C.

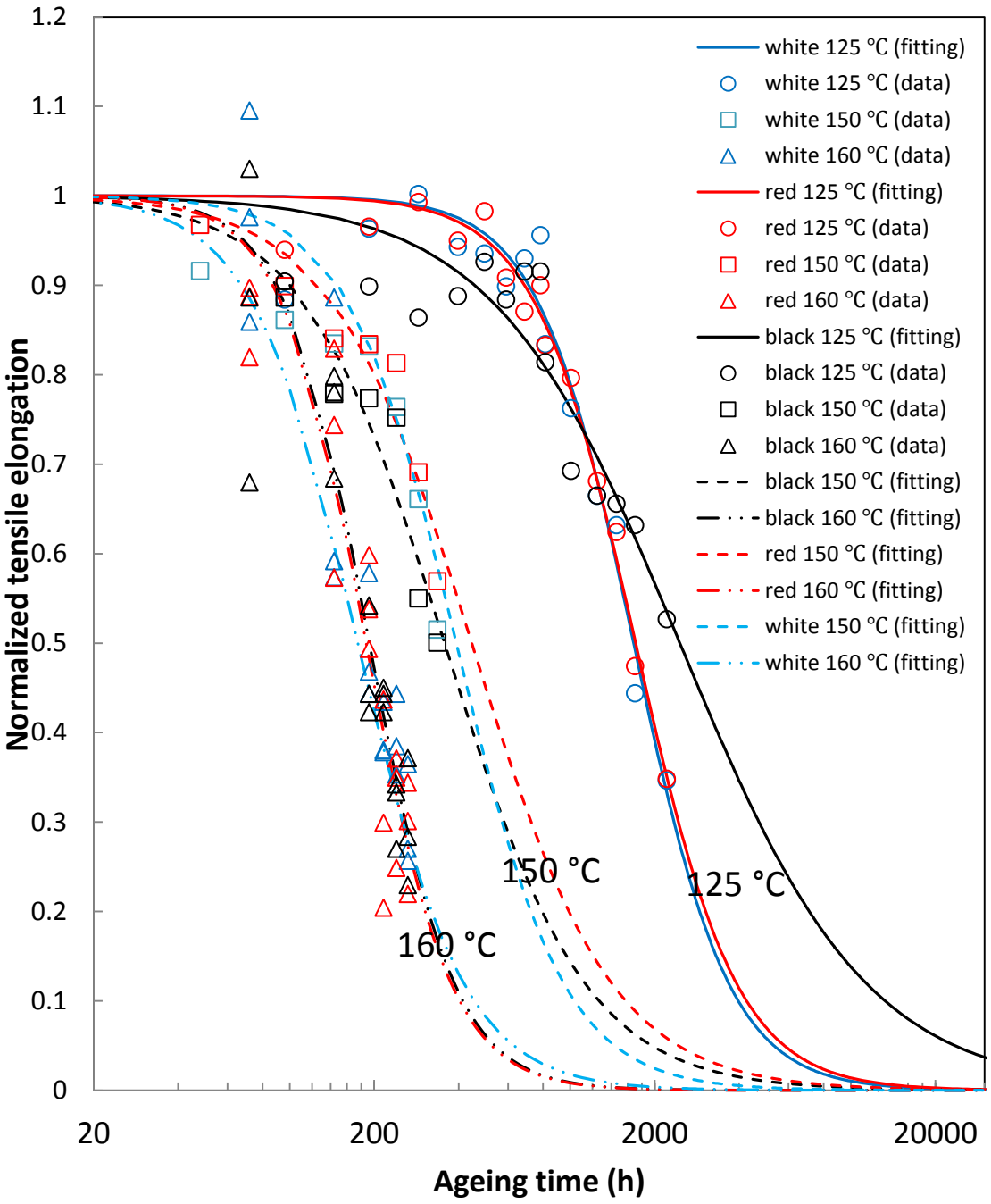

Fig.3.2 Real and approximated normalized EAB values versus ageing time for FR-EPR insulators aged with SHPVC jacket at 125 °C,150 °C, and 160 °C

3.2 Activation energy (E_a) estimations

Activation energy (E_a) is defined as the energy that must be overcome for a chemical reaction to occur. Setting accelerated test conditions as well as estimating their equivalent times at real plat conditions is mainly dependent on E_a determinations. Two well-established approaches were utilized in this study to determine E_a values from insulator EAB and ρ degradation curves, as discussed in below 3.2.1 and 3.2.2 sections.

3.2.1 Arrhenius model

Arrhenius model assumes that the activated chemical process during thermal degradation is estimated by equation 3.2[15]:

$$\boldsymbol{k} = Ae^{-E_a/RT} \qquad 3.2$$

Where

K: Rate constant of degradation reaction.

A: material constant, independent of ageing temperature

E_a*:* Activation energy [J/mol]

T: Ageing temperature [K]

R: Gas constant [8.31446 J/molK]

The estimated E_a is not the real absolute value from direct chemical reactions rate, but it is estimated from induced degradation mechanisms that alter physical insulator properties such as elongation at break and macroscopic density [56,57]. When considering that the degradation mechanisms are similar at two different temperatures, then the time ratio for similar amount of degradation level is estimated by equation 3.3:

$$\frac{\boldsymbol{t_1}}{\boldsymbol{t_2}} = e^{\frac{E_a}{R}\left[\frac{1}{T_1}-\frac{1}{T_2}\right]} \qquad 3.3$$

Where

t_1: time of accelerated ageing at initial ageing temperature T_1 [hour, or year].

t_2: time of accelerated ageing at secondary ageing temperature T_2 [hour, or year].

T_1: initial ageing temperature [K].

T_2: secondary ageing temperature [K].

Accordingly E_a can be mathematically estimated through calculating slope of natural log of time versus inverse temperature (Arrhenius plot) as can be seen in equation 3.4

$$\boldsymbol{E_a} = R\frac{\Delta(lnt)}{\Delta(1/T)} \qquad 3.4$$

Where, *t* is the time for accelerated ageing at specific degradation level. The time to specific degradation level depends on established criteria that consider margins for cable integrity against ageing. For insulator electrical properties, IAEA established insulation function criterion that is determined by resistivity (ρ) of 1×10^8 Ωm, while for EAB an ultimate or normalized 50% value is considered as insulator end-of-lifetime criterion [15]. By investigating the obtained thermal degradation results from ρ degradation for FR-EPR insulator colors as can be seen in figure 3.3, it is obvious that the values of ρ do not exceed the established threshold level (i.e. 1×10^8 Ωm). Thus, the applicability of Arrhenius model to obtain E_a is inefficient. In contrast, by investigating EAB degradation trends, EAB decrement exceeds its half initial value level (0.5 EAB_0) as shown in figure 3.4. Thus, Arrhenius model is applicable, and time to 0.5 EAB_0 is considered as end-of-lifetime for E_a estimations at each ageing temperature for all insulator colors.

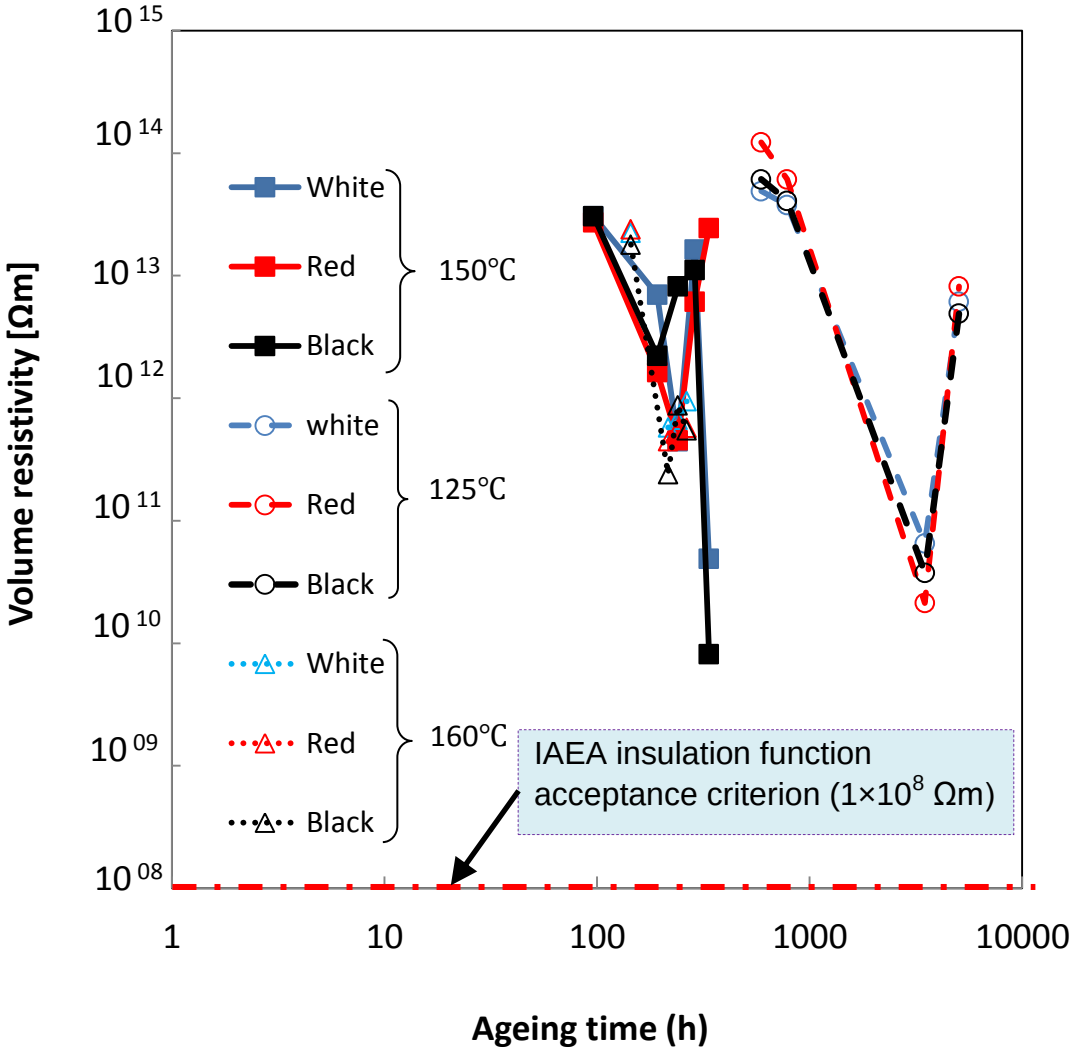

Fig.3.3 ρ degradation curves for FR-EPR thermally aged with SHPVC jacket

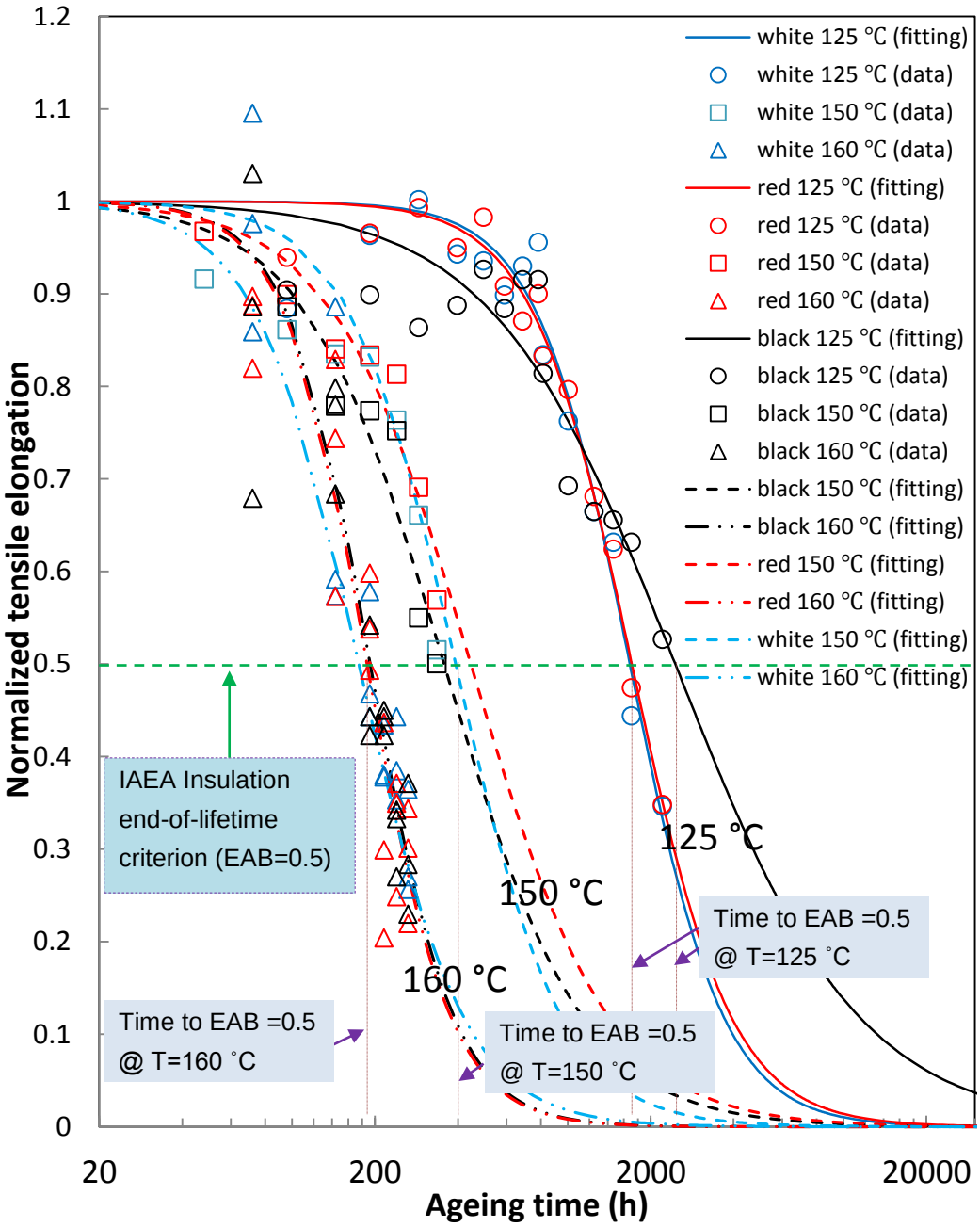

Fig.3.4 EAB degradation curves for FR-EPR thermally aged with SHPVC jacket

On the other hand, thermal accelerated testing includes uncertainties that influence E_a determinations by Arrhenius model. These uncertainties are originated from technical scattering by ageing temperature variation of ± (1-4°C), preparation of tubular-type tensile samples, and tensile testing machine. Accelerated test inaccuracies will result in EAB variation. These variations are assumed to have uniform (Gaussian) distribution around an estimated mean value. Accordingly, the

approximated EAB degradation curves by JNES-SS-0903 are considered as the mean values and standard deviation (σ) caused by EAB experimental data scattering is estimated as in equation 3.5:

$$\boldsymbol{\sigma} = \sqrt{\frac{\sum_{i=1}^{N}(EAB_{data} - EAB_{fit})^{2}}{N-1}} \qquad 3.5$$

Where

σ: standard deviation of EAB by accelerated test uncertainties from technical scattering [%]

EAB_{data}: real experimental values for EAB at each ageing temperature [%]

EAB_{fit}: approximated EAB values by JNES-SS-0903 logistic function [%]

N: Number of EAB experimental data points at each ageing temperature

Based on all above, EAB will deviate at end of lifetime criterion by 0.5 $EAB_{0\,(\mu \pm \sigma)}$. The mean 0.5 EAB value (i.e 0.5 EAB (μ)) is corresponding to the approximated 0.5 A_1 value for each insulator color which basically depends on its structure, while the deviated 0.5EAB values (i.e. 0.5 EAB_0 (μ+σ) and 0.5 EAB_0 (μ-σ)) are corresponding to EAB deviation by technical scattering. In order to evaluate effect of EAB deviation on E_a estimations through Arrhenius model, the end-of-lifetimes at 0.5 $EAB_{0\,(\mu)}$, 0.5 $EAB_{0\,(\mu-\sigma)}$, and 0.5 $EAB_{0\,(\mu+\sigma)}$ must be determined. Accordingly, JNES-SS-0903 logistic function (equation 3.1) was modified to obtain the times as in equation 3.6:

$$\boldsymbol{t} = x_0 \left(\frac{A_1 - A_2}{EAB - A_2 - 1}\right)^{\frac{1}{p}} \qquad 3.6$$

Where, A_1, A_2, x_0, and p are approximation parameters of EAB found by least-square error coding as tabulated in table 3.1.

The mean end-of-lifetime value (t_μ) (i.e. time to 0.5 EAB_0) can then be estimated as in equation 3.7:

$$\boldsymbol{t_\mu} = x_0 \left(\frac{A_1 - A_2}{0.5EAB_0 - A_2 - 1} \right)^{\frac{1}{p}} \qquad 3.7$$

Considering that $EAB_0 = A_1$, then above equation becomes as in equation 3.8:

$$\boldsymbol{t_\mu} = x_0 \left(\frac{A_1 - A_2}{0.5A_1 - A_2 - 1} \right)^{\frac{1}{p}} \qquad 3.8$$

The scattering of lifetime (time to 0.5 EAB_0 ($\mu \pm \sigma$)) is calculated by equation 3.9:

$$\boldsymbol{t_{\mu\pm\sigma}} = x_0 \left(\frac{A_1 - A_2}{0.5(A_1 \pm \sigma) - A_2 - 1} \right)^{\frac{1}{p}} \qquad 3.9$$

The values of end-of-lifetimes from equation 3.8 and 3.9 are tabulated in table 3.2 for the three insulator colors aged at 125 °C, 150 °C and160 °C. Accordingly, the corresponding E_a by deviated lifetimes [i.e. E_a (t_μ), $E_a(t_{\mu+\sigma})$, $E_a(t_{\mu-\sigma})$] can be estimated through Arrhenius model (equation 3.4) as tabulated in table 3.2 and drawn in Arrhenius plot in figure 3.5.

Table 3.2 E_a (KJ/mol) estimations from deviated times to 0.5 EAB_0 by technical scattering

FR-EPR Insulator color	**Times to 0.5 EAB_0 (hour)**			**Activation energy (E_a) (KJ/mol)**
	125 °C	**150 °C**	**160 °C**	
		t_μ		**E_a (t_μ)**
White	1681.61	392.32	174.90	90
Red	1709.90	445.43	187.23	87
Black	2457.25	356.32	192.16	105
		$t_{\mu-\sigma}$		**E_a ($t_{\mu-\sigma}$)**
White	1853.38	429.99	198.53	89
Red	1820.66	489.42	211.43	85
Black	3002.55	398.37	217.59	108
		$t_{\mu+\sigma}$		**E_a ($t_{\mu+\sigma}$)**
White	1525.76	357.95	154.08	91
Red	1605.88	405.40	165.79	89
Black	2010.98	318.71	169.70	101

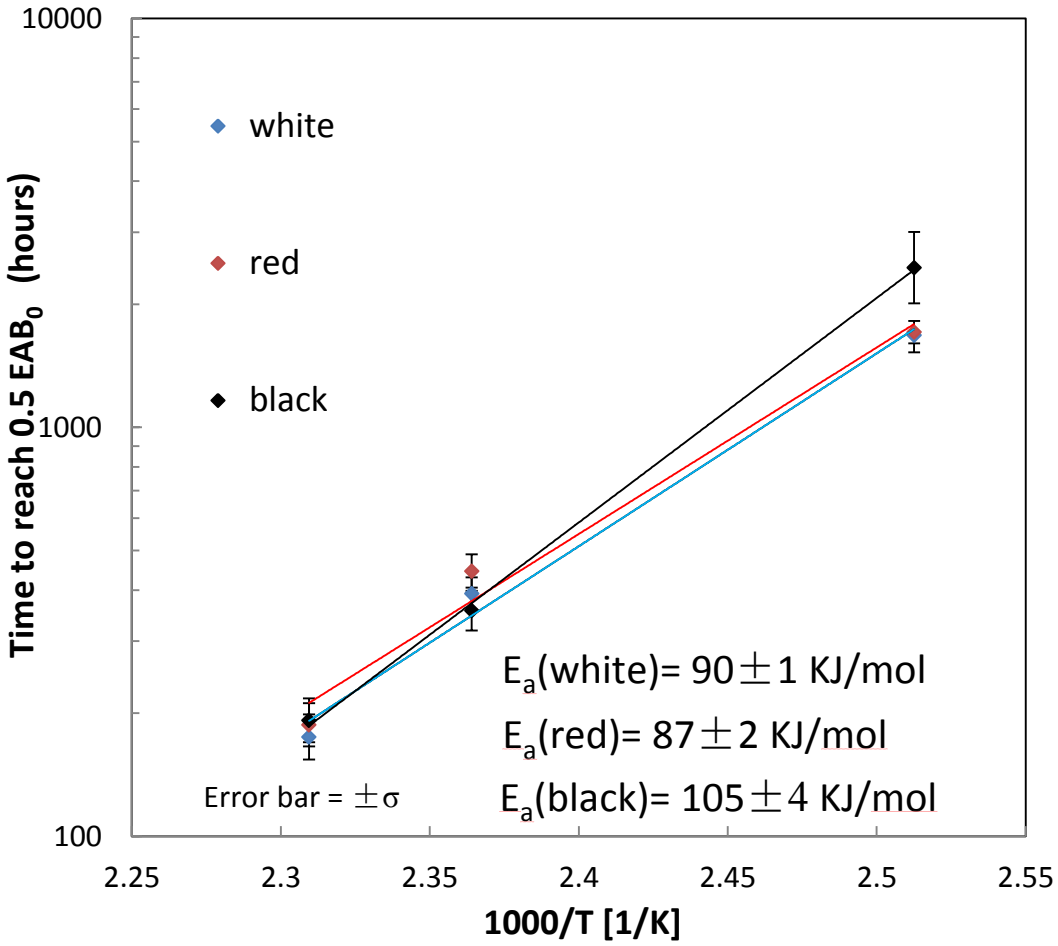

Fig.3.5 Arrhenius plot of FR-EPR insulators ageing times to 0.5 $EAB_{0\,(\mu \pm \sigma)}$

In figure 3.5, the values of E_a for both white and red insulators are very close while it largely deviates for black insulator. In addition, even if the E_a values vary within its error bars range, there will be no interference for black insulator with white and red insulators. This reveals that the effect of insulator structure by colorant pigment additives is more significant to E_a variation when compared to the effect of technical scattering. For black insulator, the higher E_a value is a result of effect of colorant pigment (carbon-black) on EAB decrement rate and thus delayed end-of-lifetimes (times to 0.5 EAB_0) compared to white and red insulators. For white and red FR-EPR insulators used in this study, the pigments materials may be titanium oxide and Azo-family, respectively that are typical colorants used for cables in JNES-SS-0903 data base since all are purchased from Japanese local makers [12]. However, the effect of these pigments on degradation progress for FR-EPR white and red insulators was not found through literature review of this study.

3.2.2 Time-temperature superposition approach

Conventional Arrhenius model analysis usually picks out single failure time corresponding to a certain amount of degradation, for example time to reach 0.5 EAB_0. However, using only single data point at each ageing temperature will waste most obtained data. Thus, time-temperature (T-t) superposition approach is involved to obtain E_a through utilizing all experimental data [56,78]. Its rational is that if degradation mechanisms are similar at range of temperature, then increasing ageing temperature will raise all underlying degradation by constant amount. This implies that higher ageing temperature curves increase ageing process by constant multiplicative shift factor (a_T), further implying that ageing curves will have same shape if plotted versus log time[56,78] which implies that a_T can follow Arrhenius behavior as in equation 3.10:

$$\boldsymbol{a_T} = e^{\frac{E_a}{R}\left[\frac{1}{(T_{ref})}-\frac{1}{(T)}\right]} \qquad 3.10$$

Where

a_T: acceleration shift factor

T_{ref}: reference temperature (master curve temperature) [K]

T : accelerated ageing temperatures higher than reference temperature [K]

Usually, The values of shift factors (a_T) are empirically estimated by superposing ageing degradation curves at higher temperatures into lower temperatures that have a_T=1 and called; reference temperature or master curve temperature [56,78]. E_a can be found from the Arrhenius plot (slope) of natural log of a_T versus inverse temperature as in equation 3.11:

$$\boldsymbol{E_a} = R\frac{\Delta(ln a_T)}{\Delta(1/T)} \qquad 3.11$$

Thanks to the developed electrode design in chapter 2 (2.3.2) for trending thermal ageing of ρ, the degradation curves of FR-EPR volume resistivity show similar trend as can be observed in figure 3.6. Accordingly, T-t is applicable to estimate a_T values that best fits superposition of degradation curves at high temperatures (i.e. 150 °C and 160 °C) to master curve at lower temperature (i.e. 125 °C). The values of a_T were estimated by empirically shifting curves that best fit their minimum ρ values. The empirically estimated a_T are summarized in table 3.3 for the three FR-EPR insulators colors aged at colors aged at 125 °C, 150 °C, and160 °C.

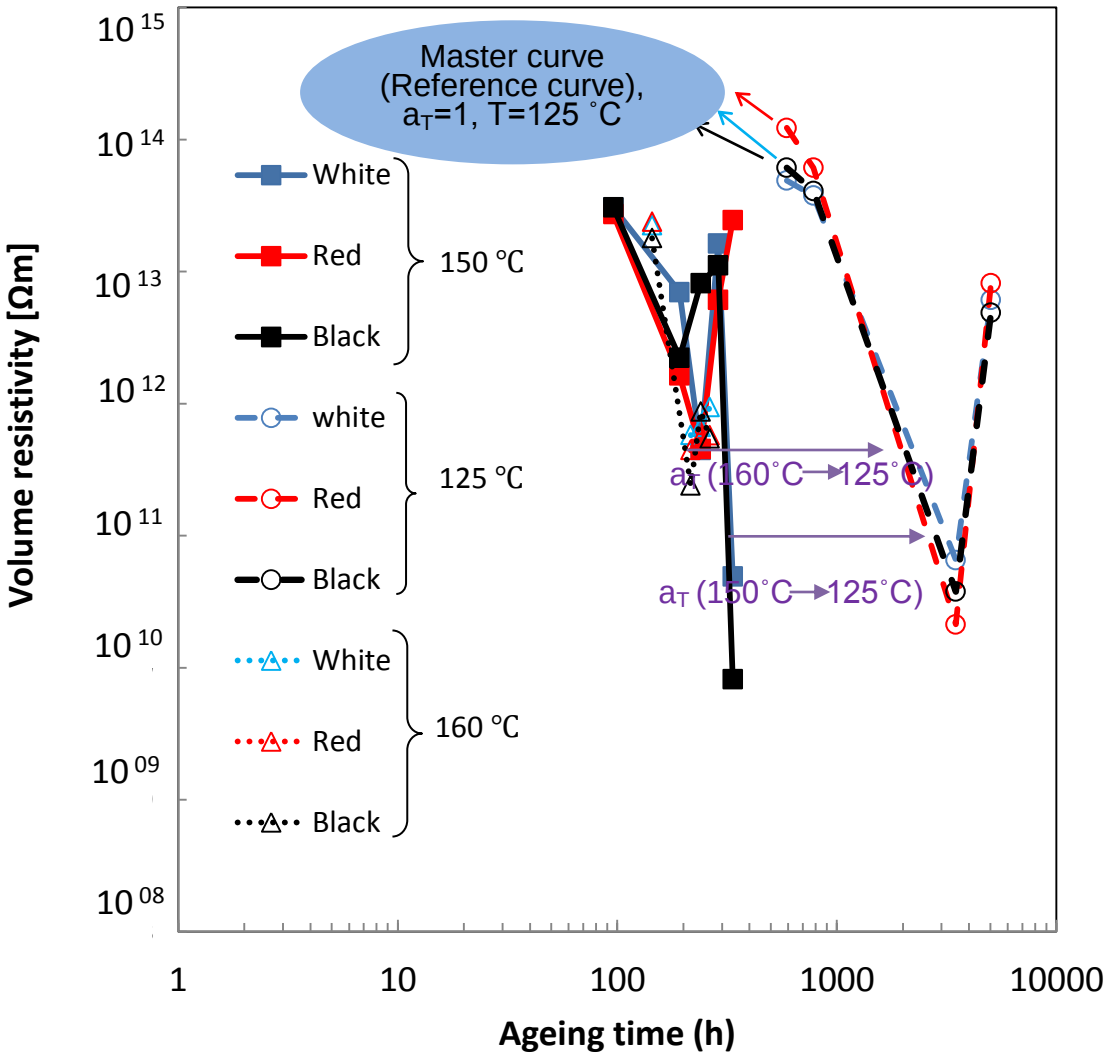

Fig.3.6 ρ degradation curves for FR-EPR thermally aged with SHPVC jacket

Table 3.3 Acceleration shift factors (a_T) values from ρ degradation curves for thermally aged FR-EPR insulators aged with SHPVC jacket

Ageing temperature	**Acceleration shift factor (a_T)**		
	White	**Red**	**Black**
125 °C	1	1	1
150 °C	11	10	11
160 °C	12	11	12

The results of T-t superposed ρ degradation curves are shown in figure 3.7. It can be noticed that ρ degradation curves at 150 °C and 160 °C properly fit master curves at 125 °C for the three insulator colors which confirm the similarity of mechanisms at each temperature.

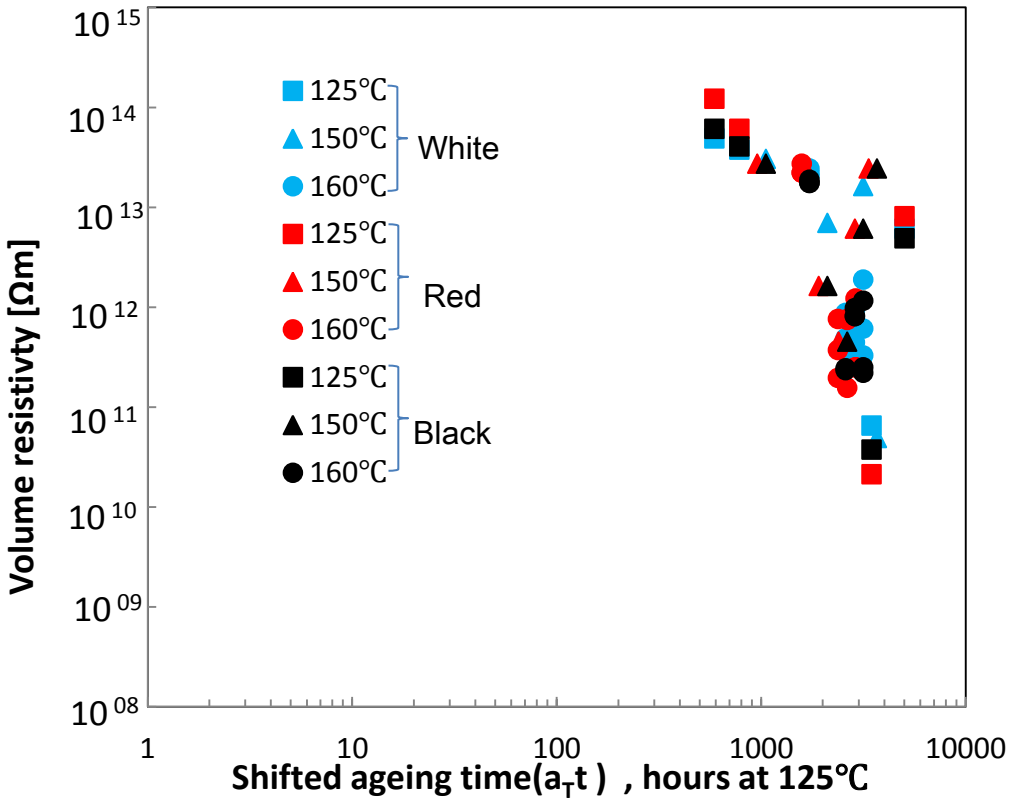

Fig.3.7 Time-temperature superposed ρ degradation curves to reference temperature of 125 ˚C, for FR-EPR thermally aged with SHPVC jacket

Hence E_a values from induced mechanisms by ρ thermal degradation can be obtained by Arrhenius plot of estimated a_T as can be seen in figure 3.8.

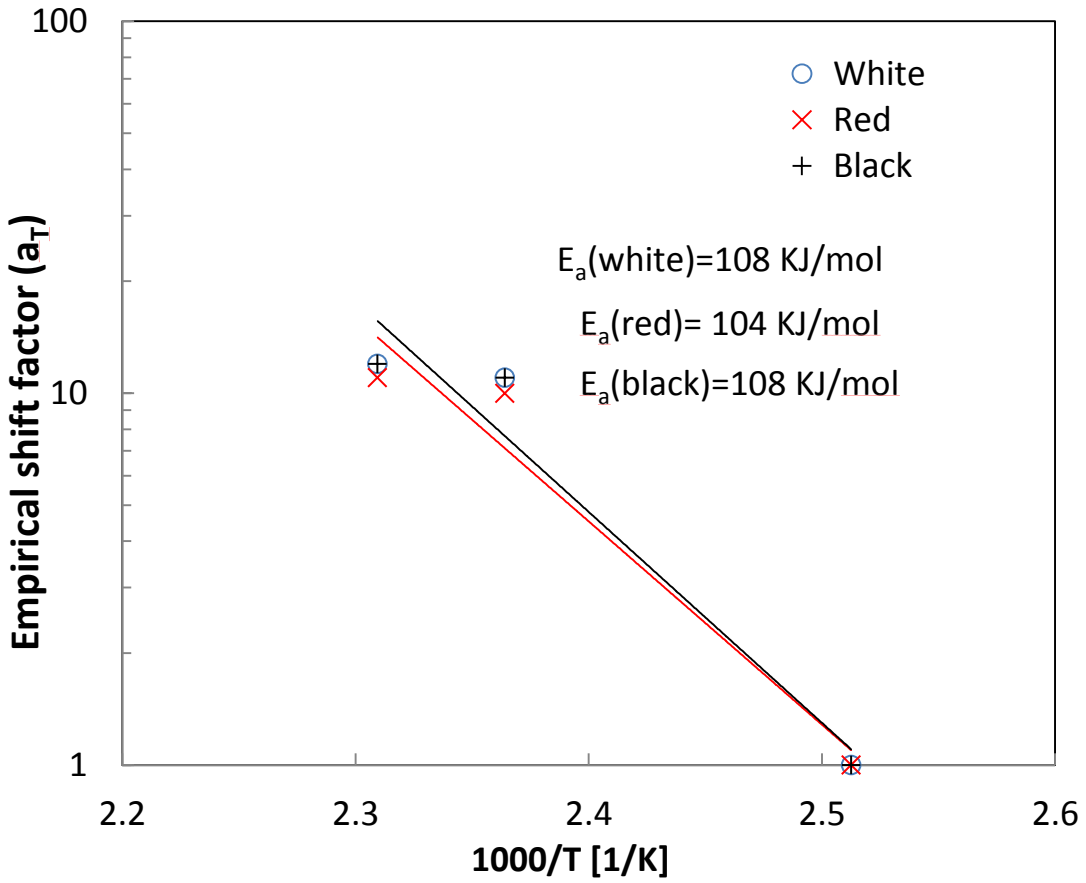

Fig.3.8 Arrhenius plot of FR-EPR insulators shift factors by ρ degradation curves superposition

For EAB degradation curves as in figure 3.9, since degradation trends have similar tendency for each color, T-t can also be applied by superposing degradation curves at high temperatures (i.e. 150 °C and 160 °C) to master curve at lower temperature (i.e. 125 °C). This requires estimating best fitted shift factor (a_T) values. Even though a_T values are usually estimated according to empirical basis [56,78], but in this study, the values of a_T were estimated by best fitting from least-square errors basis through utilizing Matlab coding and EAB degradation curves that were previously approximated by JNES-SS-0903 logistic function.

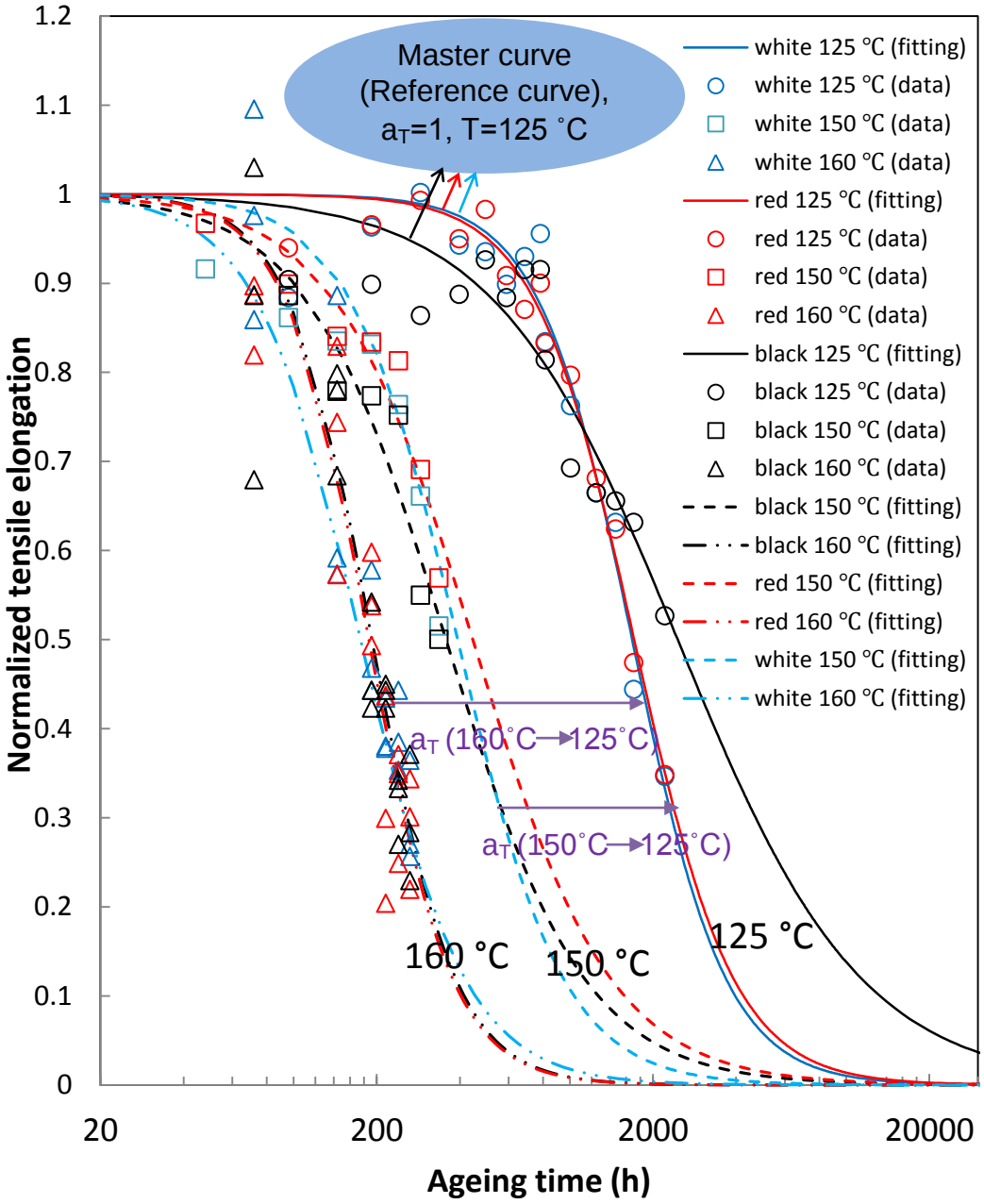

Fig.3.9 EAB degradation curves for FR-EPR thermally aged with SHPVC jacket

By utilizing JNES-SS-0903, the values of EAB at each ageing temperature were approximated as in equation 3.1. For master curve temperature of 125 °C, since EAB degradation curve is not shifted (i.e a_T=1), then EAB values are still approximated as in equation 3.1. On the other hand, at ageing temperatures 150 °C and 160 °C, EAB are superposed to master curve by corresponding a_T, accordingly the equivalent EAB values after shifting to 125 °C can be estimated by equation 3.12:

$$EAB = \frac{A_1 - A_2}{1 + \left(\frac{a_T t}{x_0}\right)^p} + A_2 \qquad 3.12$$

Besides, ageing time at temperature of 125 °C is estimated by modifying equation 3.1 into equation 3.13:

$$\boldsymbol{t_{125\,^\circ C}} = x_0 \left(\frac{A_1 - A_2}{EAB_{125\,^\circ C} - A_2 - 1}\right)^{\frac{1}{p}} \qquad 3.13$$

But for ageing temperatures 150 °C or 160 °C, the corresponding ageing times after superposition is determined by modifying equation 3.12 into equation 3.14:

$$\boldsymbol{\acute{a}_T t_{150\,^\circ C,160\,^\circ C}} = x_0 \left(\frac{A_1 - A_2}{EAB_{150\,^\circ C,160^\circ C} - A_2 - 1}\right)^{\frac{1}{p}} \qquad 3.14$$

Here, $\acute{a}_T$ is predefined vector with wide range of random numerical values. The best fitted shift factor ($a_{T\ fit.}$) is the value that achieves best superposition between degradation curves considering that degradation trends are similar. i.e.:

$$EAB_{125\,^\circ C} = EAB_{150\,^\circ C,160^\circ C}$$

This means that, $a_{T\,fit}$ is minimum difference between ageing time at 125 °C and shifted ageing times at 150 °C or 160 °C. In other words:

$$a_{T\,fit} : min. \sum (\acute{a}_T t_{150\,^\circ C,160\,^\circ C} - t_{125\,^\circ C})^2$$

A specific MATLAB M-file code was designed to find out $a_{Tfit.}$ values. These values are considered as the acceleration shift factors (a_T) from EAB degradation and tabulated in table 3.4 for each FR-EPR insulator color aged at 125 °C, 150 °C and160 °C. Both experimental and approximated EAB degradation curves are superposed based on a_T from table 3.4. The results of T-t superposed EAB degradation curves are shown in figure 3.10. It can be seen that EAB degradation curves at 150 °C and 160 °C properly fit master curves at 125 °C due to the similar induced mechanisms at each ageing temperature. For black color, tendency of

degradation is slightly varies from red and white insulators due to the impact of colorant pigment (carbon-black).

Table 3.4 Acceleration shift factors (a_T) values from EAB degradation curves for thermally aged FR-EPR insulators aged with SHPVC jacket

Ageing temperature	**Acceleration shift factor (a_T)**		
	White	**Red**	**Black**
125 °C	1	1	1
150 °C	3.74	3.28	6.95
160 °C	10.30	11.62	16.47

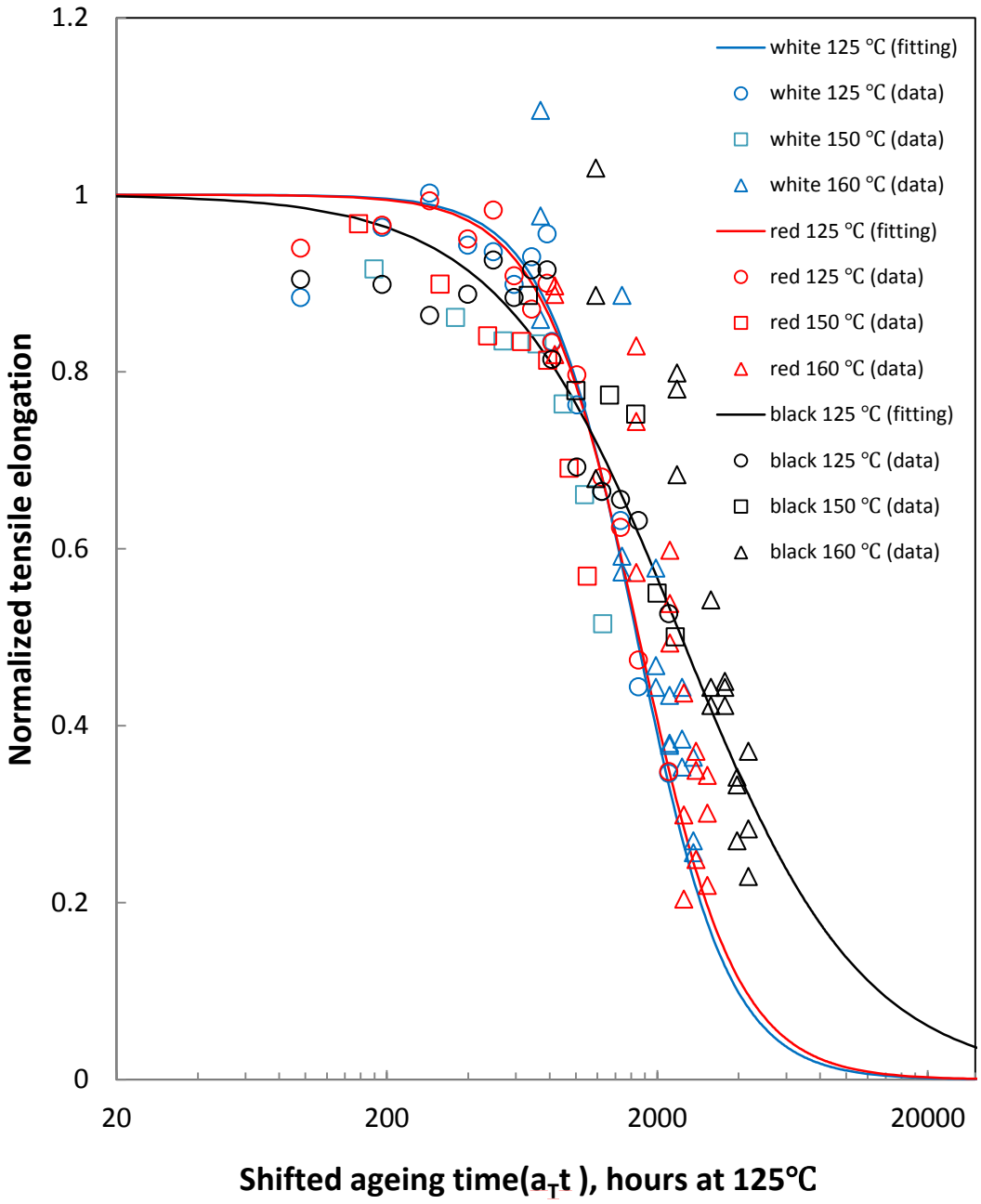

Fig.3.10 Time-temperature superposed EAB degradation curves to reference temperature of 125 ˚C, for FR-EPR thermally aged with SHPVC jacket

E_a values from induced mechanisms by EAB thermal degradation can be obtained by Arrhenius plot of estimated a_T as can be seen in figure 3.11. The E_a values are relatively close to those obtained by Arrhenius model. This reveals that thermal ageing estimations from FR-EPR insulator EAB degradation are plausible from both approaches.

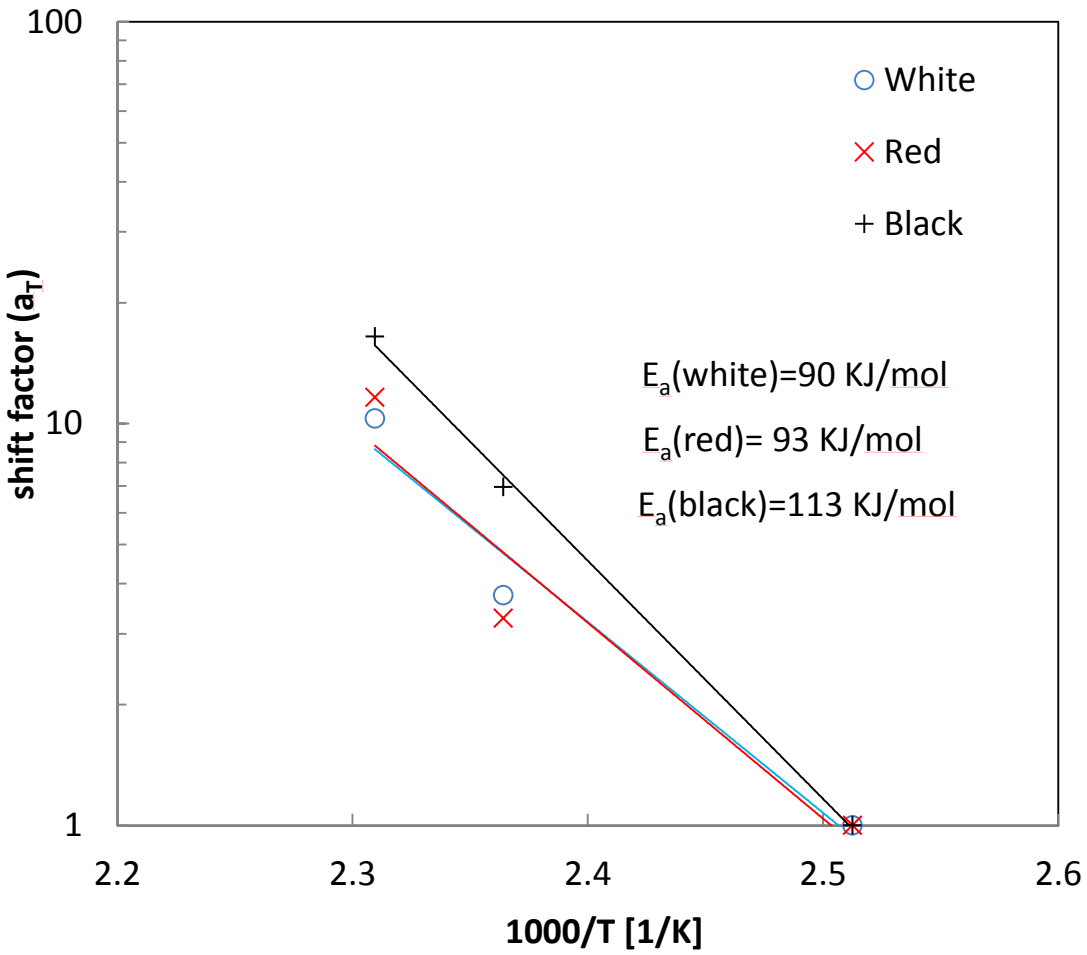

Fig.3.11 Arrhenius plot of FR-EPR insulators shift factors by EAB degradation curves superposition

3.3 Discussion on thermal ageing estimations from EAB and ρ degradations

Thermal ageing estimations from insulator mechanical and electrical properties degradations require evaluating E_a from their induced mechanisms, and examining their appropriateness to establish margins for insulator integrity against ageing at real NPP temperatures environments. Table 3.5 shows E_a values for thermally aged FR-EPR insulators from T-t superposed EAB and ρ degradation curves. The values of E_a from ρ degradation are different from those obtained by EAB degradation due to different mechanisms that alter each property. Besides, E_a variance between insulator colors is less for ρ compared to EAB. This reveals that the effect of colorant pigments on ρ chain-scission ions production is less evident when compared chain-scission and cross-linking reactions that alter EAB degradation.

Table 3.5 Activation energy (KJ/mol) values by time-temperature superposed EAB and ρ degradation curves for thermally aged FR-EPR insulators

FR-EPR insulator color	**Activation energy E_a (KJ/mol)**	
	EAB	**ρ**
White	90	108
Red	93	104
Black	113	108

On the other hand, when the supposed EAB and ρ degradation curves are trended versus their ageing times as in figure 3.12, it can be noticed that EAB values (left hand side) are gradually decreasing with ageing time and exceeding the IAEA established threshold level of half initial EAB values. In contrast, even though ρ values (right hand side) show reduction tendency, but the lowest detected ρ values are still 2-3 orders of magnitude higher than the IAEA established insulation functionality threshold of $1x10^{8}$ Ωm. This implies that thermally-induced chain scission particles from uniform-homogeneous degradation are not significant enough to facilitate larger

amount of leakage current through insulation thickness to the point that resistivity reduction exceeds functionality acceptance limits. Accordingly, the induced embrilltemnt and cracking that is evident by the gradual EAB degradation is more sufficient for cable integrity evaluations. And when considering that degradation trends are similar at normal field-aged temperatures, then the aforementioned observations is also applicable, which emphasize that thermal ageing estimations are better from trending insulator mechanical properties degradation.

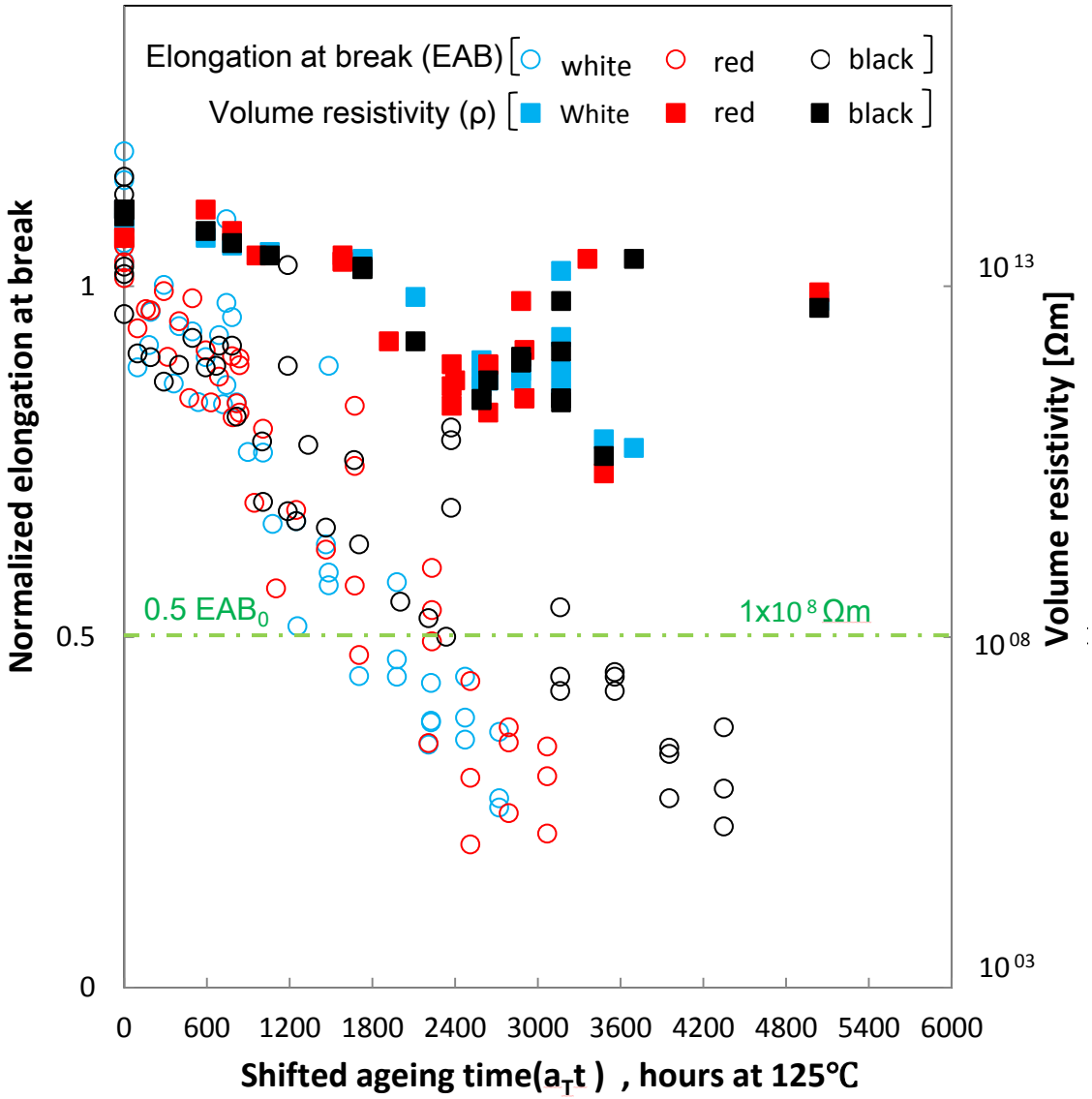

Fig.3.12 Time-temperature superposed EAB & ρ degradation curves to reference temperature of 125 ˚C, for FR-EPR thermally aged with SHPVC jacket

3.4 Comparisons of thermal ageing estimations with EAB degradation data base

Current thermal estimations are based on EAB degradation results since it is sensitive to the majority of induced degradation mechanisms within insulator material. Current research activities focus on detecting EAB for aged insulators without jacket material [12,24,25,55,56,57]. In this study EAB degradation was more severe when FR-EPR insulator environment was surrounded by SHPVC jacket material. To realize this finding, thermal ageing estimations must be considered from both ageing methods. Thus, JNES-SS-0903 EAB degradation data base from accelerating thermal ageing at 100-120 °C were utilized [12]. Two aged samples that have same insulator material as in this study (i.e. FR-EPR) were selected for comparison with FR-EPR cable of this study. Ageing method, ageing temperature range, E_a values, and prediction approach for FR-EPR insulators are summarized in table3.6.

Table 3.6 Acceleration shift factors (a_T) from EAB degradation database for thermally aged FR-EPR insulators

Insulator material		**Ageing method**	**Ageing temperature range (°C)**	**Activation energy (KJ/mol)**	**Prediction Approach**
FR-EPR	White	Insulator	125-160	90	Arrhenius
[current study]	Red	aged with		87	
	Black	jacket		105	
FR-EPR (1)	White	Insulator	100-120	85.13	Arrhenius
[JNES-SS-0903]	Red	aged with		87.34	
	Black	out jacket		84.00	
FR-EPR (2)	White	Insulator	100-120	83.81	Arrhenius
[JNES-SS-0903]	Red	aged with		85.40	
	Black	out jacket		87.23	

Even though the ageing temperature range is different between this study and JNESS-SS-0903 data base, the values of E_a are relatively close, in particular for white and red insulators. This reveals low possibility for E_a variation by physical transitions mechanisms through crystalline melting temperature points [15,56] . Accordingly, Arrhenius model is roughly considered to be appropriate methodology to compare FR-EPR insulator degradation between the two ageing methods (i.e. insulator ageing with jacket or without jacket). But for better evaluation between the two ageing methods, comparison of times to reach 0.5 EAB_0 criterion are more preferable at same ageing temperature such as 100 °C. Accordingly, the corresponding times to reach 0.5 EAB_0 at their ageing temperature values (100 °C, 110 °C and 120 °C) were regenerated for FR-EPR-1and FR-EPR-2 insulators by utilizing JNES-SS-0903 modified logistic function (equation 3.6) and approximated parameters (A_1, A_2, x_0, and p) from JNES-SS-0903 data base [12] . The calculated results of times to 0.5EAB_0 are represented by the Arrhenius plot as in figure 3.13 including the results of this study. For FR-EPR insulator aged with jacket material (this study), the ageing temperature range is 125 °C -160 °C. In order to compare with FR-EPR insulators aged without jacket material (FR-EPR-1 and FR-EPR-2) at ageing temperature 100 °C, Arrhenius model can be utilized to extrapolate time to 0.5EAB_0 from ageing temperature at 125 °C considering degradation mechanisms are similar. Thus the time to 0.5EAB_0 can be calculated as in Arrhenius equation 3.15:

$$t_1 = t_2 e^{\frac{E_a}{R}\left[\frac{1}{(273+T_1)} - \frac{1}{(273+T_2)}\right]} \qquad 3.15$$

Where

t_1: Time to 0.5EAB_0 at extrapolation temperature 100 °C [hour]

t_2: Time to 0.5EAB_0 at ageing temperature 125 °C [hour]

T_1: Extrapolation temperature (i.e. 100 °C)

T_2: Accelerated ageing temperature (i.e. 125 °C)

Times to $0.5EAB_0$ results at ageing temperature of 100 °C are shown in the extrapolation region of Arrhenius plot in figure 3.13 for FR-EPR insulators aged with jacket materials. The numerical values of times to $0.5EAB_0$ are also summarized in table 3.6 for FR-EPR insulators aged with jacket and without jacket materials.

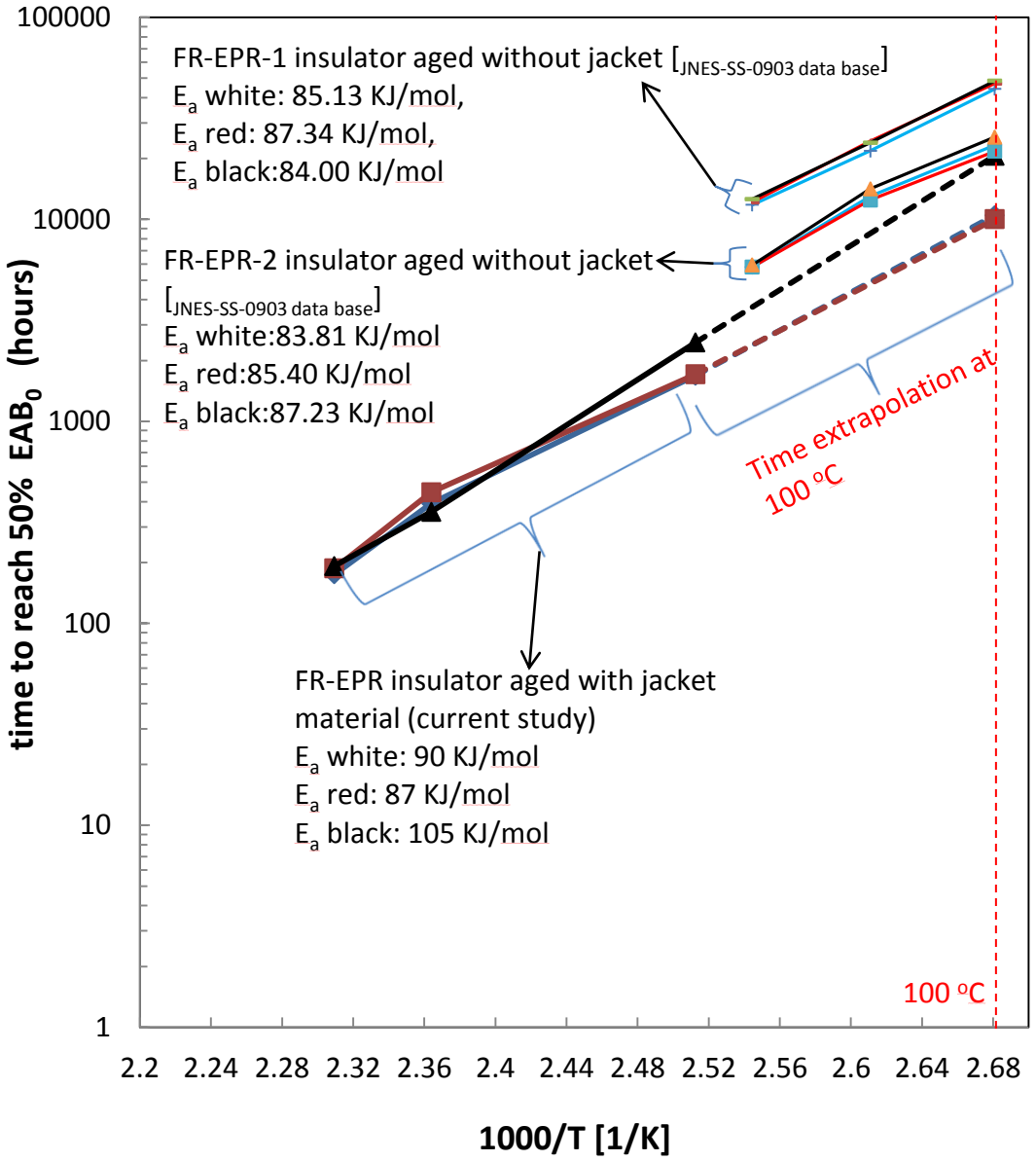

Fig.3.13 Arrhenius plot of ageing times to 0.5 EAB_0 for FR-EPR insulators aged with and without jacket materials

Extrapolation results at 100 °C show that the times to 0.5 EAB_0 are less for all FR-EPR insulators colors aged with jacket materials when compared to FR-EPR insulators aged without jacket materials. Even though insulator colorant pigments may lead to delayed degradation rates as in FR-EPR black insulator aged with jacket, the times to 0.5 EAB_0 are still (5000-28000) hours beneath corresponding times for FR-EPR-1 and FR-EPR-2 black insulators aged with no jacket as can be seen in table 3.6. Such time difference of (5000-28000) hours between ageing methods is still much higher than maximum time deviation of around ±500 hours for FR-EPR black insulator by technical scattering ($t_{\mu\pm\sigma}$) as in table 3.2. This emphasizes that the impacts of insulator pigment and technical scattering is less evident on insulator EAB reduction compared to impact of insulator environment. Further extrapolations at lower typical normal operation temperatures may lead to time imposing between black FR-EPR insulator of this study with FR-EPR -1 and FR-EPR-2 insulators. But, ageing times of FR-EPR white and red insulators of this study will remain lower than those for FR-EPR-1 and FR-EPR-2 since E_a values are very close. And since cable integrity of multi-core (multi-insulator) structure is determined from the minimum values of any of its components, then ageing time of cable at 50 °C shall be determined from the minimum value of any of the its insulators, that is white or red in this case study. In other words, the equivalent time at 50 °C is still lower for FR-EPR cable used in this study compared to FR-EPR-1 and FR-EPR-2 from JNES-SS-0903 degradation data base. This reveals that degradation rates for EAB reduction may still higher when insulator is aged within other cable components even at lower ageing temperatures. Based on these observations, thermal ageing estimations for the current environmental qualification (EQ) process shall be reevaluated as in section 3.5.

Table 3.6 Extrapolated times to 0.5 EAB_0 at 100 °C ageing from FR-EPR insulators aged with and without jacket materials

Insulator material		**Ageing method**	**times (hours) at 100 °C ageing temperature**
FR-EPR	White	Insulator aged with	10474.04
[current study]	Red	jacket	10028.50
	Black		20663.26
FR-EPR (1)	White	Insulator aged without	44273.09
[JNES-SS-0903]	Red	jacket	47117.15
	Black		48521.60
FR-EPR (2)	White	Insulator aged without	23356.45
[JNES-SS-0903]	Red	jacket	21746.03
	Black		25554.45

3.5 Considerations for thermal ageing estimations of current EQ

During environmental qualifications (EQ) process, cable is thermally aged as whole structure including jacket material and the variety of insulators colorants with different pigments additives. The basis for setting accelerated ageing test rely on available database from current cable guidelines parameters, in particular values of activation energies (E_a), accelerated ageing temperatures and accelerated ageing times [12,14,15,17,79,80]. The aforementioned knowledge is based on EAB degradation trending results for cable insulator materials aged without jacket. But based on results of this study, EAB degradation is more significant when FR-EPR insulator is aged including SHPVC jacket material, where the corresponding times to cable ageing integrity criterion of 0.5 EAB_0 were smaller than corresponding times when ageing without jacket even at ageing temperatures range similar to recommendation range from current guidelines (i.e. <120 °C) as was found in section 3.4.

Based on above, if the design basis methodology is represented as in figure 3.14, where indicator for insulator integrity is measure for degradation progress due to cable operation at ageing phase and incident phase, then the following considerations are very important for current EQ process:

1- Assuming that point 1 of figure 3.14 is the margin for ageing phase during EQ process (for example time to 0.5 EAB_0). Thus, if the degradation progress at point 1 of figure 3.14 represents the expected degradation from current EAB data base (aged only insulator), then actual degradation progress for FR-EPR cables of this study by current EQ is represented point 2 because FR-EPR insulator is actually more degraded within its whole structure.

2- This means that real degradation of FR-EPR insulator will exceed the expected planned “margin for ageing” into “margin for incident”, as can be seen in figure 3.14 where point 2 that represents real degradation by current EQ is located inside the region of “margin for incident”.

3- Even though FR-EPR insulator is more degraded compared to EQ expectations, the cable will pass the final integrity test by withstand submergence voltage test

as pre-requisite for its acceptance for operations at design basis accident (DBA) conditions.

4- This means that current EQ process is still valid and suitable for qualifying FR-EPR cables of this study. Accordingly, the margin for degradation progress in interval 3 of figure 3.14, that resulted from difference between expected thermal degradation (point 1 of figure 3.14) and actual degradation (point 2 of figure 3.14), can be converted into excessive margin for integrity (interval 4 of figure 3.14) which can be utilized for modification of current EQ at DBA conditions as will be illustrated more thoroughly in chapter 4 (section 4.5).

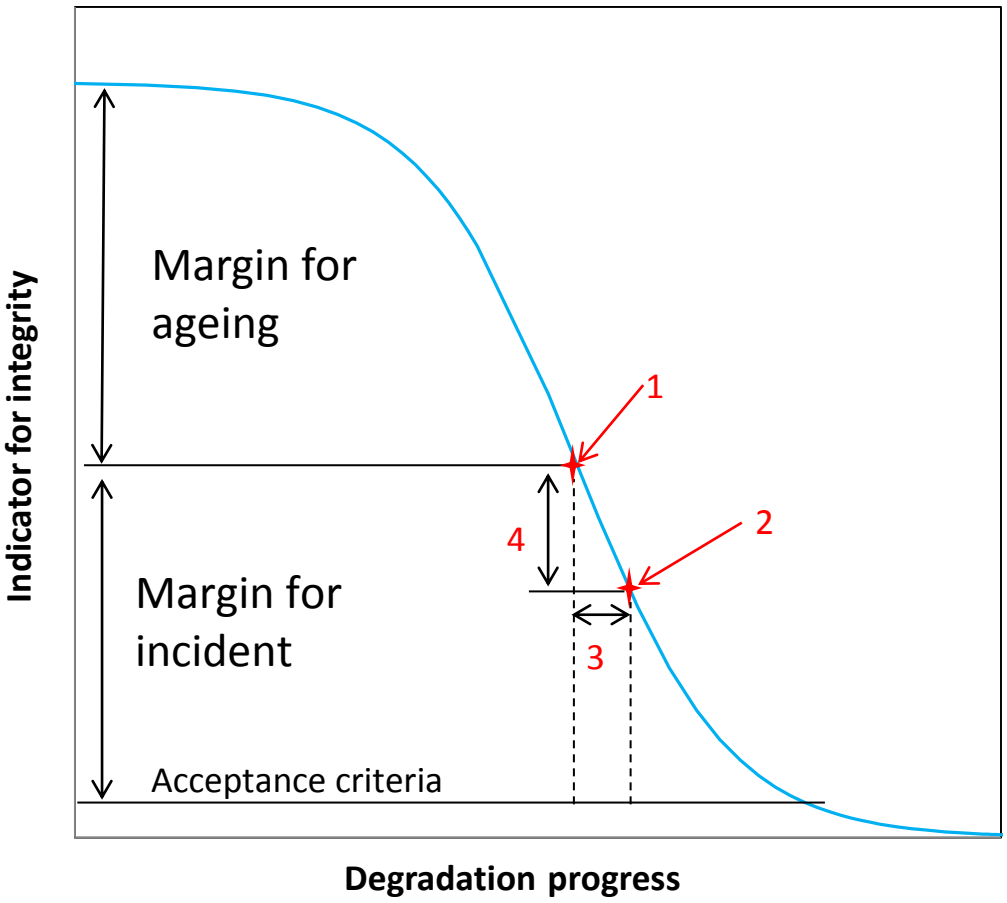

Fig.3.14 Perception of design basis methodology for cable EQ

Chapter 4 In search of design extension environments for NPPs cables

The objective of this chapter is to identify the important cables regarding design extension conditions (DECs) and propose modification of environmental qualification (EQ) process at design basis accident (DBA) phase to suit with some elevated accident scenarios accompanying DECs. In section 4.1, 18 targeted electric components were identified for boiling water reactor-4 (BWR-4) case study based on engineering judgment between plant systems understanding with 14 established severe accidents. In section 4.2, a proactive approach is introduced to establish knowledgeable-based guidelines from the identified targeted cables with their predicted cable failure phenomena through multi stress factors. In section 4.3, a methodology for cable evaluations was discussed in light of possibility for modification of current cable EQ process. Among the multi-stress factors, both DBA-peak temperature and submergence withstand voltage are considered necessary parameters for reevaluations of current EQ, thus generic approach is presented in section 4.4 for evaluating these parameters. Finally, it is found that current DBA peak temperature can be extended from remaining margins of EAB ageing and incident acceptance criteria. The DBA peak temperature trend shows possibility to increase from current value of 171 ℃ up to value range 230 ℃-250 ℃.

4.1 Cables identifications for design extensions conditions (DECs)

The start point of this study for cables identifications is based on the objectives of accident management as identified by IAEA safety guide No. NS-G-2.15 “severe accident management program (SAMP) for NPPs” [81]. The objectives “top-level” of accident management should be defined as follows [81]:

1- Preventing significant core damage.

2- Terminating the progress of core damage once it has started.

3- Maintaining the integrity of the containment as long as possible
4- Minimizing the release of radioactive materials.
5- Achieving a long term stable state.

These objectives reveal that "core melting start" event has been already affirmed or it will soon evolve after beyond-DBA (BDBA) conditions, unless preventive or corrective actions were taken to achieve these objectives. The role of cable to achieve these objectives is primarily based on identifying and evaluating its corresponding electric equipment that:

1- Keep water inventory to core cooling injection from fire water system. [i.e. achieve IAEA No.NS-G-2.15 objectives 1 and 2]
2- Keep containment vessel integrity and keep fission radioactive productive inside (components for fission products physical barrier and containment vessel ventilation)[i.e. achieve objectives 3 and 4]

Electric equipment identification by this study considered also requirements for NPP design activities that were established by IAEA safety standards series SSS- No. NS-R-1 (paragraph 5.31) [82]. These requirements consider addressing severe accidents through identifying important event sequences that may lead to sever accidents by using a combination of engineering judgment and probabilistic/deterministic methods, in addition to considering plant's full design capabilities including possible use of some systems (i.e. safety and non-safety systems) beyond their originally intended function and anticipated operational states.

In this study, boiling water reactor model 4 (BWR-4) NPP (such as Brown's Ferry units 1,2,3 & FUKUSHIMA Daiichi units 2,3,4,5) was focused for the scope of targeted cables identifications and later activities of this chapter (section 4.5). The reason behind BWR-4 focus was because this model witness two famous accidents: 1) Brown's Ferry fire accident in 1975 that resulted in safety systems spurious initiation by "hot-shorted" cables[8,9], and 2) Fukushima Daiichi units 2-5 loss of emergency power supply (metal clad (M/C) and power center (P/C)) for some emergency core cooling systems (ECCSs) by tsunami submergence in 2011 [83,84].

With all above in mind, electric equipment identification for BWR-4 NPP is

based on engineering judgment between:

1- Analyzing accident sequence parameters profiles from probabilistic and deterministic risk approaches established by NUREG/CR 2825 and NUREG/CR 2182 for BWR-4 NPPs [63,64].
2- Understanding plant systems operation and process control from General Electric (GE) systems technology manuals for BWR-4 NPP.[85,86,87,88,]

In NUREG/CR 2182 "Station Black out at Browns Ferry Unit One-Accident Sequence Analysis" [63], 6 accidents sequences resulting in core melting and initiated from prolonged complete station black out (CSB) have been identified by the following titles:

1- TB': Originated from CSB+ high-pressure coolant injection(HPCI)/reactor core isolation cooling (RCIC) systems are inoperable due to loss of DC power form unit batteries.
2- TPB': Originated from CSB+ HPCI/RCIC are inoperable due to loss of DC power form unit batteries + a stuck-open relief valve (SORV; that corresponds to small LOCA).
3- T_vB': Originated from CSB+ loss of vessel level/pressure manual control by RCIC& safety relief valve (SRV) due to loss of DC power from unit batteries.
4- T_vPB': Originated from CSB+ loss of vessel level/pressure manual control by RCIC& safety relief valve (SRV) due to loss of DC power from unit batteries+ SORV(or small LOCA)
5- TUB': Originated from CSB+ loss of HPCI/RCIC due to mechanical failure.
6- TUPB': Originated from CSB+ loss of HPCI/RCIC due to mechanical failure+ SORV(or small LOCA)

In NUREG/CR 2825 "BWR 4/ Mark I Accident Sequences Assessment " [64], 8 accidents resulting in core melting and containment breach were studied and considered as dominant contributors to public risk at a BWR according to Reactor Safety Study [89]. These accidents are initiated from large/small loss of coolant accident (LOCA) and anticipated transients events as titled as below:

1- TW: Anticipated transient initiating from loss of main condenser vacuum, and followed by loss of decay heat removal. Onsite and offsite AC power assumed available.
2- TC: Anticipated transient without scram. Manual rod insertion and standby liquid control (SLC) systems are assumed unavailable.
3- TQUV: Anticipated transient combined with failure of HPCI, RCIC, and low-pressure emergency core cooling system (LPECCS).
4- AE: Large LOCA with failure of emergency coolant injection (ECI).
5- S_1E: Small LOCA with failure of HPCI and LPECCS.
6- S_2E: Small LOCA with failure of HPCI, RCIC, and LPECCS.
7- S_2I: Small LOCA with failure of low pressure coolant recirculation system LPCRS.
8- S_2J: Small LOCA with failure of residual heat removal service water RHRSW system for cooling RHR heat exchangers. LPCI mode of RHR system is available for suppression pool cooling.

Accident progression signatures (accident parameters profiles) for all above 14 sequences were calculated by MARCH thermal-hydraulic computer codes based on ANS-5.1 standards [90]. In order to facilitate extracting targeted electrical components by this study, the coordination of these components were deliberately selected from General Electric (GE) technology manuals that contain majority of these components locations within BWR-4 [87,88], as can be seen in figures 4.1 and 4.2. The equipment inside figures are numbered according to their order in the below discussion during equipment selection. The results of selected equipment from figures 4.1 and 4.2 are categorized according to the impact of their failure on severe accident progression as summarized in figure 4.3.

Figure 4.1 shows an overview of reactor pressure vessel (RPV), primary containment vessel (PCV), automatic depressurization system (ADS) safety relief valves (SRVs), and RHR/LPCI injection valves for BWR-4 model. From these systems, electric equipment for core cooling injection, primary containment integrity in addition to some monitoring instrumentations can be extracted as characterized in

the below numbered discussion from 1-8 (corresponding to the same numbers inside figure 4.1):

1- After failure of all typical success criteria for ECCS pumps (i.e. HPCI, LPCI , low pressure core spray (LPCS)) and high pressure service water (HPSW) pumps [91], the last emergency countermeasure to provide cooled water into RPV and PCV is firewater system. Such systems is characterized by large flow rate of 2500 gpm, and discharge pressure of 120 psi [92]

2- The cascaded LPCS injection motor operated valves (MOVs) (box no. 2 in figure 4.1) on the discharge paths from system I (electrically supplied by division I) and system II (electrically supplied by division II) shall be remote-manually operable for RPV core cooling through semicircular spray headers (spargers). The motors of these valves are electrically supplied from the 480 Vac emergency power system buses, in particular motor control centers (MCC). LPCS injection valves motors are categorized in figure 4.3 as important electrical equipment for mitigating accident, in particular for core cooling injection from firewater systems.

3- The cascaded RHR/LPCI mode injection MOVs (box no. 3 in figure 4.1) on the discharge paths from system I (electrically supplied by division I 480 Vac MCC) and system II (electrically supplied by division I 480 Vac MCC) shall be remote-manually operable in order to restore and maintain core water level inventory. LPCI injection valves motors are categorized in figure 4.3 as important electrical equipment for mitigating accident, in particular for core cooling injection from firewater systems.

4- The cascaded RHR/containment spray mode drywell (DW) spray sparger supply MOVs (box no. 4 in figure 4.1) from systems I& II (electrically supplied by division I&II 480 Vac MCC) shall be remote-manually operable to condense radioactive steam mixture for PCV pressure and airborne activity reduction. The DW spray sparger valves motors are categorized in figure 4.3 as important electrical equipment for mitigating accident, in particular for fission products barrier and PCV ventilation.

5- The cascaded RHR/containment spray mode suppression chamber spray headers supply MOVs (box no. 5 in figure 4.1) from systems I& II (electrically supplied by division I&II 480 Vac MCC) may not be necessary for operation, since suppression pool water temperature almost remain below 60 °C as can be seen from temperature profiles of AE, A_1E and S_2E accident sequences [64]. But if the Zircaloy-water (Zr-H_2O) decomposition reaction begins, then the valves are required to cool pool water and prevent temperature rapid increase from 57 °C to 227 °C as in temperature profile of TUB' accident sequence [63].With all above in mind, suppression chamber spray headers supply valves motors are attached with DW spray spargers as one component in figure 4.3.

6- The ADS equipped air/nitrogen (N_2) pilot SRVs are required for automatic rapid depressurization of RPV below 150 psi to enable low-pressure core water level inventory. Among 11-13 total SRVs , only 6-7 SRVs are assigned for ADS [63,85]. Each ADS/ SRV is controlled by two solenoid coils from two channels "A" and "B". Channel "A" is electrically supplied from division I 125Vdc panels, while channel "B" is supplied from division II 125 Vdc panels. Only 2 of (11-13) SRVs solenoid coils are required to be remote-manually operable [91]. The ADS/SRV solenoid coil is categorized in figure 4.3 as important electrical equipment for mitigating accident, in particular for core cooling injection from firewater systems.

7- There are 37-46 copper–constantan temperature thermocouples (TCs) distributed at RPV vessel, vessel top head , head stud and vessel/head flange in order to evaluate vessel thermal stress [86]. The corresponding instrumentation cables of these TCs are connected to junction box located inside DW. The maximum indicating range for these TCs is 315.6 °C. When TCs located near vessel bottom reach maximum range (315.6 °C), the operator confirms core uncovery. But following core melting start event, the expected maximum core temperature can raise to 4727 °C as long as core is not cooled as can be seen from temperature profiles at AE sequence [64]. This means that

TCs can not indicate RPV temperature during elevated accident scenarios. Besides, TCs instrumentation cables installed inside DW will certainly melt and electrically fail when considering that the DW temperature can raise to 927 °C -1200 °C as can be tracked from temperature profiles of TUB',S_1E and S_2E accident sequences [63,64]. Nevertheless, the expected failure of RPV TCs with elevated accident scenarios is not necessary for mitigating accident progression, thus RPV temperature thermocouples are categorized in figure 4.3 as supplementary electric components, in particular for monitoring instrumentations.

8- The pressure and temperature sensors mounted inside DW are useful for monitoring accident parameters until their maximum design range. DW For pressure sensor, the maximum detectable value is 5.5 Bar [63]. DW pressure will raise between 2-9 Bar (until containment venting due electric penetration assembly (EPA) elastomer seal failure by over temperature at 260 °C) and may continue rising until containment over pressure failure at 12.2 Bar as can be tracked from AE accident sequence parameters [64]. DW temperature sensors are not expected to be operable when considering that DW temperature can raise to 927 °C -1200 °C as can be tracked from temperature profiles of TUB',S_1E and S_2E accident sequences [63,64]]. On the other hand, DW pressure and temperature sensors are not vital in light of mitigating severe accident progression. Thus, DW temperature and pressure sensors are categorized in figure 4.3 as supplementary electric components, in particular for monitoring instrumentations.

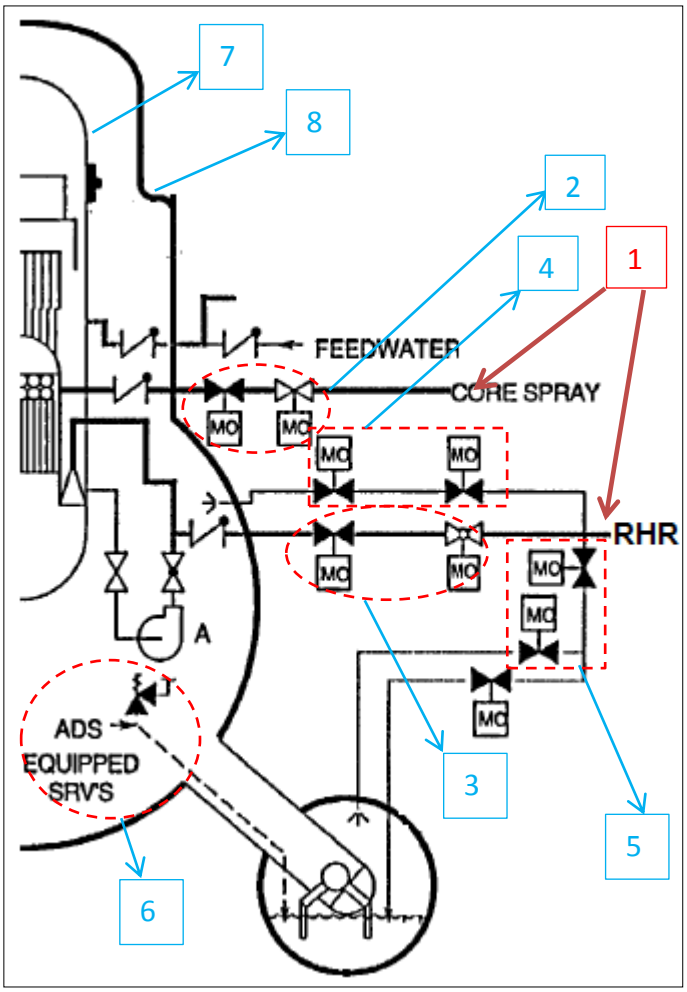

Fig.4.1 BWR-4 cut view for RPV, PCV, RHR/LPCS injection valves, and ADS SRVs from system I side

Figure 4.2 shows an overview of primary containment auxiliary systems for BWR-4 model. From these systems, electric equipment for, primary containment integrity and some monitoring instrumentations can be extracted as characterized in the below numbered discussion from 1-8 (corresponding to the same numbers inside figure 4.2):

1- During DBA , primary containment auxiliary systems will automatically isolate (at high drywell pressure signal (1.7 psig), RPV level 2 signal, etc.). All primary containment purging/inerting and venting valves automatically close. At same time, reactor building standby ventilation system (RBSVS) automatically initiates to keep containment pressure less than outside pressure by (0.25-0.3) inch water gage and limit radiation does to less than limit

requirements established in 10CFR100. But considering elevated accident scenarios beyond their design basis, primary containment pressure can increase beyond its design basis (3.3 Bar)[88] until containment overpressure failure at 12.2 Bar according to AE accident sequence [64]. At such scenarios, the RBSVS functionality to keep same differential pressure is questionable. Accordingly, to keep primary containment integrity and limit radioactive fission products, a venting path starting from suppression chamber until exhaust stack (green path with box no. 1 in figure 4.2) shall be remote-manually initiated. The start point for venting shall be from suppression chamber side not DW side for these reasons:

a. The relapsed water and steam during accident into DW environment will increase DW pressure and hence force the released mixture into suppression pool through the interconnecting downcomers vents. This leads to temporary reduction in DW pressure before pressure is re-equalized by vacuum breakers. If DW is directly vented, then higher dose levels can release through station ventilation exhaust into exhaust stack. While by selecting venting from suppression chamber side, the leaked radioactive dose will be limited because the suppression chamber will seize the released fission products during its transfer from dwncomers vents.
b. Venting suppression chamber will reduce hydrogen amount initiated by Zr-H_2O decomposition reaction which is responsible for sharp increment of suppression chamber temperature and pressure as can be observed from TUB' accident sequence parameters profiles [63]. Accordingly, venting suppression chamber will reduce pressure and can make chamber cooling, which can in turn leads to enhanced water inventory to DW spray spargers and core cooling injection considering that RHR injection valves are supplied from same source (such as firewater system)

2- Based on above discussion, the cascaded suppression chamber venting air pilot directional valves (two upper valves of box no. 2 in figure 4.1) shall be remote-manually operable for PCV venting from suppression chamber side. The cascaded suppression chamber purging air pilot directional valves (two lower valves of box no. 2 in figure 4.1) can also be utilized as a back-up in case. The solenoid coils of directional valves are electrically supplied from the 125 Vdc distribution buses. The solenoid coils of these valves are categorized in figure 4.3 as a electric components for fission products physical barrier (venting valves) , and as a back-electrical components for mitigating accident (purging valves).

3- The isolation damper valve and fan of the primary containment purging system (PCPS) (above cascaded equipment of box no. 2 in figure 4.2) shall be remote-manually operable for processing primary containment effluent atmosphere prior to release. The PCPS filter consists of high efficiency particulate absolute (HEPA) filter that remove radioactive particles of 0.3 micron size and larger with 99.95 % efficiency, and charcoal filter for removing 99.95 % of radioactive iodine in the form of elemental iodine and 85 % of radioactive iodine in the form of methyl iodine. The fan beyond the filter system flow and delivers 1000 scfm at 8.5 inches water gage pressure. Besides, the bypass purge exhaust fan and valve (the below cascaded equipment of box no. 3 in figure 4.2) can be utilized as a back-up in case of PCPS filter train failure. The fan motors and solenoid coils of these equipment are categorized in figure 4.3 as a electric components for fission products physical barrier (PCPS filter fan and damper valve) , and as a back-electrical components for mitigating accident (purge exhaust fan and valve).

4- Reactor building exhaust fans and outlet isolation dampers (cascaded equipment of box no. 4 in figure 4.2) can be maintained operable as supplementary equipment for secondary containment recirculation. The reactor building has three exhaust fans (45000 scfm each). Two of these three exhaust fans are usually in operation providing 100% capacity (90000 scfm)

exhaust flow. The failure of these components will not affect the initiated venting path for radioactive fission products. Besides, the impellers of inoperable exhaust fans can still isolate secondary containment from discharged steam mixture in the venting line. Accordingly, the fan motors and damper solenoid coils of these components are categorized in figure 4.3 as back-up electric components for mitigating severe accident.

5- Reactor building ventilation exhaust radiation sensor (box no. 5 in figure 4.2) is selected for monitoring radiation level of vented steam. This sensor is categorized in figure 4.3 as a monitoring instrumentation.

6- Reactor building standby ventilation system (RBSVS) mixing plenum inlet (MOVs) (box no. 6 in figure 4.2) shall be remote-manually closed in order to isolate secondary containment from excessive steam pressure which can reach 12.2 bar according to AE accident sequence parameters profiles[64]. Accordingly, valve motor is categorized in figure 4.3 as electrical components for fission products physical barrier and PCV ventilation.

7- The cascaded reactor building exhaust isolation valves (box no. 7 in figure 4.2) shall be remote-manually open for directing the steam mixture to the exhaust stack. The valves solenoids coils are categorized in figure 4.3 as electrical components for fission products physical barrier and PCV ventilation.

8- The station ventilation booster exhaust fan (box no. 8 in figure 4.2) shall be remote-manually open for diluting discharged steam mixture. The fan motor categorized in figure 4.3 as electrical components for fission products physical barrier and PCV ventilation.

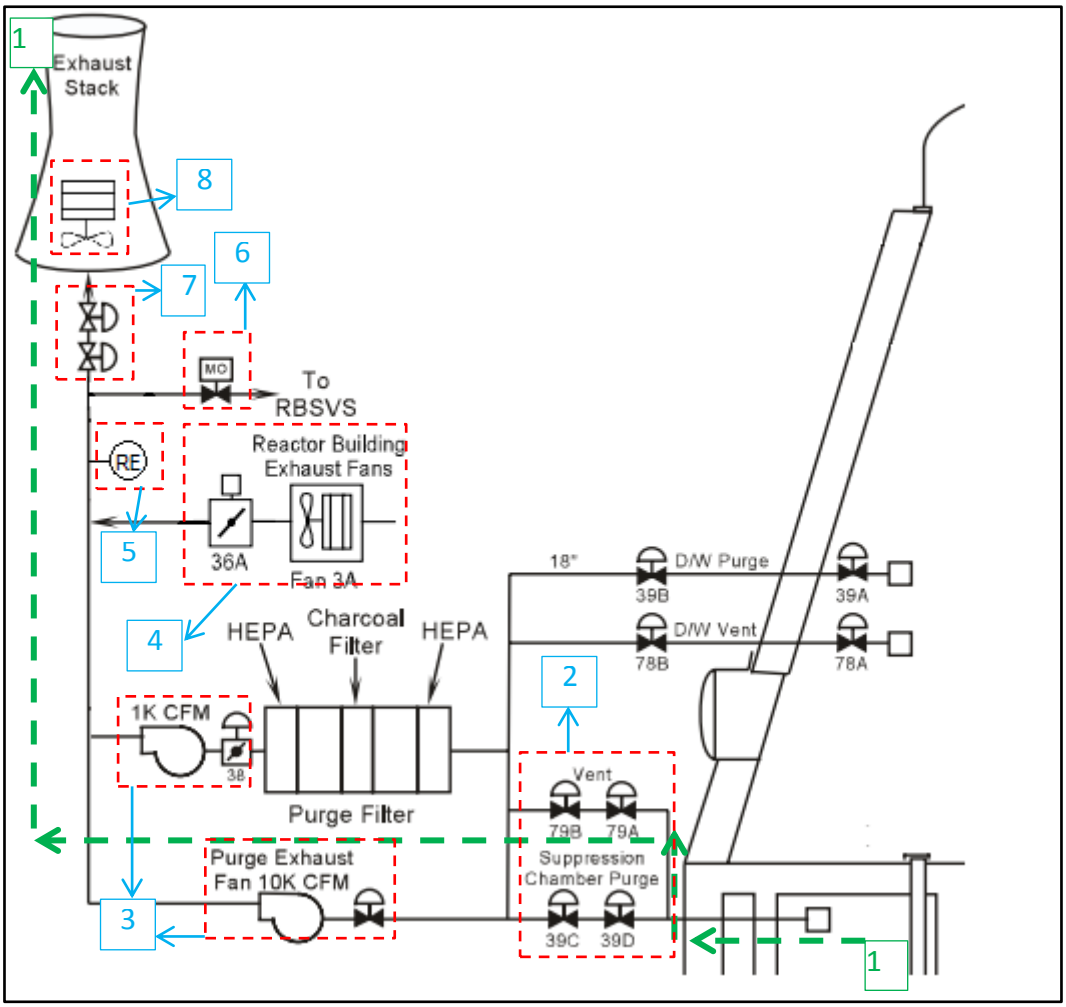

Fig.4.2 BWR-4 cut view for primary containment auxiliary systems

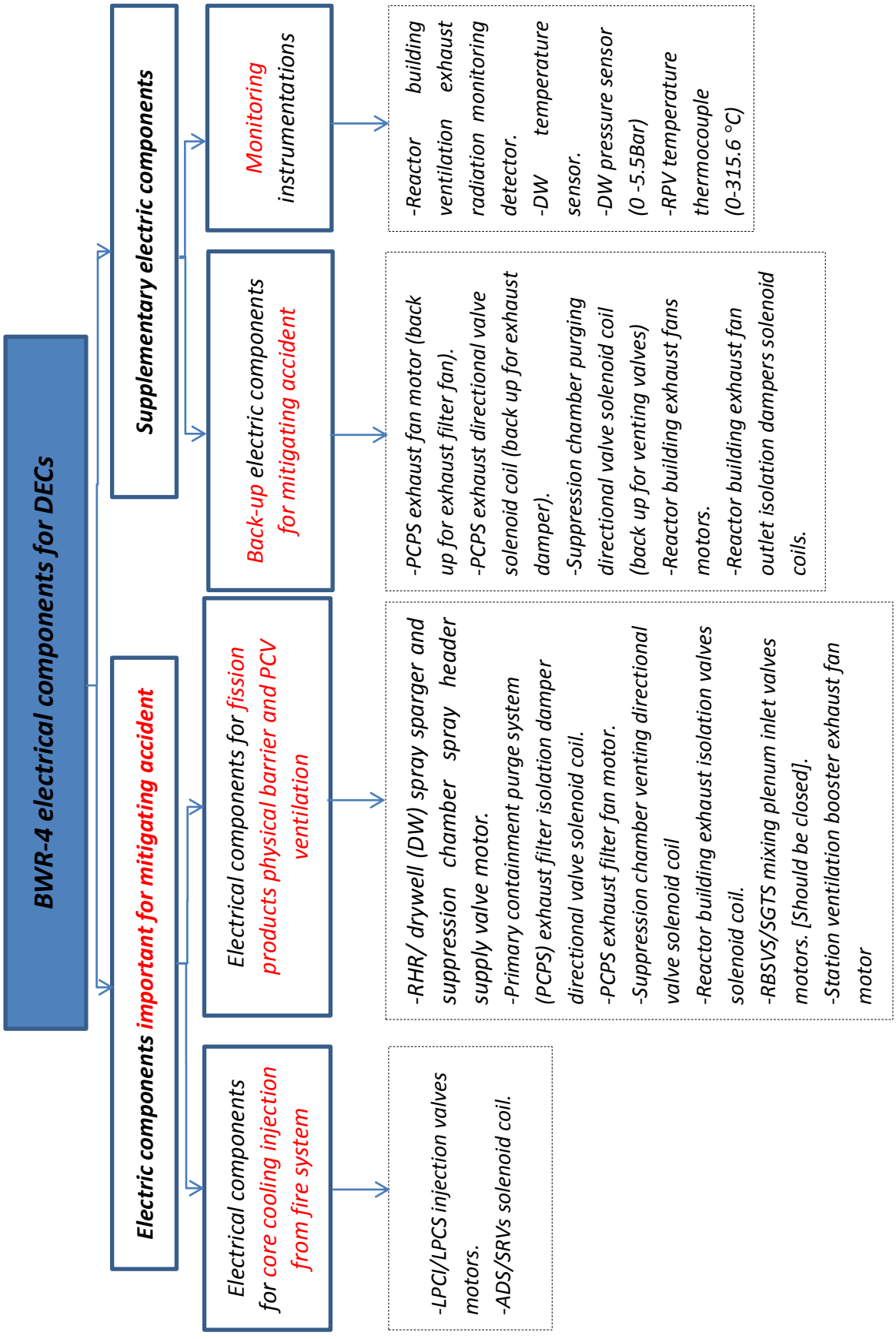

Fig.4.3 BWR-4 electrical components for design extension conditions

4.2 Knowledgeable-base proactive approach for targeted cables regarding DECs

The identified targeted electric equipment and their cables regarding DECs are systemically coordinated with other three items to establish a proactive approach for predicting failure phenomena at elevated accidents scenarios as can be seen in figure 4.4. The data base for these items are collected from understanding NPP model technical manuals (such as GE systems technology manuals for BWR-4 model [87,88,85,86]), probabilistic/deterministic approaches (such as NUREG/CR 2182 and NUREG/CR-2825 for BWR-4 accident analysis [63,64]), in addition to knowledge from experienced accidents (such as TEPCO technical reports after FUKUSHIMA Daiichi accidents for BWR-4 model [83,84]). Collecting the required information for each identified components will flow into developing knowledgeable-base in the form of technical guidelines. An example of such guidelines can be seen in Annex 2 for FUKUSHIMA Daiichi unit 2 BWR-4 ADS/SRV as a case study.

In figure 4.4, each identified component (as those for BWR-4 case study shown in figure 4.3) is the primary item including details about its safety function (functional classification and designed function) and rated voltage/power (such as 125 Vdc, 3ϕ 480 Vac). Features and interfaces with other systems are also useful for thorough understanding during analysis of cable failure modes. The second item “cable installation locations” should include the detailed locations from both cable ends; equipment side (such as reactor building basement outside PCV), and nearest power/signal side (such as junction box, electric penetration assembly (EPA), metal clad/high voltage switch gear (MC), power center (PC), motor control center (MCC)). These identified locations can save times and efforts for tracking sources of errors between cables ends once they occur during accident. The third item “cable failure phenomena” determine expected impact on cable integrity initiated from mainly four stress factors (BDBA temperature, fire, earthquake, and flooding). BDBA temperature or fire result in cable melting, earthquake may result in cable cut/wear while flooding can lead to water intrusion. Cable failure modes initiated from aforementioned events

depend on cable category which was assigned for the fourth item. The instrumentation cables (such as twisted pair, coaxial and triaxial cables) can deliver attenuated signal or erroneous measurements from associated sensors when cable is molten, cut or flooding-immerged. For control and power cables with low voltage (LV) and medium voltage (MV) ratings (such as multi-conductors cables), the failure modes can be either by:

1- Short circuit between two conductors (such as phase-phase) or ground short due to cable melting, cable cut or water intrusion.
2- Power/signal loss due to loss of single phase or multi-phases as result of possible cable cut during earthquake.

Failure modes of identified cables can lead to spurious initiation or termination of other components that are electrically connected by logic –interfered systems. In same manner, the failure of logic-interfered components can lead to spurious initiation or termination of the targeted equipment. Accordingly, this approach addressed the impact of mutual cable failure initiating events between targeted equipment and the logically interfered equipment as can be seen in ADS/SRV case study (annex 2).

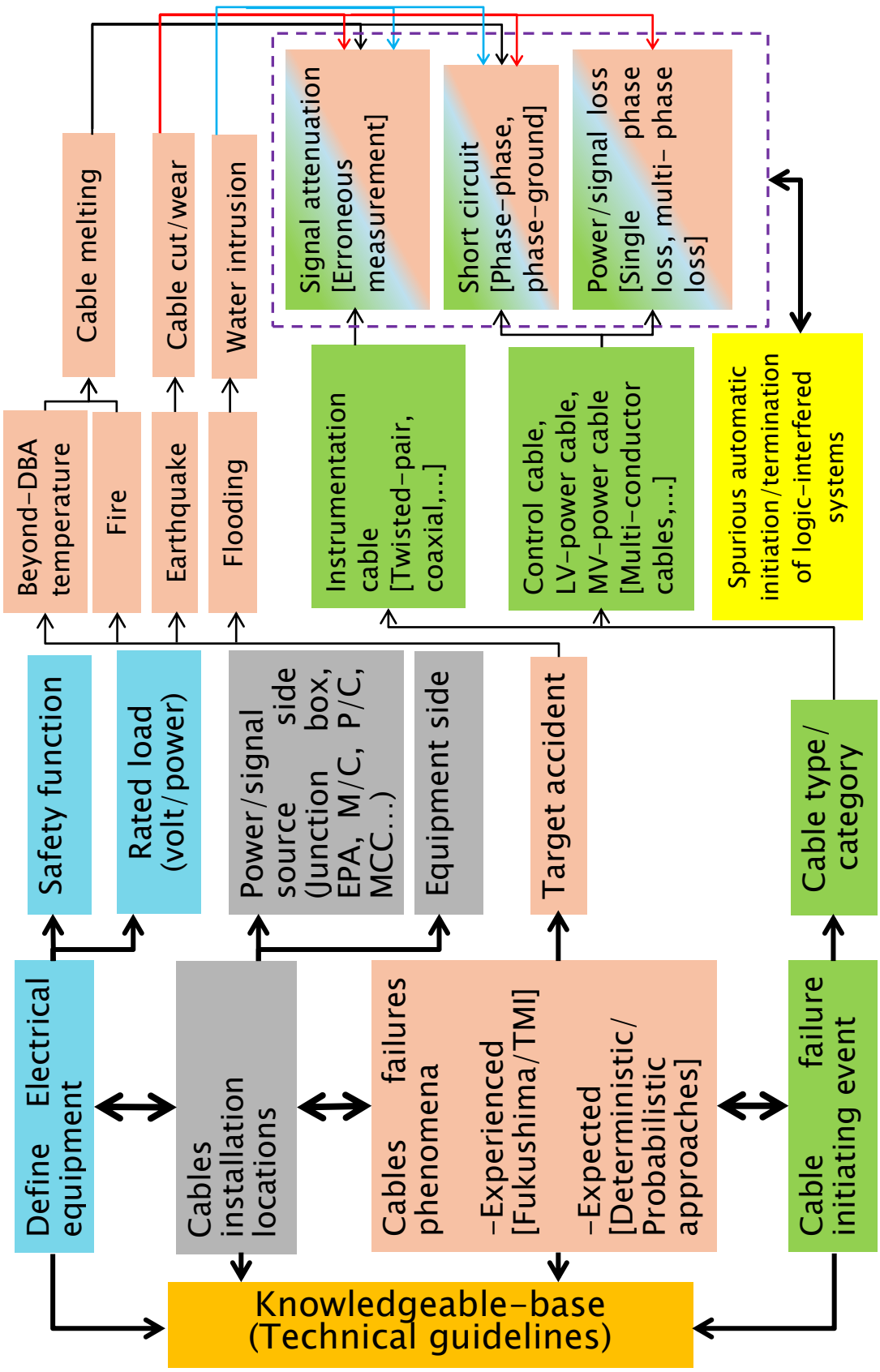

Fig. 4.4 Proactive approach for establishing knowledgeable-base guidelines from targeted cables regarding design extension conditions

4.3 Perception for cable evaluations at DECs

The presented proactive approach in figure 4.4 predicts cables failures at elevated accidents scenarios where the stress factors are beyond their initially designed basis. Some of these targeted cables are safety-related cables and must be evaluated under the current EQ prior to their installations. Under severe accident scenarios, the stress factors may exceed their designed values at EQ, thus cables will certainly fail and their failure cause loss of corresponding safety systems functions. Based on these expectations, design extension conditions (DECs) process of some stress factors in the current EQ process is necessary. In order to evaluate cables at DECs, the flowchart in figure 4.5 is presented based on operator behaviors at severe accident conditions and proactive approach understanding from figure 4.4.

Once accident occurs from internal or external initiating events (such as earthquake, tornado, flooding, anticipated transients, LOCA, SBO), the operator shall prepare the technical-guidelines for targeted cables regarding DECs that were established according to approach in figure 4.4. If ECCS succeeds to terminate accident progression during the initial stage of the accident and while the stress factors are within DBA values, then there are no further requirements in terms of cable evaluations. But if the accident is still progressing due to loss of ECCS systems, then the operator shall electrically isolate the automatic operation mode of targeted equipment and set “remote-manual” mode in order to achieve functional independency and avert spurious automatic initiation/termination from logic interfered signals with other systems. If any target equipment (regardless whether cable part or other electrical/mechanical part) fails to operate due to impacts of accident progression, then the operator shall take corrective actions to mitigate accident utilizing redundancy principle of targeted equipment (such as ADS/RSV diversity), and utilizing the supplementary back-up equipment (for example, BWR-4 PCPS exhaust fan motor and valve solenoid coil can be a back-up in case of PCPS exhaust filter fan or valve failure as shown in figure 4.3). In order to determine whether the equipment failed as consequence of cable failure, the vicinity stress

factors between cable ends installation location shall be evaluated, thus the following three cases can evolve by which current cable EQ can be judged:

1- In the first case, the stress factor is lower than its design basis limits and the cable is still functional, thus the equipment did not fail by failure of its cable. In addition, this reveals that the current cable EQ process is enough and no requirements for DECs considerations.

2- In the second case, the cable is still functional in spite the stress factor value is higher than its design basis limit, thus the electric equipment did not fail by cable failure. But in contrast, the current EQ is not enough and targeted cables shall be reevaluated with extended environments beyond those established in current design basis.

3- In the most severe case, the failure of equipment was a result of cable failure due to elevated stress factors beyond their design limits. This reveals that the current EQ process is not valid for cable evaluations at DECs. Accordingly, modifications for plant design shall be considered such as relocating cable to milder environments during severe accident conditions.

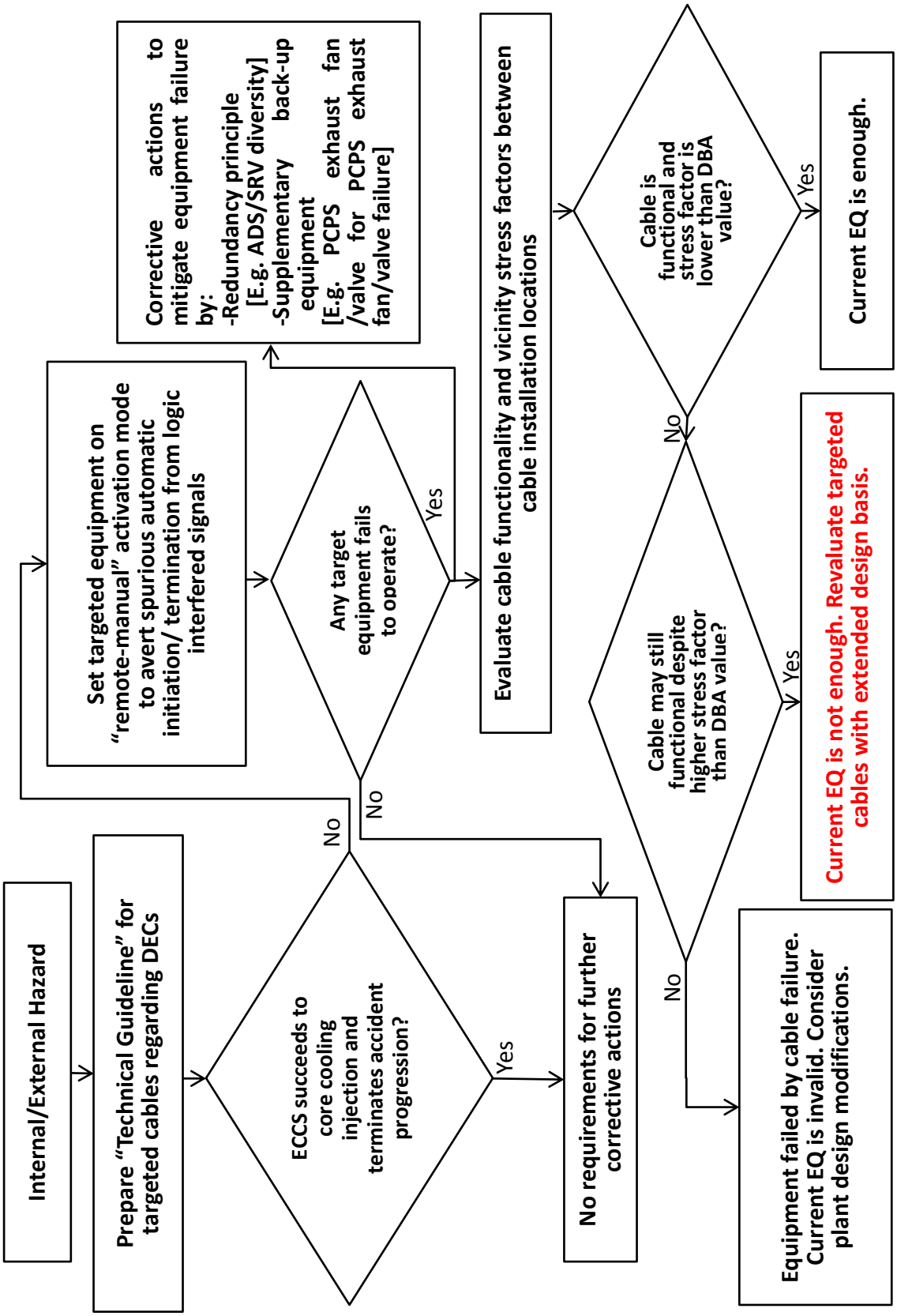

Fig. 4.5 Perception for cable evaluations at design extension conditions

4.4 Generic approach for modifying current EQ

For the BWR-4 case study, 18 targeted electric components at DECs (figure 4.3) were identified from engineering judgments between 14 severe accident sequences (section 4.1) with understanding BWR-4 systems and process control. The corresponding cables of these components are all classified as low voltage (LV) power cables, or instrumentation and control (I&C) cables. In addition, at the initial scenarios of 14 accident sequences, the current EQ is suitable to evaluate cable integrity against temperature, radiation and water submergence (flooding). But considering stress factors of target accident from technical guidelines (figure 4.4), the most important stress factors to be considered for design extension process for current cable EQ are BDBA temperature and flooding. Accordingly, current EQ should be reevaluated for both DBA temperature-profile and submergence withstand voltage.

A generic approach is presented in figure 4.6 that addresses basic requirements to modify DBA temperature and withstand voltage stress for current EQ process. Keeping in mind polymeric-based structure of jacket and insulator materials, the thermo-physical characteristic shall consider the variety of these materials types. Accordingly, evaluating DBA temperature is preferably to be in compliance with threshold failure temperature of each type which is identified by CAROLFIRE project [8,9,10]. In CAROLFIRE project, the threshold failure temperature is basically selected according to cable insulation resistance IR failure criteria at 1 KΩ or less. For thermoplastic polymeric materials such as PE and PVC, the threshold failure temperature is 200-250 °C [8,9,10]. While for thermoset polymeric materials such as XLPE, EPR/EPDM, SiR and CSPE the threshold failure temperature is 400-450 °C [8,9,10]. For withstand voltage during final integrity judgment test, the basis for modifications shall suits with cable function and maker standards.

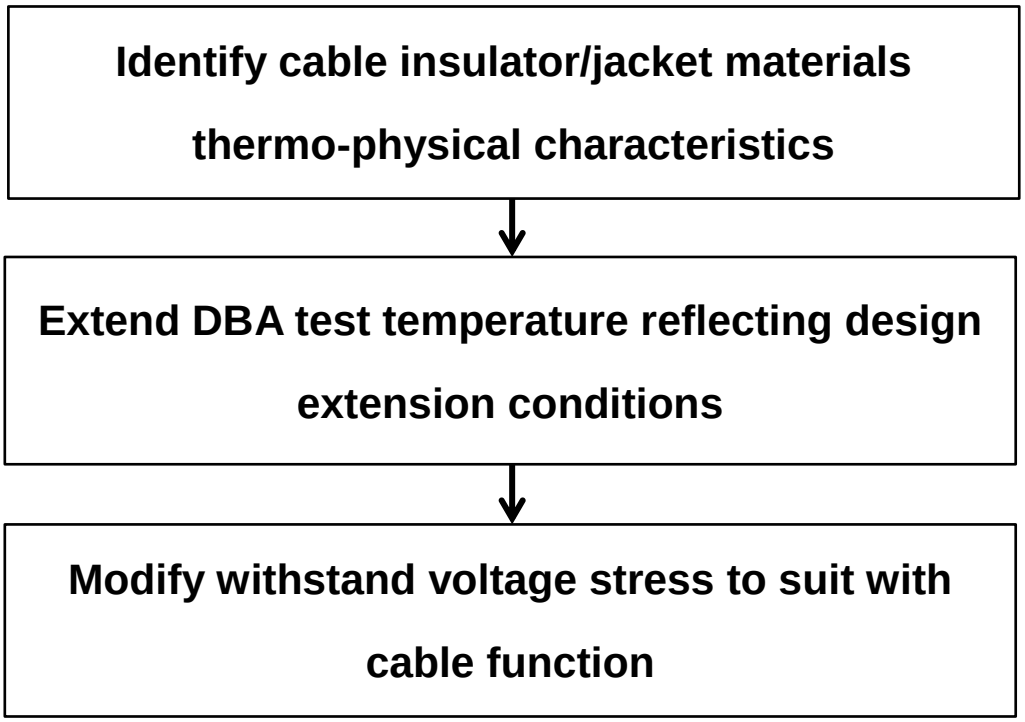

Fig. 4.6 General approach for modification of current EQ

Proposing modified values for DBA peak temperature and withstands voltage, requires reviewing status quo of their corresponding values separately as below:

1. **Temperature:** Figure 4.7 summarizes current temperature schemes inside NPP that can have different benchmark on cable ageing. Temperature value at 50 °C forms a typical hot spot environment that can be found in some areas of NPPs, but cables integrity can withstand operation at such hot spot environments beyond their initially designed lives of 40 years. Temperature up to 120 °C is considered practical to set accelerated ageing test for thermal ageing extrapolations at lower temperatures, considering chemical stability and thermodynamics transitions above glass transition temperature and crystalline melting temperature for some cable polymer materials [15]. The temperature range from 125 °C to 160 °C represents the accelerated ageing temperature span for this study (chapter 2 and 3). Elevated temperature value at 171 °C is the established current DBA peak temperature corresponding to LOCA for Japanese BWR plants [12]. Raising temperatures lead to cable polymer structure failure by rapid melting, thus the criteria for cable evaluations cannot be based on Arrhenius model since the ageing

will be heterogeneous. At such conditions, failure criterion is mainly dependent on electrical integrity, in particular insulator resistance (IR), while failure time will rapidly decrease from days or hours at uniform thermal ageing to minutes at such conditions. 200°C is the minimum threshold temperature for thermoplastic materials electrical failure (i.e. IR< 1KΩ) with an average time of 8 minutes [10]. At 400 °C, the thermoset polymeric materials will electrically fail within an average time of 15 minutes [10]. Beyond threshold failure points, cable is certainly un-functional thus modification of DBA temperature profile is implausible. Based on above, DBA temperature profile is possible in the range of current peak temperature value (171 °C) and threshold failure points depending on insulator material. Considering the possible existence of thermoplastic material within cable structure (such as the SHPVC jacket of the tested specimens in this study), and maintaining the mechanical integrity of cable structure to apply Arrhenius model, then a proposed value for DBA-peak temperature can be between the span of 171 °C -200 °C. Literature review shows that at 180 °C there will be no electrical failure for thermoplastic materials [93]. Accordingly, the extended temperature can be in the remaining range between 180°C -200°C with no need for further experiments. 190 °C is conservative example considering dominance of cable mechanical integrity thereby applicability of thermal ageing estimations from Arrhenius model to extrapolate the modified DBA peak time as will be illustrated more thoroughly in section 4.5.

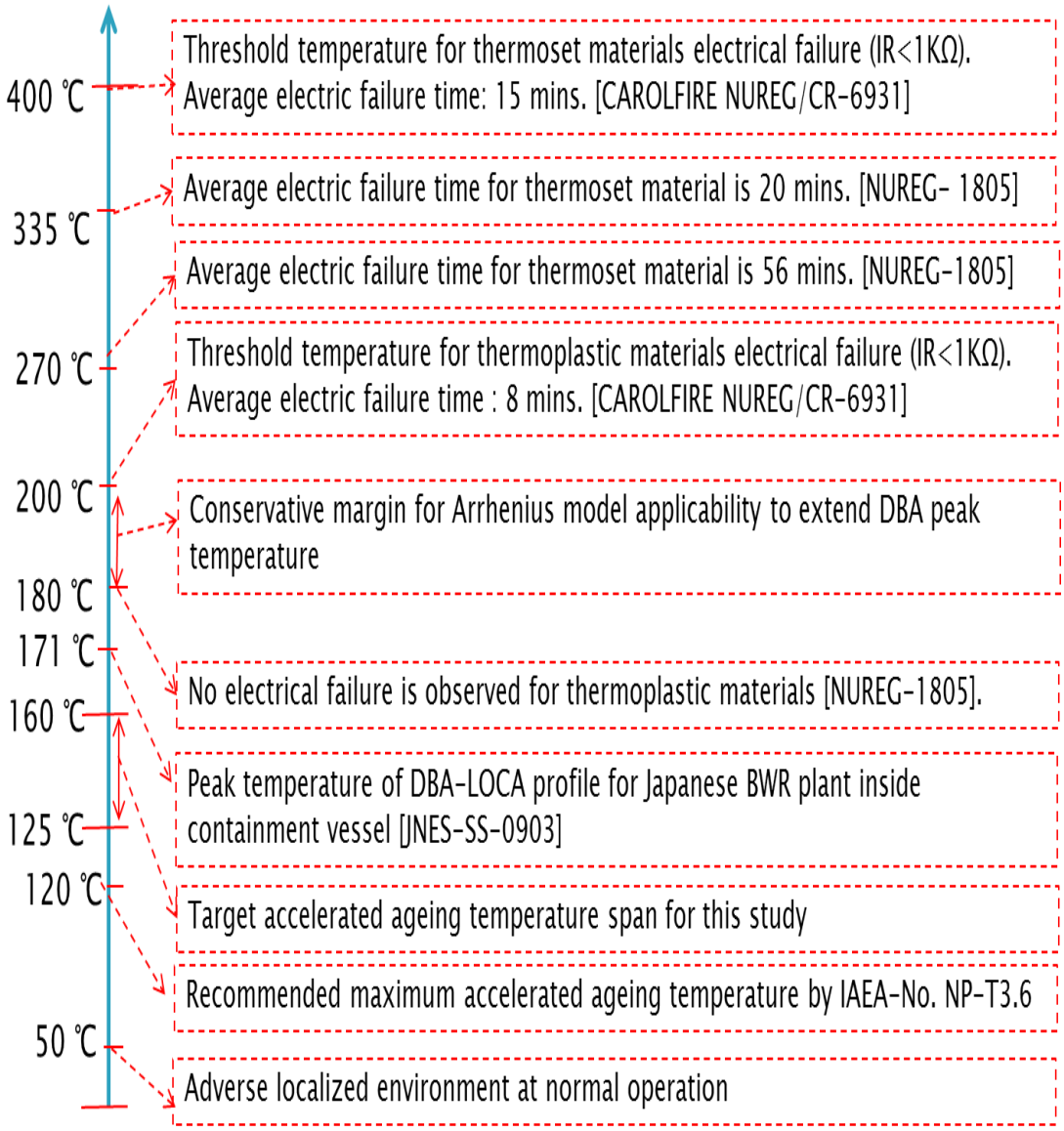

Fig. 4.7 Temperature schemes of NPPs cables

2. **Withstand voltage:** In current EQ submergence bending withstand voltage test, voltage stress value is set to 3.2 KVac/mm along with insulator thickness for 5 minutes as recommended by the institute of electrical engineering of Japan (IEEJ). But this value is actually much larger than actual voltage stress for NPP cables. For example, the targeted cables for DECs at this study are all LV cables with nominal/rated values less than 1000 V. In case of power or control cables with typical 3ϕ 480 Vac and thickness of 1 mm (as of the selected FR-EPR specimens in this study), the voltage stress during normal operation as well as all accident scenarios is estimated by $(480/\sqrt{3})$/1mm or

277.13 V/mm. The voltage stress is even less for instrumentation cables with nominal rated voltage class of 24/48 V [4]. Besides, insulator inner layers near conductor are exposed to higher voltage stress levels than outer layers due to dependence on electric field intensity on distance reciprocal from conductor. Thus, even if the outer layers absorb water due to submergence, the dielectric capability of inner layers may not be equally impacted. Based on these observations, current EQ settings for voltage stress (as well as humidity) during submergence withstand voltage test include ultimate corresponding environments that can be encountered at real plant conditions including any accident scenario of DECs. In other words, the values of voltage stress cannot further extended. However, since insulation design criteria provides large margin for dielectric strength inspections against water intrusion by submergence, this study suggested modification of current withstand voltage values (3.2 KV/mm) as in figure 4.8. The recommended withstand voltage from manufacturer standard for the LV cables (as identified in this study) are ranging between 1-2 KV/mm insulation thickness. Accordingly, the new modified voltage stress can be set between 3.2KV/ mm and 2KV/mm in order to suit with DBA temperature profile extension. Once DBA temperature profile is modified, the following submergence leads to more water intrusion compared to those induced by current DBA temperature profile settings. Thus if the cable fails at current voltage stress of 3.2KV/mm , then the test is repeated at gradually decreased voltage stress values (not less than 2 KV/mm) until cable passes. The new voltage stress can then be fixed at the value at which cable passes considering the minimum value from the variety of cable polymer materials types.

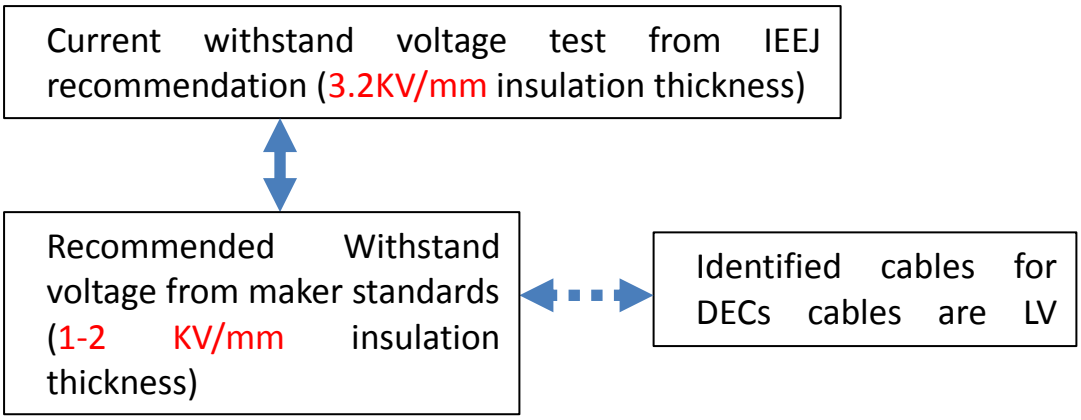

Fig. 4.8 Basis for modifying withstand voltage in order to maintain extended DBA temperature profile

4.5 DBA peak-temperature extension from EAB degradation

In chapter 3 (section 3.5), an excessive margin for cable integrity was found from thermal ageing difference between current EQ process expectations and real degradation of FR-EPR cable used in this study. In addition, NPPs temperature schemes (figure 4.7) shows that current DBA peak temperature (e.g. 171 °C for BWR-4) can be extended beyond current values. With all above in mind, this study proposes two systematic methods for DBA-peak temperature extension. The basic rational is that the DBA-peak temperature limit is mainly reliable on the dominance of mechanical degradation through EAB reduction at ageing phase and incident phase of EQ process as thoroughly explained below:

1- **Extensions from equivalent time margins to service life criterion:** EAB reduction to 0.5 EAB_0 was utilized in chapter 3 to evaluate equivalent times for thermally aged FR-EPR insulators. Thermal ageing estimation by Arrhenius model was performed considering dominance of mechanical integrity (EAB) degradation at thermal ageing phase of EQ process. Besides, the excessive margin during thermal ageing (figure 3.14) reveals that the equivalent times of accelerated tests have adequate margin until EAB reduction reaches 50% normalized value (i.e. 0.5 EAB_0). Accordingly, the time beyond the initially designed qualified life (for example 40 years) can be utilized to extend the current DBA-peak temperature through Arrhenius model. But this requires in advance estimating temperature limit that has same degradation trends in order to apply Arrhenius model. Accordingly, the temperature span between (180 -200) °C in figure 4.7 was estimated to be suitable for DBA-peak temperature extension, and 190 °C is considered suitable limit DBA-peak temperature extension. Based on all above discussion, equivalent times for FR-EPR insulators in this study at normal operation environment of 50 °C were firstly extrapolated from ageing at 125 °C by Arrhenius model (equation 4.1) assuming that ageing trends are similar between 50 °C and 125 °C:

$$t_1 = t_2 e^{\frac{E_a}{R}\left[\frac{1}{(273+T_{real})} - \frac{1}{(273+T_{test})}\right]} \quad 4.1$$

Where

t_1: Time to 0.5EAB$_0$ at real NPP environment [year]

t_2: Time to 0.5EAB$_0$ at accelerated test temperature [year]

T_{real}: Real operating temperature at NPP environment (i.e. 50 °C).

T_{test} : Extrapolation temperature at accelerated test region (i.e. 125 °C).

The values of t_2 of equation 4.1 are obtained from table 3.2 at t_{μ}, while E_a are E_a (t_{μ}) (converted from hour units to year units). The results of equivalent time estimations form above equation are shown in figure 4.9. For ageing phase, the normal qualified life is 40 years, but there is still large remaining margin to the service lifetime criterion (0.5 EAB$_0$). The remaining equivalent time to 0.5 EAB$_0$ is estimated after subtracting the total equivalent time from the quailed service life (40 years), and resulted in 68, 50, and 408 years for white, red and black insulators, respectively. This remaining equivalent time margin can be converted into extended DBA-peak time by applying Arrhenius model.

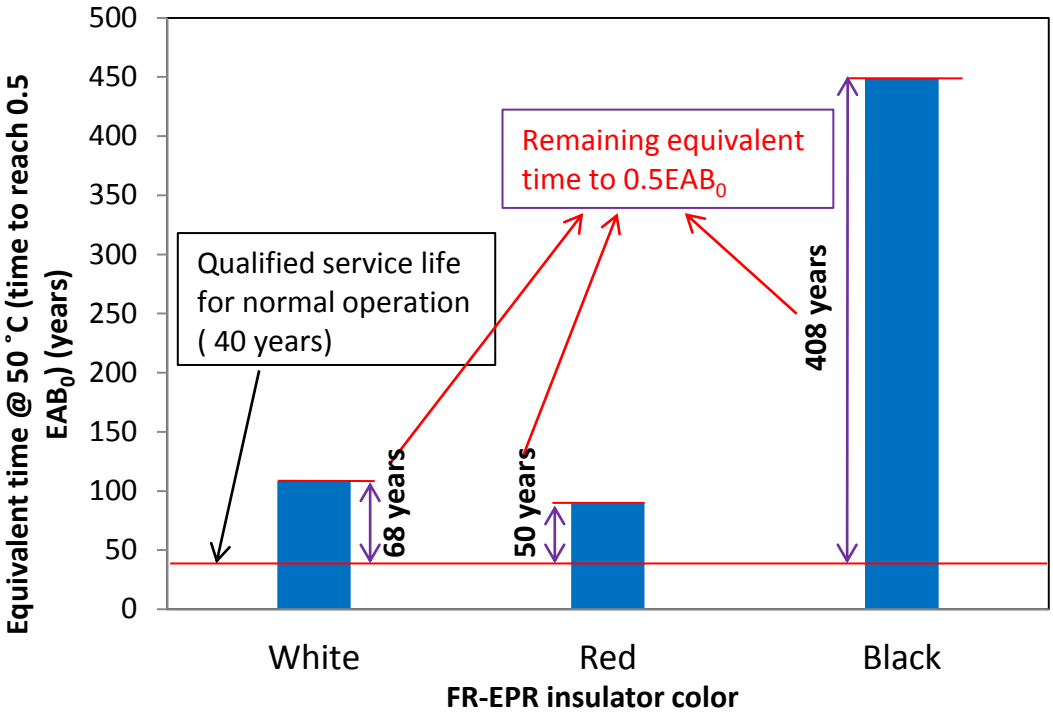

Fig. 4.9 Equivalent time for FR-EPR insulators at normal operation temperature of 50 °C extrapolated from accelerated ageing at 125 °C

But before extension, the effect of DBA secondary sequential temperature degradation (i.e. 121 °C for 13 days) shall be considered. Figure 4.10 shows BWR DBA-temperature profile (black lined profile was utilized from JNES-SS-0903[12]) which has two temperatures; one is the DBA peak temperature of 171°C for 9 hours, while the other is the sequential temperature profile of 121 °C for 13 days. The sequential temperature (121 °C) is very close to ageing range of this study , and thus the time period (13 days) can be converted into equivalent time at 50 °C by Arrhenius (equation 4.1). The values of equivalent times are 15.25, 12.50 and 41.23 years for FR-EPR white, red and black colors respectively. Thus modified time margin at 50 °C after subtracting equivalent time of sequential temperature from initial time margin is the margin from which DBA-peak temperature/time are extended through Arrhenius model as in equation 4.2:

$$Extended\ peak\ time = \boldsymbol{t'} e^{\frac{E_a}{R}\left[\frac{1}{(273+T_{ext.})}-\frac{1}{(273+50)}\right]} \qquad 4.2$$

Where

$T_{ext.}$: Extended peak temperature (°C)

t': Modified time margin at 50 °C, after subtracting equivalent time of sequential temperature from initial time margin.

When $T_{ext.}$ =190 °C, the peak-times are 17.48, 17.61 and 23.26 hours for FR-EPR white, red and black colors, respectively. But a second option includes keeping same peak-temperature of 171°C, thus peak-time can even increase to 47.70, 46.49 and 74.85 hours for FR-EPR white, red and black colors respectively. Figure 4.10 includes the original DBA temperature profile in addition to the extended profiles by increasing peak temperature or by keeping same current DBA-temperature. Considering whole cable structure, the extended peak time shall be determined from insulator color with minimum value which indicates minimum integrity of its components. In other words, the extended peak-temperature/time of whole FR-EPR insulated cable in this study is set to 190 °C×17 hours or 171 °C×46 hours. These new set

points are presented in the blue and green temperature profiles in figure 4.10. The blue temperature profile of figure 4.10 (i.e. 190 °C×17 hours) is more suitable to scenarios with higher accident temperatures than LOCA but lower accident durations. While the green temperature profile in figure 4.10 (i.e. 171 °C×46 hours) is more suitable for scenarios with similar temperature of LOCA but longer periods. Both green and blue temperature profiles in figure 4.10 imply that current EQ is inherently suitable to some elevated scenarios of DECs considering dominance of mechanical integrity (EAB) degradation to 0.5 EAB_0 (indicator for ageing). However, there is still temperature range between achieved peak-temperature at 190 °C and minimum threshold failure point of FR-EPR insulator (i.e. 400 °C for thermoset materials). Thus, this study considered utilization this range to further increase peak temperature above 190 °C. However, this requires experimental design to verify dominance for mechanical degradation even beyond ageing region (0.5 EAB_0) and within incident region of design basis methodology (figure 3.14).

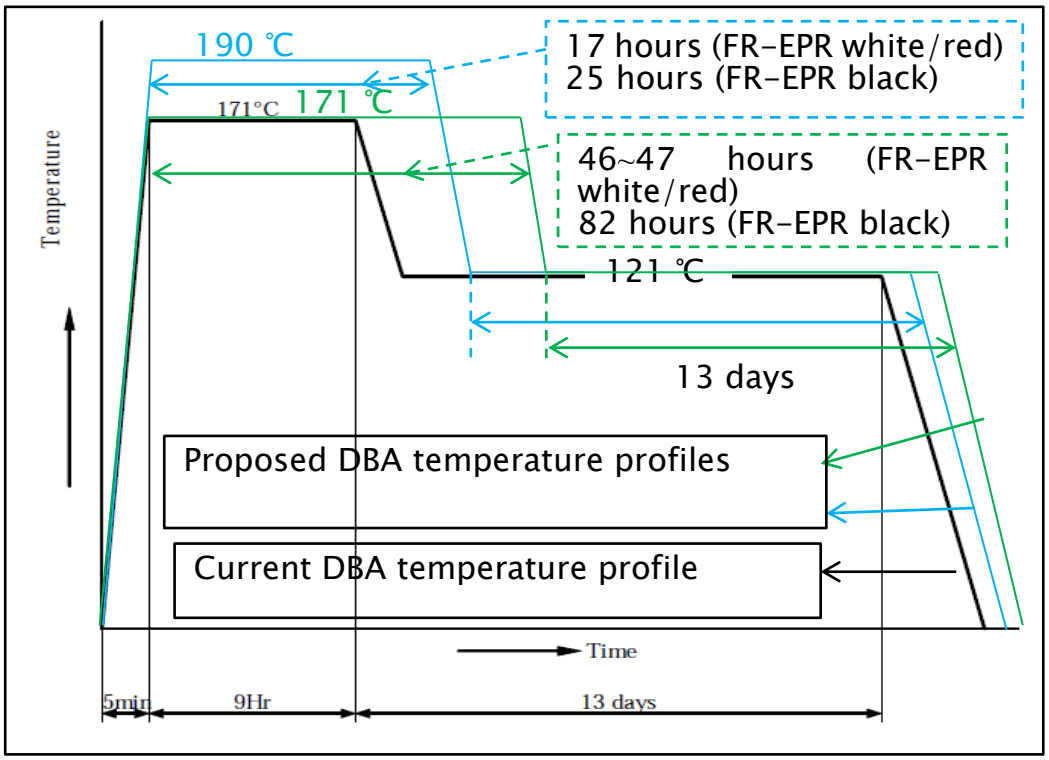

Fig. 4.10 Proposed DBA-temperature profile at peak temperatures of 171°C and 190 °C for FR-EPR cables installed inside BWR containment vessel

2- **Extensions from EAB incident retention:** To understand rational of peak-temperature extension from EAB degradation below $0.5EAB_0$, design basis methodology of cable EQ (figure 3.14) is represented again as in figure.4.11. Assuming dominance of mechanical degradation, design methodology is characterized by EAB as indicator of insulator integrity to evaluate degradation progress that can be systemically represented by ageing time (at ageing phase) and shorter incident period (at incident phase). EAB degradation for FR-EPR cables will follow induction-time behavior as represented by blue curve in figure 4.11. Following degradation at ageing phase (after EAB is $<0.5\ EAB_0$), cable operation at incident phase is assumed to have mechanical degradation that does not largely shift from those at ageing phase provided that incident peak temperature is not so close to the minimum threshold failure point of thermoset material (i.e. 400 °C). This means that EAB degradation will continue reduction within same blue curve or will slightly shift from this curve. Accordingly, suitable value of DBA- peak temperature (T_N) can be experimentally determined from EAB reduction at incident phase. However, to confirm dominance of mechanical degradation at incident phase, there must be acceptance limit or criteria of cable mechanical integrity reduction. The criteria is determined by IAEA established EAB of 50 % ultimate which can provide retention against movement during accident [15].Based on above, after ageing phase, the margin of incident can be utilized to extend DBA-peak temperature (T_N) up to level where EAB retention is almost zero as can be seen in figure 4.11. EAB retention here means; EAB at T_N – 50% ultimate. In other words, determination of DBA peak temperature, when EAB retention approaches zero, is assumed to verify dominance of mechanical degradation.

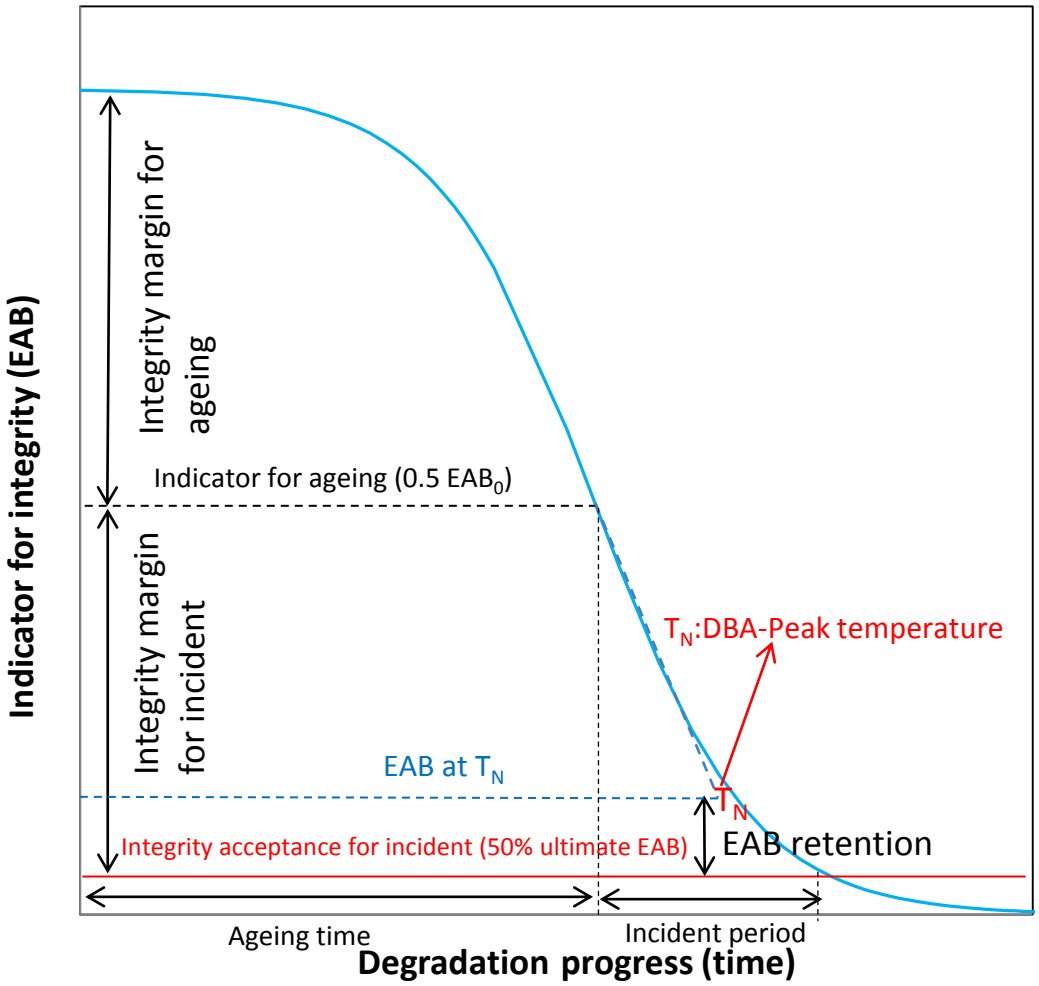

Fig. 4.11 Rational of DBA-peak temperature extension from EAB retention

Based on above understanding, this study performed additional experiment to find out suitable DBA peak temperature above 190 °C and below 400 °C for FR-EPR cables. Experimental design considered sequential accelerated heating test consisted of pre-ageing corresponding to normal operation conditions (i.e ageing phase) followed by isochronal ageing corresponding to some scenarios of DECs (i.e. incident phase). For pre-ageing testing, FR-EPR cables were aged for 160 °C up to 50 % normalized EAB_0. The time for ageing at 160 °C considered the service life of cable as approximated by minimum time of the three insulators to reach $0.5EAB_0$ at 160 °C from table 3.2. Ageing time was set to174.9 hours as was found minimum time for white insulator. Besides, the effect of sequential temperature profile at 121 °C ×13 days was added to ageing time at 160 °C from

Arrhenius model extrapolations (equation 4.1). The equivalent times from 121 °C to 160 °C were: 26.05, 28.27 and 17.33 hours for FR-EPR white, red and black insulators respectively. The minimum time of 17.33 hours was selected considering whole cable structure as determined from minimum integrity of its components. Based on all above the total ageing time at 160 °C is 192 hours (8 days). After pre-ageing, same aged FR-EPR cables were further isochronally aged at elevated temperatures starting from 171 °C which is the current DBA-peak peak temperature. The isochronal ageing period is 9 hours which is the same original time for DBA-peak temperature. Temperature increment step was approximately 20 °C. Following isochronal ageing, EAB was measured for each aged FR-EPR samples to confirm whether EAB retention approaches zero (i.e. whether EAB exceeds 50% ultimate).

Figure 4.12 shows the results of isochronal ageing at temperature range from 171 °C to 250 °C. EAB values gradually decrease in similar tendency for the three FR-EPR insulators; white, red, and black. This reveals identical degradation mechanisms through whole ageing temperature range. At temperature range 230-250 °C, EAB degradation slightly accelerates and approach integrity level of 50% ultimate EAB. This means that mechanical degradation is almost dominant up to 230-250°C. Thus, the mechanical integrity still has some safety margin against induced cracking from vibration and bending during accident conditions. In addition, literature review reports that electrical failure of thermoset materials (as for EPR-based insulators) will not start below 270 °C [93]. This reveals that mechanical degradation is still dominant in the range 230-250 °C. Accordingly, DBA- peak temperature for FR-EPR cables have tendency to further extend from previous achieved temperature value of 190 °C to the range of 230-250 °C. In other words, original DBA-peak temperature of 171 °C is proposed to increase up to 230-250 °C as presented by red profile in figure 4.13 (black lined profile was utilized from JNES-SS-0903[12]).

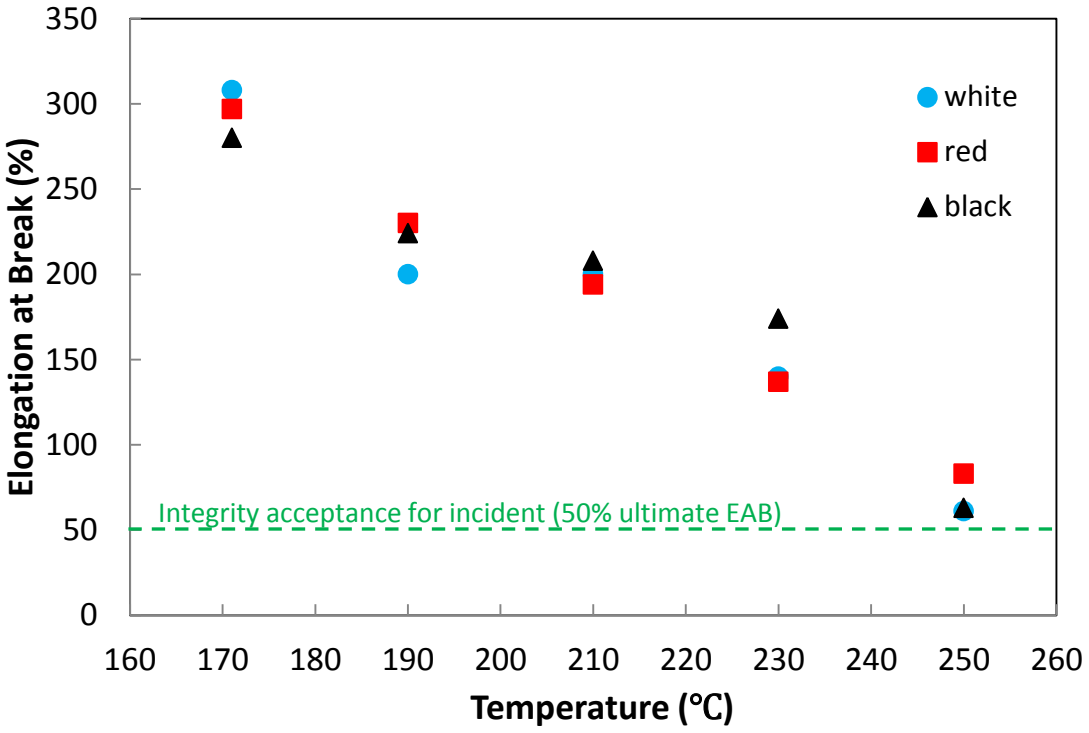

Fig. 4.12 EAB versus ageing temperature for FR-EPR insulators isochronally aged with SHPVC jacket for 9 hours, after pre-ageing for 192 hours at 160 °C

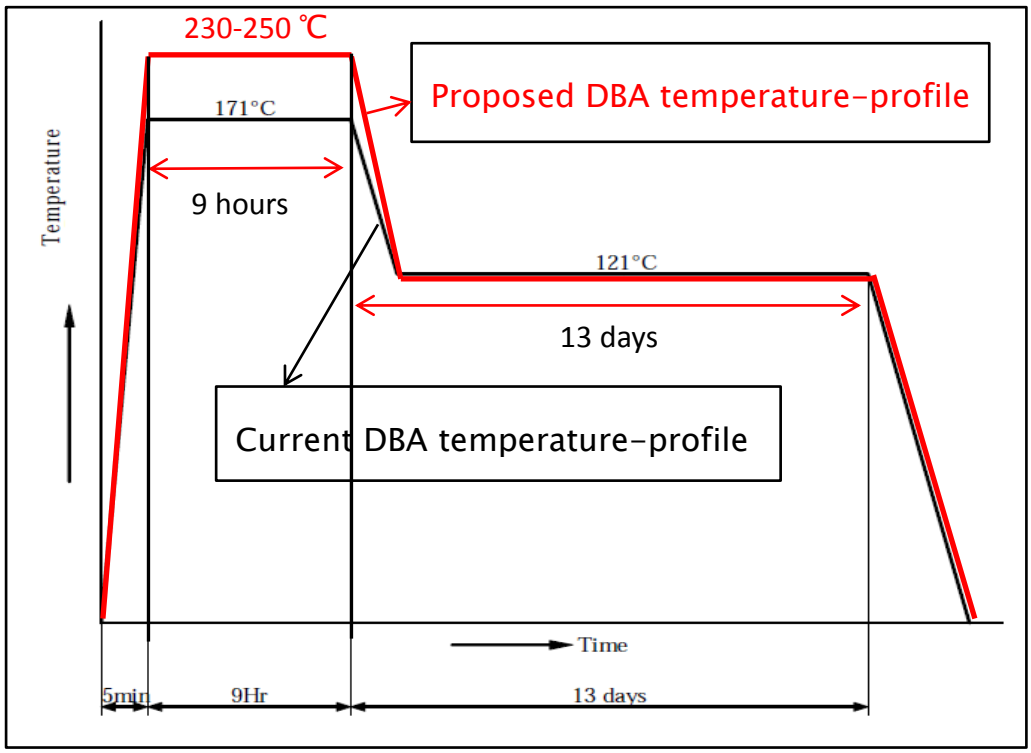

Fig. 4.13 Proposed DBA-temperature profile at peak temperature of 230-250 °C for FR-EPR cables installed inside BWR containment vessel

The three proposed temperature profiles in figure 4.10 (blue and green temperature profiles) and figure 4.13 (red temperature profile) confirm dominance of mechanical degradation and retain safety margin against crack induced by vibration and bindings. However, electrical integrity after mechanical degradation (i.e. when EAB approaches 50% ultimate value) shall also be maintained against humidity combined with voltage stress effects. Accordingly steam exposure test followed by submergence withstand test are considered as good evaluation tools to confirm electrical integrity of cable insulator that suits with postulated environments during DECs. Besides, the updated EQ shall consider cable location to suit with elevated accident environment. For example, the green temperature profile (figure 4.10) may envelop typical severe accident scenario that is identical to Fukushima Daiichi unit-2 suppression chamber temperature increment to 147 °C for around 5 days [94].

Chapter 5 Conclusions

Nuclear power plants (NPPs) cable ageing is key concern for research activities in order to evaluate its integrity at normal operation phase and accident phase. The outcome of cable ageing research activities is mainly reflected on accelerated thermal ageing estimations test and design basis accident (DBA) test of environmental qualification (EQ) process. Status quo of EQ process indicates that thermal estimations focus only on elongation at break (EAB) degradation of insulator material without estimating the variety of insulator properties and insulator existence within whole cable structure. Besides, DBA testing is limited to loss of coolant accident (LOCA) scenario, while expected design extensions conditions for new regulations may be beyond current DBA. This study reconsidered accelerated ageing testing for better understanding of cable real degradation during normal operation phase, and for searching design extension environments during accident phase. Nuclear grade low voltage flame retardant- ethylene propylene rubber (FR-EPR) insulated cables and boiling water reactor (BWR-4) were considered as case study during the activities of this research work. The main findings of this study as well as recommendations for future research are pointed out below:

5.1 Major findings and contributions of this study

1-Effect of cable structure by SHPVC jacket material is more significant on FR-EPR insulator degradation:

The effect of cable structure on FR-EPR insulator homogenous thermal ageing was evaluated from mechanical properties (EAB) and electrical properties (volume resistivity (ρ)). In this study, a specific tubular-shape electrode was designed and electrically connected by Wheatstone bridge circuit configuration for ρ detection. The maximum detected ρ by the developed design was in the order level of 10^{14} Ωm. Besides, the developed design helped evaluate post-ageing behavior for ρ which was governed by recovery to highest order of magnitude within 10 days. Through the

accelerated ageing temperature span 125°C -160°C, EAB and ρ degradation was more significant when FR-EPR insulator was aged including special heat resistant polyvinyl chloride (SHPVC) jacket material compared to ageing without jacket. Thermally induced embrittlement/cracking through insulator structure, that was evidenced by continuous EAB gradual degradation, overlapped ρ detection at increased aged times which in turn resulted in ρ increment after reaching its minimum value range in the order level (10^{10} -10^{11}) Ωm. Oxidative carbonyl (C=O) compounds (acid, ester aldehyde, and anhydride) were detected on FR-EPR insulator surface by Fourier transform infrared (FTIR) characterizations in the bandwidth (1700-1800) cm^{-1} for samples aged including SHPVC jacket material. Nevertheless, the chain-scission and cross linking reactions are not governed by oxidation degradation, since EAB and ρ decrement rates were faster for FR-EPR insulators aged with SHPVC jacket materials and diffusion limited oxidation (DLO) impacts are higher. This reveals that the jacket material will accelerate chain-scission and cross-linking degradation reactions. From ρ degradation, jacket environment will enhance the chain-scission moieties generation or will complicate ions absorption and quenching by anti-oxidant additives. Even though immigrated additives and reaction products from SHPVC jacket into FR-EPR insulation during thermal ageing is also possible on its degradation. But effect of HCL dehydrochlorination from SHPVC jacket material into insulator degradation was not evident as investigated from FTIR spectra analysis at bandwidth (2926-2932) cm^{-1}. Finally, it was difficult to evaluate the effect of different colorant pigments from trending EAB and ρ time-dependent degradation, due to interference of error bars that are originated from technical scattering.

2-Current EQ process misestimates insulator degradation due to the existence of jacket material:

Thanks to the developed tubular-electrode design, time-temperature superposition approach was successfully utilized to estimate activation energy (E_a) values for FR-EPR insulators from induced mechanisms by ρ degradation. The effect of colorant pigments was small on E_a values variations between insulator colorants (E_{awhite}=108 KJ/mol, E_{ared}=104 KJ/mol, E_{ablack}=108 KJ/mol). Nevertheless, this study affirmed the

superiority of thermal ageing estimations from EAB degradation compared to ρ degradation. That is because the induced chain-scission moieties are not enough to facilitate leakage current passage to the level that ρ decrement exceeds the IAEA established insulation function criterion of 1×10^{8} Ωm. The effect of colorant pigments was evident from E_a estimations for EAB degradation by Arrhenius model even when considering the effects of technical scattering on E_a variations (E_{awhite}=90±1 KJ/mol, E_{ared}=87±2 KJ/mol, E_{ablack}=105±4 KJ/mol). E_a large deviation for black insulator from white and red insulators is resulted from the usage of carbon-black as colorant pigment additive which acts as anti-oxidant and radical quencher. Comparisons of thermal ageing estimations between EAB degradation results of this study with EAB degradation data base shows that extrapolated times at mild temperatures are less for FR-EPR insulators aged with jacket materials. This reveals that the current EQ degrades FR-EPR insulator of this study more severely during accelerates thermal ageing process. But since cable can still pass the final withstand voltage integrity testing, then the EQ is still valid, and excessive margins from thermal ageing phase to accident phase were found to be useful for systematic modification of current EQ at DBA test.

3-Modification of DBA peak-temperature is proposed for FR-EPR cables up to 230-250 °C:

This study identified 18 targeted low-voltage electrical equipment /cables that are important for plant operations at elevated accident scenarios of design extension conditions (DECs) based on engineering judgment between 14 severe accident scenarios with plant technical guidelines for systems understanding. This study also developed proactive approach for predicting failure behaviors of targeted cables at elevated accident scenarios from four main stress factors; BDBA temperature, fire, earthquake, and flooding. Besides, this approach addressed spurious automatic activation/termination of logically interfered systems from cable failure initiating events. The outcome of this approach flows into establishing knowledgeable-base technical guidelines for the targeted equipment. Such knowledgeable-base is very vital for new designs modifications, since it can help addresses the weak points of

current design for operating cables at NPPs. Considering the aforementioned stress factors, current EQ process for DBA phase was reevaluated by modifying DBA temperature profile and submergence withstand voltage test. The excessive margin during thermal ageing phase was utilized to extend current DBA- peak temperature from 171°C up to 190 °C through Arrhenius model considering mechanical integrity criterion of $0.5EAB_0$. The DBA-peak temperature increment trend showed further tendency to increase up to temperature of 230-250 °C when considering thermoset insulator materials and mechanical integrity level of 50% EAB absolute. This study suggested modifying withstand voltage between current regulations (3.2 KV/mm insulator thickness) and cables makers specifications (1-2KV/mm insulator thickness) in order to suit with real cable functional classification and maintain extended DBA temperature profiles.

5.2 Recommendations for future work

- This study focused on investigating effect of cable structure on EPR-based insulators degradation since they are dominant for current NPPs. In order to strengthen the finding of whether jacket environment has more or less effect on insulator EAB and ρ degradation, the variety of cable insulator and jacket polymer materials can be also focused that can help enrich the database of current findings. Such work should be in conjunction with research efforts to investigate the microstructure change of insulator during accelerated ageing in order to understand the real mechanisms schemes of insulator degradation under jacket environment.
- The developed tubular-electrode design can be extensively utilized to trend time-dependent behavior of other electrical parameters, such as insulator capacitance, real and imaginary permittivity. There is no need to reconsider the placement of guard electrodes for gap width since these parameters are mainly dependent on insulator geometry not on the detected property.
- Cable identification for DECs was considered for BWR-4 in this study. The current knowledge can be broadened considering the other NPPs models. In addition, modification for current DBA phase did not consider the effect of steam exposure, chemical spray and pressure profile on electrical integrity during elevated accident scenarios. Accordingly, it is preferable to include steam exposure, pressure profile and chemical spray based on country specific requirements to validate extended DBA-peak temperature limit after investigating electrical integrity. Thus, electrical integrity of cable insulator can also be verified beside mechanical integrity to suit with severe accident scenarios. Besides, the accident scenarios that suit the modified DBA-temperature profile can be identified including the variety of NPP models.

Annex

1 ρ measurement results for aged FR-EPR insulators with SHPVC jacket material at 150 °C by direct circuit configuration and Wheatstone bridge configuration

Ageing time(hour)[1]	White insulator		Red insulator		Black insulator	
	Direct [2]	Bridge[3]	Direct[2]	Bridge[3]	Direct[2]	Bridge[3]
0 (un-aged)	I_x= 3pA $R_x=1.67\times10^{14}\Omega$ $\rho=8.17\times10^{13}\Omega m$	R_N=1 GΩ R_B=500 MΩ R_A=2 KΩ $R_x=2.50\times10^{14}\Omega$ $\rho=1.23\times10^{14}\Omega m$	I_x= 3pA $R_x=1.67\times10^{14}\Omega$ $\rho=8.17\times10^{13}\Omega m$	R_N=1 GΩ R_B=500 MΩ R_A=2 KΩ $R_x=2.50\times10^{14}\Omega$ $\rho=1.23\times10^{14}\Omega m$	I_x= 2.5pA $R_x=2.00\times10^{14}\Omega$ $\rho=9.80\times10^{13}\Omega m$	R_N=1 GΩ R_B=500 MΩ R_A=2.5 KΩ $R_x=2.00\times10^{14}\Omega$ $\rho=9.80\times10^{13}\Omega m$
96	I_x= 9pA $R_x=5.56\times10^{13}\Omega$ $\rho=2.72\times10^{13}\Omega m$	R_N=1 GΩ R_B=500 MΩ R_A=8 KΩ $R_x=6.25\times10^{13}\Omega$ $\rho=3.06\times10^{13}\Omega m$	I_x= 9pA $R_x=5.56\times10^{13}\Omega$ $\rho=2.72\times10^{13}\Omega m$	R_N=1 GΩ R_B=500 MΩ R_A=9 KΩ $R_x=5.56\times10^{13}\Omega$ $\rho=2.72\times10^{13}\Omega m$	I_x= 8pA $R_x=6.25\times10^{13}\Omega$ $\rho=3.06\times10^{13}\Omega m$	R_N=1 GΩ R_B=500 MΩ R_A=8 KΩ $R_x=6.25\times10^{13}\Omega$ $\rho=3.06\times10^{13}\Omega m$
192	I_x= 35pA $R_x=1.43\times10^{13}\Omega$ $\rho=7.00\times10^{12}\Omega m$	R_N=1 GΩ R_B=500 MΩ R_A=35 KΩ $R_x=1.43\times10^{13}\Omega$ $\rho=7.00\times10^{12}\Omega m$	I_x= 150pA $R_x=3.33\times10^{12}\Omega$ $\rho=1.63\times10^{12}\Omega m$	R_N=1 GΩ R_B=500 MΩ R_A=150 KΩ $R_x=3.33\times10^{12}\Omega$ $\rho=1.63\times10^{12}\Omega m$	I_x= 110pA $R_x=4.55\times10^{12}\Omega$ $\rho=2.23\times10^{12}\Omega m$	R_N=1 GΩ R_B=500 MΩ R_A=110 KΩ $R_x=4.55\times10^{12}\Omega$ $\rho=2.23\times10^{12}\Omega m$
240	I_x= 550pA $R_x=0.91\times10^{12}\Omega$ $\rho=4.45\times10^{11}\Omega m$	R_N=1 GΩ R_B=500 MΩ R_A=550 KΩ $R_x=9.09\times10^{11}\Omega$ $\rho=4.45\times10^{11}\Omega m$	I_x= 540pA $R_x=9.26\times10^{11}\Omega$ $\rho=4.54\times10^{11}\Omega m$	R_N=1 GΩ R_B=500 MΩ R_A=540 KΩ $R_x=9.26\times10^{11}\Omega$ $\rho=4.54\times10^{11}\Omega m$	I_x= 30pA $R_x=1.67\times10^{13}\Omega$ $\rho=8.17\times10^{12}\Omega m$	R_N=1 GΩ R_B=500 MΩ R_A=30 KΩ $R_x=1.67\times10^{13}\Omega$ $\rho=8.17\times10^{12}\Omega m$
288	I_x= 15pA $R_x=3.33\times10^{13}\Omega$ $\rho=1.63\times10^{13}\Omega m$	R_N=1 GΩ R_B=500 MΩ R_A=15 KΩ $R_x=3.33\times10^{13}\Omega$ $\rho=1.63\times10^{13}\Omega m$	I_x= 40pA $R_x=1.25\times10^{13}\Omega$ $\rho=6.13\times10^{12}\Omega m$	R_N=1 GΩ R_B=500 MΩ R_A=40 KΩ $R_x=1.25\times10^{13}\Omega$ $\rho=6.13\times10^{12}\Omega m$	I_x= 22pA $R_x=2.27\times10^{13}\Omega$ $\rho=1.11\times10^{13}\Omega m$	R_N=1 GΩ R_B=500 MΩ R_A=22 KΩ $R_x=2.27\times10^{13}\Omega$ $\rho=1.11\times10^{13}\Omega m$
336	I_x= 5nA $R_x=1.00\times10^{11}\Omega$ $\rho=4.90\times10^{10}\Omega m$	R_N=1 GΩ R_B=1 MΩ R_A=10 KΩ $R_x=1.00\times10^{11}\Omega$ $\rho=4.90\times10^{10}\Omega m$	I_x= 10pA $R_x=5.00\times10^{13}\Omega$ $\rho=2.45\times10^{13}\Omega m$	R_N=1 GΩ R_B=500 MΩ R_A=10 KΩ $R_x=5.00\times10^{13}\Omega$ $\rho=2.45\times10^{13}\Omega m$	I_x= 0.03μA $R_x=1.67\times10^{10}\Omega$ $\rho=8.17\times10^{09}\Omega m$	R_N=1 GΩ R_B=1 MΩ R_A=60 KΩ $R_x=1.67\times10^{10}\Omega$ $\rho=8.17\times10^{09}\Omega m$

Notes:

[1] Measured after at least 10 days sampling at 20.6-21.1 °C and 43-46 %. temperature and relative humidity respectively

[2] Vdc=500 V, $R_x=500/I_x$, leakage current is recorded after 60 seconds electrification, $\rho=0.49R_x$

[3] Vdc=500V, bridge circuit is balanced after passing 60 seconds electrification, $R_x= R_B R_N /R_A$, $\rho=0.49R_x$

2 Descriptive case study on technical guidelines items (BWR-4 ADS/SRV)

Electrical equipment	Cable installation locations	Cables failure phenomena/initiating event
Target component : Double stage target rock safety relief valve (SRV) pilot solenoid coil . Functional classification: Safety-related. Function : Actuate the normally-closed (N.C) nitrogen operated valves for rapid reactor pressure vessel (RPV) depressurization. Rated voltage: 125 V/250V DC. Features and interfaces: - 6/7 SRVs of 11/13 total SRVs assigned for automatic depressurization system (ADS). -2 channels ADS logic (channel "A " logic from Div.1 125V DC panel, channel "B" logic from Div.2 125 VDC panels). -ADS auto actuation logic for channel A: [following sequences combine]: 1-low RPV level "level 3". 2-lo-lo-lo RPV level "level 1". 3-Any system 1's LPCS/LPCI pump is running. 4-105 sec. time delay.	-Cable end installation location at valve solenoid side: R/B outside PCV. -Cable end installation location at DC power supply side: *Fukushima Daiichi unit 2: 1-ADS Channel A (Div.1 125 V DC): DC 3A 125V panel at C/B basement (flooded by last tsunami). 2-ADS Channel B (Div.2 125 V DC): DC 3B 125V panel at C/B basement (flooded by last tsunami).	Cable category: Low voltage (LV) power cable. -Cable failure modes initiating events : 1-Fire/Beyond DBA temperature: Insulator melting- hot short circuit - solenoid coil trip failure-loss of valve function. 2-Flooding (internal/tsunami): Submergence-water intrusion-insulation resistance failure -short circuit- solenoid coil trip failure- loss of valve function. 3-Earthquake: valve solenoid cable break damage /cable connection loosen : a-Loss of solenoid coil electric power supply- loss of valve function. b-Short circuit solenoid coil trip failure-loss of valve function. -Other cables failure initiating events (logic-interfered systems): 1-RPV level transmitter deviated/erroneous ATTUS signal or sensor actuated trip switch cable contact short (by fire , flooding, earthquake)- level 1 /level 3 spurious permissive signal for ADS auto actuation logic. 2- RPV level transmitter ATTUS instrumentation cable break/ cable connection loosen by earthquake- sensor actuated trip switch cable break /cable connection loosen by earthquake - loss of lo-lo-lo level 1 /low level 3 actuation signal for ADS logic at RPV lo-lo-lo level 1 /RPV low level 3. 3- Any system 1 /2 LPCS/LPCI pump discharge pressure switch cable contact short (by fire, flooding, earthquake)- spurious permissive system "pump is running" signal for corresponding ADS channel A/B auto actuation logic. 4- Any system 1 /2 LPCS/LPCI pump pressure switch cable break / cable connection loosen by earthquake -loss of "pump is running" signal for corresponding ADS channel A/B auto actuation logic.

Bibliography

1. International Atomic Energy Agency. Power reactor information system, Operational Reactors by Age. Available at: http://www.iaea.org/PRIS/WorldStatistics/OperationalByAge.aspx. Accessed August 4, 2015.
2. International Energy Agency. Technology Roadmap.; 2015. doi:10.1007/SpringerReference.
3. VERARDI L. Aging of nuclear power plant cables: In search of non-destructive diagnostic quantities. Thesis. University of Pologna. 2013.
4. Fuse N, Homma H, Okamoto T. Remaining issues of the degradation models of polymeric insulation used in nuclear power plant safety cables. IEEE Trans Dielectr Electr Insul. 2014;21(2):571-581. doi:10.1109/TDEI.2013.004086.
5. Fuse N, Homma H, Okamoto T. Kinetic degradation model for insulating materials used on nuclear power plant safety cables. IEEE Trans Dielectr Electr Insul. 2014;21(1):24-32. doi:10.1109/TDEI.2013.004049.
6. Hashemian HM. Ageing of electric cables in light water reactors (LWRs). In: Murty KL, ed. Materials Ageing and Degradation in Light Water Reactors. Woodhead Publishing; 2013:284-311. doi:10.1533/9780857097453.2.284.
7. United States Nuclear Regulatory Commission. Essential Elements of an Electric Cable Condition Monitoring Program, NUREG/CR-7000.; 2010.
8. United States Nuclear Regulatory Commission. Cable Response to Live Fire (CAROLFIRE) Volume 1: Test Descriptions and Analysis of Circuit Response Data, NUREG/CR-6931, Vol. 1.; 2008.
9. United States Nuclear Regulatory Commission. Cable Response to Live Fire (CAROLFIRE) Volume 2: Cable Fire Response Data for Fire Model Improvement, NUREG/CR-6931, Vol. 2.; 2008.
10. United States Nuclear Regulatory Commission. Cable Response to Live Fire (CAROLFIRE) Volume 3: Thermally-Induced Electrical Failure (THIEF) Model,NUREG/CR-6931, Vol. 3.; 2008.
11. OECD/NEA (2010). Technical Basis for Commendable Practices on Ageing Management, SCC and Cable Ageing Project (SCAP), (NEA/CSNI/R(2010)15). Available at: http://www.oecd-nea.org/nsd/docs/2010/csni-r2010-15.pdf.
12. Japan Nuclear Energy Safety Organization. JNES System Safety Report, The Final Report of The Project of “Assessment of Cable Aging for Nuclear Power Plants”, JNES-SS-0903.; 2009.
13. International Atomic Energy Agency. Ageing Management for Nuclear Power Plants, IAEA Safety Standards Series No. NS-G-2.12. Vienna; 2009.
14. International Atomic Energy Agency. Assessment and Management of Ageing of Major Nuclear Power Plant Components Important to Safety: In-Containment Instrumentation and Control Cables Volume I,

IAEA-TECDOC-1188. Vienna; 2000.
15. International Atomic Energy Agency. Assessing and Managing Cable Ageing in Nuclear Power Plants, IAEA Nuclear Energy Series No. NP-T-3.6. Vienna; 2012.
16. International Atomic Energy Agency. Approaches to Ageing Management for Nuclear Power Plants, International Generic Ageing Lessons Learned (IGALL) Final Report, IAEA-TECDOC-1736. Vienna; 2014.
17. Japan Nuclear Energy Safety Organization. JNES System Safety Report, Review Manual for Technical Assessment for Ageing Management, Insulation Degradation of Electric/Instrumentation Equipments (Including Performance Degradation of Electric/Instrumentation Equipments), JNES-SS-0511-02.; 2009.
18. Institute of Electrical and Electronics Engineers. IEEE Standard for Qualifying Class 1E Electric Cables and Field Splices for Nuclear Power Generating Stations, IEEE 383.; 2003.
19. Brookhaven National Laboratory. Condition Monitoring of Cables, Task 3 Report: Condition Monitoring Techniques for Electric Cables, BNL-90735-2009-IR.; 2009.
20. Toman GJ, Mantey A. Cable system aging management for Nuclear Power Plants. In: 2012 IEEE International Symposium on Electrical Insulation. IEEE; 2012:315-318. doi:10.1109/ELINSL.2012.6251480.
21. Electric Power Research Institute. Plant Engineering: Aging Management Program Guidance for Medium-Voltage Cable Systems for Nuclear Power Plants, EPRI 3002000557, Revision 1.; 2013.
22. International Electrotechnical Commission. Nuclear Power Plants – Instrumentation and Control Important to Safety – Management of Ageing of Electrical Cabling Systems, IEC 62465. Geneva; 2010.
23. Pacific Northwest National Laboratory. Determining Remaining Useful Life of Aging Cables in Nuclear Power Plants: Interim Study FY13, PNNL-22812.; 2013.
24. Seguchi T, Tamura K, Ohshima T, Shimada A, Kudoh H. Degradation mechanisms of cable insulation materials during radiation–thermal ageing in radiation environment. Radiat Phys Chem. 2011;80(2):268-273. doi:10.1016/j.radphyschem.2010.07.045.
25. Kudo H, Shimada A, Idesaki A. Degradation Mechanisms of Cable Insulation Materials by Radiation and Thermal Ageing. In: International Symbosium on the Ageing Management and Maintenace of Nuclear Power Plants.; 2010:84-91.
26. Gillen KT, Bernstein R, Clough RL, Celina M. Lifetime predictions for semi-crystalline cable insulation materials: I. Mechanical properties and oxygen consumption measurements on EPR materials. Polym Degrad Stab. 2006;91(9):2146-2156. doi:10.1016/j.polymdegradstab.2006.01.009.
27. Verardi L, Fabiani D, Montanari GC. Electrical aging markers for EPR-based low-voltage cable insulation wiring of nuclear power plants. Radiat Phys Chem.

2014;94:166-170. doi:10.1016/j.radphyschem.2013.05.038.
28. Sugimoto M, Shimada A, Kudoh H, Tamura K, Seguchi T. Product analysis for polyethylene degradation by radiation and thermal ageing. Radiat Phys Chem. 2013;82(1):69-73. doi:10.1016/j.radphyschem.2012.08.009.
29. Zhao Q, Li X, Gao J. Surface degradation of ethylene–propylene–diene monomer (EPDM) containing 5-ethylidene-2-norbornene (ENB) as diene in artificial weathering environment. Polym Degrad Stab. 2008;93(3):692-699. doi:10.1016/j.polymdegradstab.2007.12.009.
30. Wu Q, Qu B, Xu Y, Wu Q. Surface photo-oxidation and photostabilization of photocross-linked polyethylene. Polym Degrad Stab. 2000;68(1):97-102. doi:10.1016/S0141-3910(99)00171-8.
31. Wang W, Qu B. Photo- and thermo-oxidative degradation of photocrosslinked ethylene-propylene-diene terpolymer. Polym Degrad Stab. 2003;81(3):531-537. doi:10.1016/S0141-3910(03)00154-X.
32. Zhao Q, Li X, Gao J. Aging of ethylene–propylene–diene monomer (EPDM) in artificial weathering environment. Polym Degrad Stab. 2007;92(10):1841-1846. doi:10.1016/j.polymdegradstab.2007.07.001.
33. Ohki, Y., Hirai, N., Yamamoto, T., Minakawa, T, Okamoto T. Improvement of Inspection and Maintenance Procedures of Polymeric Cable Insulation Used in Nuclear Power Plants in Japan. CIGRE Sess. 2012;44:D1-109.
34. Celina MC. Review of polymer oxidation and its relationship with materials performance and lifetime prediction. Polym Degrad Stab. 2013;98(12):2419-2429. doi:10.1016/j.polymdegradstab.2013.06.024.
35. Seguchi, T., Hashimoto, S., Arakawa, K., Hayakawa, N., Kawakami, W., Kuriyama I. Radiation induced oxidative degradation of polymers-I. Oxidation region in polymer films irradiated in oxygen under pressure. Radiat Phys Chem. 1981;17:195–201.
36. Sandia National Laboratories. Nuclear Power Plant Cable Materials: Review of Qualification and Currently Available Aging Data for Margin Assessments in Cable Performance. SAND2013-2388. Albuquerque, New Mexico, U.S.A; 2013.
37. Santhosh TV, Ghosh a. K, Fernandes BG. Remaining life prediction of I&C cables for reliability assessment of NPP systems. Nucl Eng Des. 2012;245:197-201. doi:10.1016/j.nucengdes.2012.01.020.
38. Ohki Y, Hirai N, Yamada T, Kumagai S. Highly sensitive location method of an abnormal temperature point in a cable by frequency domain reflectometry. Proc IEEE Int Conf Solid Dielectr ICSD. 2013:117-120. doi:10.1109/ICSD.2013.6619799.
39. Ohki Y, Hirai N. Location feasibility of degradation in cable through Fourier transform analysis of broadband impedance spectra. Electr Eng Japan (English Transl Denki Gakkai Ronbunshi). 2013;183(1):1-8. doi:10.1002/eej.22384.
40. Alshaketheep T, Murakami K, Sekimura N. A Study on Insulation Degradation in Thermally Aged Ethylene Propylene Rubber Using Volume Resistivity Measurement. E-Journal Adv Maintenance, Japan Soc Maintenology.

2015;7(1):102-107.

41. Clavreul R. Thermal ageing of ethylene propylene copolymer. Proc Conf Electr Insul Dielectr Phenom - CEIDP '96. 1996;2:0-3. doi:10.1109/CEIDP.1996.564632.
42. Ramteke PK, Ahirwar a. K, Shrestha NB, Sanyasi Rao VVS, Vaze KK, Ghosh a. K. Thermal ageing predictions of polymeric insulation cables from Arrhenius plot using short-term test values. 2010 2nd Int Conf Reliab Saf Hazard, ICRESH-2010 Risk-Based Technol Physics-of-Failure Methods. 2010:325-328. doi:10.1109/ICRESH.2010.5779569.
43. Institute of Electric Engineers of Japan (IEEJ) Technical Report (Division II), No.139. Recommended Practice for Methods of Environmental Test and Flame Resistance Test for Electrical Wires and Cables for Nuclear Power Plants.; 1979.
44. Institute of Electrical and Electronics Engineers. IEEE Standard for Qualifying Class IE Equipment for Nuclear Power Generating Stations, IEEE-323. 1974.
45. Institute of Electrical and Electronics Engineers. IEEE Standard for Qualifying Class 1E Electric Cables and Field Splices for Nuclear Power Generating Stations, IEEE 383.; 1974.
46. Hsu YT, Chang-Liao KS, Wang TK, Kuo CT. Monitoring the moisture-related degradation of ethylene propylene rubber cable by electrical and SEM methods. Polym Degrad Stab. 2006;91(10):2357-2364. doi:10.1016/j.polymdegradstab.2006.04.003.
47. Hsu YT, Chang-Liao KS, Wang TK, Kuo CT. Correlation between mechanical and electrical properties for assessing the degradation of ethylene propylene rubber cables used in nuclear power plants. Polym Degrad Stab. 2007;92(7):1297-1303. doi:10.1016/j.polymdegradstab.2007.03.027.
48. Plaček V, Bartoníček B, Hnát V, Otáhal B. Dose rate effects in radiation degradation of polymer-based cable materials. Nucl Instruments Methods Phys Res Sect B Beam Interact with Mater Atoms. 2003;208(1-4):448-453. doi:10.1016/S0168-583X(03)00626-8.
49. Plaček V, Kohout T. Comparison of cable ageing. Radiat Phys Chem. 2010;79(3):371-374. doi:10.1016/j.radphyschem.2009.08.031.
50. Plaček V, Kohout T, Kábrt J, Jiran J. The influence of mechanical stress on cable service life-time. Polym Test. 2011;30(7):709-715. doi:10.1016/j.polymertesting.2011.06.005.
51. International Atomic Energy Agency. Management of Life Cycle and Ageing at Nuclear Power Plants: Improved I&C Maintenance, IAEA TECDOC-1402. Vienna; 2004.
52. Institute of Electrical and Electronics Engineers. IEEE Guide for Field Testing of Shielded Power Cable Systems Using Very Low Frequency (VLF) (less than 1 Hz), IEEE 400.2.; 2013.
53. Ralph P. Water Trees are Significant. 2005:1-3. Available at: http://www.netaworld.org/sites/default/files/public/neta-journals/NWsu05-feaPATTERSON.pdf. Accessed August 4, 2015.

54. Muto H, Motohashi K, Maruyama Y, Iwata Z. Studies on the initiation and growth of electrical trees from water trees. In: 4th International Conference on Conduction and Breakdown in Solid Dielectrics. IEEE; 1992:461-469.
55. Celina M, Gillen KT, Clough RL. Inverse temperature and annealing phenomena during degradation of crosslinked polyolefins. Polym Degrad Stab. 1998;61(2):231-244. doi:10.1016/S0141-3910(97)00142-0.
56. Gillen KT, Bernstein R, Clough RL, Celina M. Lifetime predictions for semi-crystalline cable insulation materials: I. Mechanical properties and oxygen consumption measurements on EPR materials. Polym Degrad Stab. 2006;91(9):2146-2156. doi:10.1016/j.polymdegradstab.2006.01.009.
57. Gillen KT, Celina M, Bernstein R, Shedd M. Lifetime predictions of EPR materials using the Wear-out approach. Polym Degrad Stab. 2006;91(12):3197-3207. doi:10.1016/j.polymdegradstab.2006.07.027.
58. Gillen KT, Clough RL. Inhomogeneous radiation degradation in polymers studied with a density gradient column. Radiat Phys Chem. 1983;22(3-5):537-544. doi:10.1016/0146-5724(83)90061-4.
59. Western European Nuclear Regulation Association. Safety of New NPP Designs- Study by Reactor Harmonization Working Group RHWG.; 2013.
60. International Atomic Energy Agency. Safety of Nuclear Power Plants : Design, IAEA Safety Standard SeriesNo. SSR-2/1.; 2012.
61. Powerstream. Wire Gauge and Current Limits Including Skin Depth and Strength. Available at: http://www.powerstream.com/Wire_Size.htm. Accessed August 4, 2015.
62. Orza R. INVESTIGATION OF PEROXIDE CROSSLINKING OF EPDM RUBBER BY SOLID-STATE NMR.Thesis. Eindhoven University of Technology. 2008.
63. Oak Ridge National Laboratory. Station Blackout at Browns Ferry Unit One-Accident Sequence Analysis, NUREG/CR-2182, Vol.1. Oak Ridge, Tennessee, U.S.A; 1981.
64. Oak Ridge National Laboratory. BWR 4/Mark I Accident Sequences Assessment, NUREG/CR-2825. Oak Ridge; Tennessee; U.S.A; 1982.
65. Matsunami U, Mikami M. Study on the Ageing Degradation Diagnosis of Electric Cables Based on Indenter Modulus Method [Japanese]. INSS J. 2008;15:236-242.
66. International Electrotechnical Commission. Nuclear Power Plants – Instrumentation and Control Important to Safety – Electrical Equipment Condition Monitoring Methods – Part 3: Elongation at Break, IEC 62582-3. Geneva; 2012.
67. Behera a. K, Akhtar S, Alsammarae AJ. Performance Of Cables Under Local Submergence Resulting From A Design Basis Accident. In: 1990 IEEE Nuclear Science Symposium Conference Record.; 1990. doi:10.1109/NSSMIC.1990.693501.
68. Simmons KL, Ramuhalli P, Pardini A, et al. Determining Remaining Useful Life of Aging Cables in Nuclear Power Plants using Non-Destructive

Evaluation. Trans Am Nucl Soc. 2014;111:456-458.
69. Gaffari T. Electrical Testing and Characterization. In: Characterization and Failure Analysis of PLASTICS. American Society of Metals interantional; 2003:164-176.
70. American Society for Testing and Materials. Standard Test Methods for DC Resistance or Conductance of Insulating Materials, ASTM-D257-07.; 2007. doi:10.1520/D0257-07.
71. Indian Standards Institution. METHODS OF TEST FOR VOLUME AND SURFACE RESISTIVITY OF SOLID ELECTRICAL INSULATING MATERIALS, IS:3396-1979.; 1980.
72. International Electrotechnical Commission. Nuclear Power Plants – Instrumentation and Control Important to Safety – Electrical Equipment Condition Monitoring Methods – Part 2: Indenter Modulus, IEC 6258-2. Geneva; 2011.
73. Nakanishi K. Infrared Absorption Spectroscopy,Practical. San Fransisco: Holden-Day; 1962.
74. Xu J, Liu C, Qu H, Ma H, Jiao Y, Xie J. Investigation on the thermal degradation of flexible poly(vinyl chloride) filled with ferrites as flame retardant and smoke suppressant using TGA–FTIR and TGA–MS. Polym Degrad Stab. 2013;98(8):1506-1514. doi:10.1016/j.polymdegradstab.2013.04.016.
75. The Free Library. Identification of polymers by IR spectroscopy. Available at: http://www.thefreelibrary.com/Identification+of+polymers+by+IR+spectroscopy.-a0119376722. Accessed August 4, 2015.
76. Seguchi T, Tamura K, Shimada A, Sugimoto M, Kudoh H. Mechanism of antioxidant interaction on polymer oxidation by thermal and radiation ageing. Radiat Phys Chem. 2012;81(11):1747-1751. doi:10.1016/j.radphyschem.2012.06.011.
77. Sun Y, Luo S, Watkins K, Wong CP. Electrical approach to monitor the thermal oxidation aging of carbon black filled ethylene propylene rubber. Polym Degrad Stab. 2004;86(2):209-215. doi:10.1016/j.polymdegradstab.2004.04.013.
78. Li Z, Moon KS, Yao Y, et al. Carbon nanotube/polymer nanocomposites: Sensing the thermal aging conditions of electrical insulation components. Carbon N Y. 2013;65:71-79. doi:10.1016/j.carbon.2013.07.105.
79. International Atomic Energy Agency. Assessment and Management of Ageing of Major Nuclear Power Plant Components Important to Safety: In-Containment Instrumentation and Control Cables Volume II, IAEA-TECDOC-1188. Vienna; 2000.
80. Japan Nuclear Energy Safety Organization. JNES Safety Research Report, Guide for Ageing Evaluation of Cables for Nuclear Power Plants, JNES-RE-2013-2049.; 2014.
81. International Atomic Energy Agency. Severe Accident Management Programmes for Nuclear Power Plants Safety Guide, IAEA Safety Standards

Series No. NS-G-2.15. Vienna; 2009.

82. International Atomic Energy Agency. Safety of Nuclear Power Plants: Design, IAEA Safety Standards Sereies No. NS-R-1. Vienna; 2000.
83. Kawano A, Tokyo Electric Power Company. Fukushima Nuclear Accident Interim Report: Effects of the Earthquake and Tsunami on the Fukushima Daiichi and Daini Nuclear Power Stations, especially on electric and I&C systems and equipments. 2011. Available at: http://grouper.ieee.org/groups/npec/N11-02/N11-02_TEPCO_IEEEpresenkawanorev8.pdf. Accessed August 4, 2015.
84. Tokyo Electric Power Company. Technical Knowledge of the Accident at Fukushima Dai-ichi Nulcear Power Station, TEPCO Diagrams (Provisional Translation). 2011. Available at: https://www.nsr.go.jp/archive/nisa/english/press/2012/06/en20120615-1-2.pdf. Accessed August 4, 2015.
85. USNRC Technical Training Center. General Electric BWR/4 Tecnnology Manual-10.2-Automatic Depressurization System. Available at: http://pbadupws.nrc.gov/docs/ML0228/ML022840049.pdf. Accessed August 4, 2015.
86. USNRC Technical Training Center. Boiling Water Reactor- General Electric BWR/4 Technology Manual-Chapter 3.0-Process Instrumentation and Control Systems. Available at: http://atominfo.ru/files/fukus/023020088.pdf. Accessed August 4, 2015.
87. USNRC Technical Training Center. Boiling Water Reactor- General Electric BWR/4 Technology Advanced Manual- Chapter 6.0- BWR Differences. GE Technol Adv Man. Available at: hhttp://pbadupws.nrc.gov/docs/ML0230/ML023010606.pdf. Accessed August 4, 2015.
88. USNRC HRTD. General Electric Systems Technology Manual-Chapter 4.1-Primary Containment System. Available at: http://pbadupws.nrc.gov/docs/ML1125/ML11258A322.pdf. Accessed August 4, 2015.
89. United States Nuclear Regulatory Commission. Reactor Safety Study, WASH 1400 (NUREG 75/014).; 1975.
90. American Nuclear Society Standards Committee. Decay Heat Power in Light Water Reactors, ANSI/ANS-5.1-1979.; 1979.
91. United States Nuclear Regulatory Commission. Analysis of Core Damage Frequnecy From Internal Events : Methodology Guidleines, Volume 1, NUREG/CR-4550 V1.; 1987.
92. Mandelli D, Smith C, Riley T, et al. Light Water Reactor Sustainability Program, Support and Modeling for the Boiling Water Reactor Station Black Out Case Study Using RELAP and RAVEN, INL/EXT-13-30203.; 2013.
93. United States Nuclear Regulatory Commission. Fire Dynamics Tools (FDTs) Quantitative Fire Hazard Analysis Methods for the U.S. Nuclear Regulatory Commission Fire Protection Inspection Program, NUREG-1805.; 2004.

94. Tokyo Electric Power Company. Analysis and evaluation of the operation record and accident record of Fukushima Daiichi Nuclear Power Station at the time of Tohoku-Chihou-Taiheiyou-Oki-Earthquake. 2011. Available at: http://www.tepco.co.jp/en/press/corp-com/release/betu11_e/images/110524e16. Accessed August 4, 2015.